Scuola Normale Superiore

Phenomenological aspects of Extra Dimensions

Candidate

Marco Cirelli

Supervisors

Prof. Riccardo Barbieri
Dr. Andrea Romanino

Pre-Ph.D. Thesis

Pisa, November 2002

Contents

Chapter 1

Introduction

1.1 Getting motivated

Any honest discussion on possible extensions of the Standard Model [1] of strong and electroweak interactions cannot obviously omit the fact the Standard Model works astonishingly well.

Besides the well known conceptual successes (the unification of three forces under the spell of the gauge invariance principle, the prediction of neutral current interactions and of the properties of the weak bosons, the necessity of charm quark...), the focus is rather on the overall agreement beetwen the Theory and the vast set of experimental data coming from electron–positron annihilations, hadronic collisions and neutrino interactions, often measured at an accuracy level better than one part per mille. The present status of this good agreement is depicted in fig.1.1.[1, 2]

The most important message of these ElectroWeak Precision Tests (EWPT) concernes possible physics beyond the Standard Model (SM): only very delicate deviations from the SM predictions are allowed. This is a very strong constraint on theorist's immagination.

Nevertheless, technical and conceptual flaws of the Standard Model have been the spurring force for particle physics of the last decades and theorists' immagination has proved to be not too much curbed.

In the following I briefly review how and why the Standard Model itself calls for New Physics, before focusing on the single issue of Extra Dimensions.

1.1.1 Beyond the Standard Model!

A short list of unsatisfactory features and drawbacks of the Standard Model should include at least the following:

1. too much arbitrariness,
2. no masses for neutrinos, and no description of neutrino oscillations,
3. unification of known forces incomplete, gravity being not included.

[1]See however [4] (for instance) for recent comments on some of the few open discrepancies.

[2]The discrepancy between SM prediction and experimental value of muon anomalous magnetic moment should also be mentioned in this context; see Chapter 5.

Figure 1.1: Precision Electroweak measurements and the pulls they exert on a global fit to the Standard Model. [2]

1. Even if one accepts the rather odd set of group representations and hypercharges, the Standard Model contains at least 18 free parameters (3 gauge couplings, 6 quark masses and 3 lepton masses, 4 Cabibbo-Kobayashi-Maskawa free elements, 2 parameters to characterize the scalar sector of theory).[3] The common feeling of this fact is that a more fundamental theory should be invoked to naturally explain the pattern. Unification theories stem from this point. They set a new high energy scale somewhere around 10^{15} GeV.

2. There is now compelling evidence that neutrinos have masses [5, 43, 6] while in the minimal Standard Model these are strictly vanishing. All most popular extensions of the SM that can account for non zero neutrino masses call for a higher energy scale (should it be the mass scale suppressing higher dimensional operators that yield (Majorana) masses for left-handed neutrinos or the explicit mass for right-handed neutrino fields in the see-saw mechanism). This mass scale sits naturally close to the Unification scale and indeed small neutrino masses are addressed as the "third pillar of Unification" in [7].

3. The Standard Model is not the "Theory of Everything" since gravitational interaction is not included in the game. The unification of gravity calls for a even higher energy scale around 10^{19} GeV, at which gravitational interaction becomes comparable with gauge forces. This is called Planck mass (M_{Pl}). String theory/M-theory is the only candidate to be the ultimate answer to this need.

1.1.2 The Hierarchy Problem

From the sketchy picture above, it seems that it is all a matter of energy scales: first we meet the well known ElectroWeak Symmetry Breaking (EWSB) scale at $few \cdot 100$ GeV $\div 1$ TeV, then a large energy desert opens, up to the Unification scale, and above all is the Planck scale. It seems that we are simply being informed that physics is not ended at the EWSB energy and we could go and look for some New Physics at those large scales.

No, there is more: we *must* look for New Physics at *low* energy ($\lesssim 1$ TeV) scales. Why is it so? After all the SM is a renormalizable field theory and it could be valid well above the energy scale at which it is presently tested and at which EWSB happens, if one is willing to accept (at least a portion of) the energy desert.

The compelling argument to look for New Physics at low scales is known as **hierarchy problem**. It originates in the very existence of the scalar sector of the theory coupled to the presence of higher energy scales.

The standard argument goes as follows:

a. The scalar sector of the Standard Model leaves the Higgs mass as a free parameter.

Such sector is the most hazardous in the theory: we postulate the existence of an elementary Higgs scalar that spontaneously realizes the EWSB since we assume a tree level potential which is characterized by the negative mass parameter μ^2 and the dimensionless quartic coupling λ. The measured value of the Fermi constant fixes a combination of these parameters (essentially μ^2/λ) but the squared mass of the physical Higgs boson, proportional to μ^2, is undetermined.

[3] The angle related to strong CP problem is an additional free parameter.

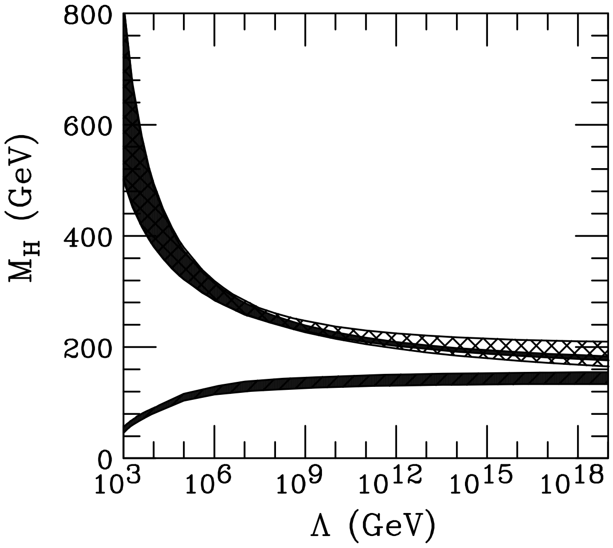

Figure 1.2: The upper (and lower) bound on Higgs mass as a function of the scale Λ at which the Standard Model ceases to be meaningful. [8]

b. However, Higgs boson has to be light.

This comes from the requirement of the Higgs self coupling λ not to develop a Landau pole before the high energy scales. This sets an overall upper bound on the Higgs mass of the order of 600 GeV, as depicted in figure 1.2. [4] More precisely, the limit depends on the high energy scale that one aims to reach: if New Physics shows up at a scale close to the Unification scale, the Higgs is confined to be roughly under 200 GeV. Notice that this point is so even in absence of any experimental hint on Higgs mass, it simply has to do with the self-consistency of the theory itself.

c. But the mass of the Higgs boson receives divergent contributions, quadratic in the cut-off Λ, already at one loop in perturbation theory, as we will check later. If the nearest cut-off at disposal is at Unification scale or even at Planck scale, the quantum corrections to Higgs mass dwarf the physical value by about 34 orders of magnitude (the Hierarchy). In other words, the tree level value is to be choosen with an accuracy of 10^{-34} compared to the Planck mass, which is so unnatural...

As well known, the Hierarchy Problem has been attacted along two main directions:
I. Technicolor models aim to eliminate the fundamental scalar field from the theory, replacing it with some fermion condensate: the energy scale of EWSB is then understood as the scale at which some new gauge force becomes strong. These models encounter several theoretical and phenomenological problems, I will not be interested in them here.

II. Low energy SuperSymmetry relies on the existence of an additional (although broken) symmetry that can motivate the smallness of Higgs mass. In other words, low energy SuperSymmetry aims to interpose a new energy scale low enough to shield scalar masses from the harm of very high energies.

[4] The unitarity bound also sets a larger upper limit of about 1 TeV.

This scale is related to the scale of SuSy breaking. SuperSymmetric models, and in particular the Minimal SuperSymmetric Standard Model (MSSM), feature a lot of new particles (the superpartners) that enter the game with a mass comparable to that scale. In the optic of the necessity of a light touch on EWPT, this approach is very successful since the superpartners contributions decouple very fast. Unfortunately, one should also mention that a lot more parameters are introduced: in the unconstrained MSSM, for instance, we end up with 105 new ones with respect to the SM, that is certainly not one wants in the spirit of point 1 in 1.1.1 above.

Recently, a new idea has opened a third brilliant way:
III. The only fundamental scale in nature is assumed to be the ElectroWeak Breaking scale ($\sim$ 1 TeV); it also settles the scale of gravitational interactions, the enormity of the Planck scale is only a mirage produced by the presence of **large extra (space) dimensions** accessible to gravity. From this idea, a huge quantity of different realizations and applications spurted. See chapter 2 for a brief overview.

1.1.3 Tightening the siege: the Lep Paradox or Little Hierarchy Problem

I now want to take a step backward and enforce the arguments given above, relying more heavily on the experimental evidences at our disposal (and making concrete what was a bit speculative).

Suppose we do not want to extrapolate the Standard Model up to those incredibly high scales, suppose that we can leave gravity alone. Do the Standard Model still faces a problem of hierarchy? The answer is yes and it ironically comes from the data of the ElectroWeak Precision Tests that I used at the beginning to state the success of the SM.
Indeed, on the one hand, EWPT say that the Higgs boson (most probably exists and) is light: this is intuitively inferred from figure 1.3 and figure 1.4, for instance.

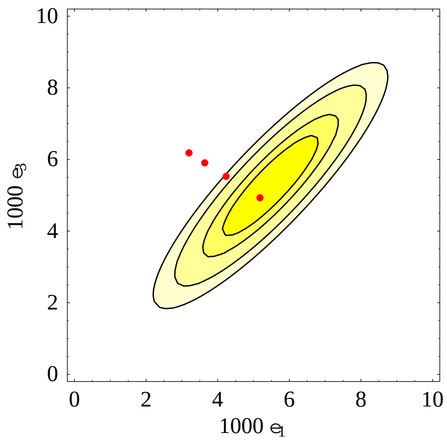

Figure 1.3: Level curves at 68, 90, 99, 99.9 per cent of confidence level of the ElectroWeak Parameters ϵ_1 and ϵ_3 compared with the SM prediction for Higgs mass equal to 100, 300, 600, 1000 GeV (dots from right to left) [9]. The agreement is best for $m_H \simeq 100$ GeV.

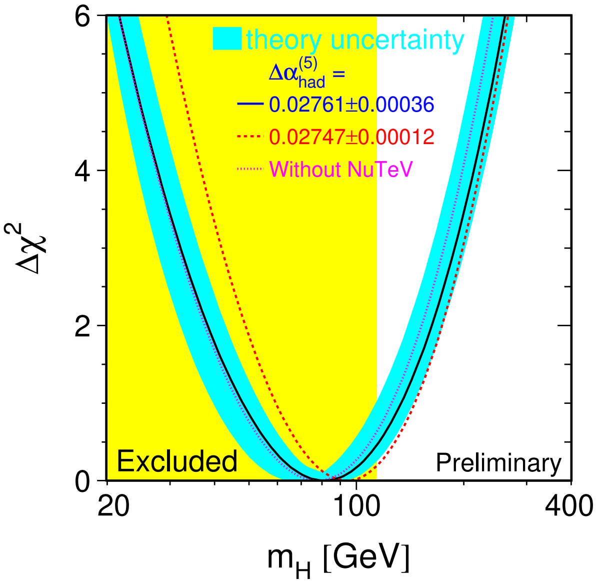

Figure 1.4: The $\Delta\chi^2$ curve derived from the Precision ElectroWeak measurements, performed at LEP and by SLD, CDF, D0, NuTeV and others, as a function of the Higgs boson mass. The preferred value, corresponding to the minimum of the curve, is around 81 GeV, with an experimental uncertainty of +52 and −33 GeV (at 68% confidence level. The mass is lower than about 193 GeV (one-sided 95% confidence level upper limit derived from $\Delta\chi^2 = 2.7$ for the blue band, thus including both the experimental and the theoretical uncertainty). [2]

On the other hand EWPT yields enough information to say that a characteristic scale of any New Physics cannot be lower than, say, 5 TeV [9].

Schematically:

$$\begin{array}{ccc} \text{EWPT} & & \text{EWPT} \\ \Downarrow & & \Downarrow \\ \text{Higgs is } \textit{light} & \textbf{VS} & \text{New Physics is } \textit{high} \\ (m_H \lesssim 190 \text{ GeV}) & & (\Lambda \gtrsim 5 \text{ TeV}). \end{array}$$

With these elements in hand, let us focus on the most significant divergent contributions to the Higgs mass: they are the one-loop diagrams involving the top quark, the $SU(2) \times U(1)$ gauge bosons and the Higgs itself (see figure 1.5).

The *top loop* is the most important and gives a correction:

$$\delta m_H^2(\text{top}) = -\frac{3}{\sqrt{2}\pi^2} G_F\, m_t^2\, \Lambda^2 = -\,(120\,\text{GeV})^2 \left(\frac{\Lambda}{400\,\text{GeV}}\right)^2 \tag{1.1}$$

where G_F is the Fermi constant and m_t the top mass. Even when the New Physics scale Λ is at its lower value, the correction is roughly 100 times larger than the most probable physical Higgs mass.

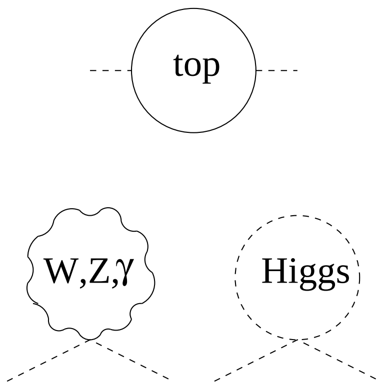

Figure 1.5: The most significant quadratically divergent contributions to the Higgs mass in the Standard Model.

Is it sensible for the quantum correction be so larger than the physical value? A disturbing large *fine tuning* cancellation between the correction and the tree level value is to be assumed (see figure 1.6).

This is nothing but the usual Hierarchy Problem that has gained a low energy aspect (a "**Little Hierarchy Problem**"), more concretely based on experimental evidence. I traded the Planck mass for a much lower scale Λ but the difficulties are still there. One can call this a paradox, springing from the EW Precision Tests data. Given the rôle of Lep accelerator in EWPT, this can be called "**Lep Paradox**" [9].

Where to look for a solution? As alreasy mentioned, a successful approach to the (usual) Hierarchy Problem is based on SuperSymmetric particles to intervene between the Higgs mass and the New Physics scales. Every quadratic divergent loop diagram is accompanied by another with a superpartner running in the loop (figure 1.7).

Let's then introduce the loops of the stop, whose mass is $m_{\tilde{t}}$, and equation (1.1) becomes:

$$\delta m_H^2(\text{top} - \text{stop}) = -\frac{3}{\sqrt{2}\pi^2} G_F\, m_t^2\, m_{\tilde{t}}^2\, \log\frac{\Lambda^2}{m_{\tilde{t}}^2} = -0.1\, m_{\tilde{t}}^2\, \log\frac{\Lambda^2}{m_{\tilde{t}}^2} \tag{1.2}$$

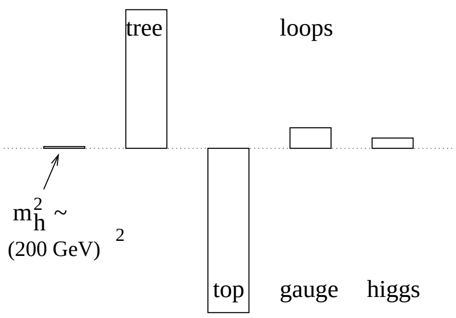

Figure 1.6: The fine tuning required to obtain an acceptable Higgs mass in the Standard Model, computed with cut-off $\Lambda = 10$ TeV. [10]

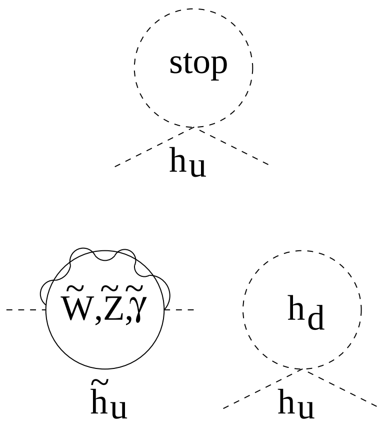

Figure 1.7: The superpartner diagrams of the loops in figure 1.5, cancelling the quadratic divergencies.

which is again divergent, although less severely.

Nevertheless, another "*puzzle*" arises: if one does not want to reproduce the problem, the numbers say that $m_{\tilde{t}}$ should not be much above ~ 200 GeV, which in turn causes other supersymmetric particles to have similar mass ranges [11], and they should have already been discovered at Lep.

This state of embarrassment and dissatisfaction is more or less where we stand.

1.1.4 The ElectroWeak Symmetry Breaking Problem

We have focused on the origin of the ElectroWeak Symmetry Breaking scale, but another aspect of the same problems concerns the *physical mechanism* of EWSB itself. In the Standard Model the spontaneous breaking of the ElectroWeak symmetry is inserted artificially through the parameters μ^2 and λ.

In the Minimal SuperSymmetric Standard Model (MSSM) it is possible to describe the breaking as a radiative effect but this is governed by the soft (SuSy) breaking terms, which must be again somewhat adjusted by hand. This opens one more time the issue of which mechanism realizes the SuperSymmetry breaking...

The open question is: what triggers naturally the ElectroWeak Symmetry Breaking?

1.1.5 Try Extra Dimensions!

Summarizing the qualitative discussions above, one can say that the Standard Model and the MSSM do not provide a theory of ElectroWeak Symmetry Breaking in a two-faced sense: (i) they do not provide an explanation for the origin and the stabilization of the low energy scale (Hierarchy Problem); (ii) they do not provide a satisfactory justification for the mechanism of this breaking (ElectroWeak Symmetry Breaking Problem).

New Physics is kindly asked to yield an answer to both points.

It is in this perspective that the idea of the existence of Extra space Dimensions is worth being pursued. One one hand I will be interested in the framework of the general idea that is successfull in addressing the Hierarchy Problem (see chapter 2 for some details) and in its consequences and limitations. On the other hand I will also present a specific realization of this idea (see also chapter 4 for some details) that is successful in addressing the ElectroWeak Symmetry Breaking Problem.

1.1.6 Down to the SM?

Actually, one can forget all arguments given above and realize that the stronger motivation to study Extra Dimensions comes from turning upside-down the energy scale presented so far. Indeed, we believe that gravity, sooner or later, must be quantized and string/M-theory is the only known candidate to do the job.

"By coincidence", string/M-theory features both Extra Dimensions and SuperSymmetry as corner stones of mathematical consistency. In string theory the extra six-dimensional space is usually thought as squeezed in a manifold of tiny volume, the compactification scale being of the order of the inverse Planck mass. In this case the low energy world (in which we remain interested) would definitely appear as four-dimensional. However, as we will see, this belief can be questioned and the study of low energy theories with Extra Dimensions (with SuSy) receive further motivation.

1.2 Organization of the work

The subject of this thesis are some selected phenomenological aspect of Extra Dimensions.

In chapter 2 I give a brief introduction to the generalities of extra dimensions, focusing on the possible realizations and their usefulness for different problems.

In chapter 3 the framework is that of Compact Gravitational Extra Dimensions; I discuss the phenomenology of neutrino mixing with bulk fermions in the context of supernova physics. The main point is to revise the limits on the size of extra dimensions implied by SN physics, but I will also be interested in the consequences that the existence of Extra Dimensions can carry on SN evolution.

In chapter 4 I shift to the framework of Universal Extra Dimensions and I present the main features of the theory proposed by Barbieri, Hall and Nomura, underlining the motivations for which the theory is worth studying.

In chapter 5 I present a sample calculation (the muon anomalous magnatic moment) in the framework of that theory. The aim is to show an example of its virtue of computability and to assure its compatibility with such a precise experimental datum.

In chapter 6 I present the computation of the Higgs boson production rate via gluon fusion in the framework of the same theory. The output is the discovery of a non trivial suppression of the rate, that is an interesting aspect of the phenomenology of the model.

In chapter 7 I draw some general conclusions.

Chapter 2

Generalities of Extra Dimensions

Motivated by the Introduction above, we are willing to assume that one or more extra space dimensions exist.[1] However, we do not experience more than 3 spatial dimensions in our everyday life and in current physical investigation. Thus the first issue in the physics of Extra Dimensions is of course how to hide them. Two main streams have emerged since the beginning:

- **(Flat) Compactified Extra Dimensions**;
  depending on which fields experience the extra space one can also distinguish:
  - **Gravitational Extra Dimensions** (only the graviton [2] in extra dimensions)
  - **Universal Extra Dimensions** (also SM fields in extra dimensions)
- **Warped Extra Dimensions**.

In theories with extra dimensions, the additional space is usually named "bulk". In the bulk can be embedded a hyper-surface (often a (3+1)-dimensional space) called "brane", on which some fields are possibly confined by some mechanism.

2.1 Compact Extra Dimensions

Each extra dimension is assumed to be compactified on a circle, the radius R of which is the crucial parameter.[3] If the size of the extra dimensions is enough microscopic, the space-time is effectively four dimensional at distances that largely exceed R. Equivalently: experiments probing energies much lower than the compactification scale $1/R$ will see no hint of their presence. A more precise statement on the maximum size allowed depends of course on what physics is extended into the extra space and on which experiments can probe it, as we will see later.

[1] For general reviews on Extra Dimensions see [12].

[2] ...and possibly some SM gauge singlet, see chapter 3.

[3] If more than one extra dimension are present the resulting compactification manifold is a torus that can also be beautifully endowed with a non trivial shape [13].

In general, the physics of Extra Dimensions is effectively described from a 4-dimensional point of view in terms of Kaluza-Klein fields. As a reference, let us consider the case of one extra dimension y, so that the complete set of coordinates in (4+1)-dimensional space time is $x^M = (x^\mu, y)$, $M = (0,1,2,3,5)$, $\mu = (0,1,2,3)$. Every field allowed in the extra dimension is a function of all 5 coordinates: $\Phi(x^\mu, y)$. The compactification implies that the points $y = 0$ and $y = 2\pi R$ are identified so that the wave function of the field is periodic and can be expanded in Fourier series

$$\Phi(x^\mu, y) = \sum_{n \in \mathbb{Z}} e^{in\frac{y}{R}} \phi_n(x^\mu) \tag{2.1}$$

where $\Phi_n(x^\mu)$ are an infinite tower of 4-dimensional (Kaluza-Klein, KK) fields. The kinetic lagrangian term for a 5D massless scalar, for instance, reads

$$\int d^4x\ dy\ \left(\partial_M \Phi^*\ \partial^M \Phi\right) = \int d^4x\ dy\ \left(\partial_\mu \Phi^*\ \partial^\mu \Phi + \partial_5 \Phi^*\ \partial^5 \Phi\right) = \int d^4x \sum_{n \in \mathbb{Z}} \left(\partial_\mu \phi_n^*\ \partial^\mu \phi_n - \frac{n^2}{R^2} \phi^* \phi\right) \tag{2.2}$$

Each KK mode ϕ_n, therefore, can be interpreted as a separate particle with mass $m_n = |n|/R$. At low energies, only massless modes are relevant, while at energies $\sim 1/R$ heavy modes will be produced in collision and take part in physical processes.

2.1.1 Gravitational Extra Dimensions

This framework of Extra Dimensions (the first that was investigated [14]) blossomed from the simple observation that the behaviour of gravitational interaction is not known at distances in the sub-mm range[4]. This opens the possibility that the graviton can experience a certain number δ of extra space dimensions of size up to $\sim 100\ \mu$m.

The general set-up is very simple: all Standard Model fields are (somehow) confined on a 4D brane while the graviton is free to propagate in all the $4 + \delta$ dimensions. The extra ones are compactified on circles of radii R_i.

The Hierarchy Problem is solved (as mentioned in 1.1.2) thanks to the volume of the extra space: the only fundamental scale is $M_* \sim$ TeV while the hugeness of the Planck mass is produced by

$$M_{Pl}^2 = \prod_{i=1}^{\delta} (2\pi R_i M_*)\ M_*^2\,. \tag{2.3}$$

This formula is simply obtained from the consistency of the Gauss law in 4D and in $4+\delta$ dimensions. The Newton potential at distances smaller than the compactification radius is modified and goes with r like $1/r^{1+\delta}$ instead of $1/r$.

A lot of different physical processes have to be considered in order to guarantee the experimental viability of such a scenario. Schematically, relevant constraints or confirmations can come from (besides of course the detection of a modification of Newton law at small distances):

[4]See [15] for the latest results.

- **collider physics** [16, 18, 19], via the phenomenon of graviton production and virtual exchange or even, since the gravity scale is lowered to TeV, black hole production;

- **astrophysics** [16, 48], since the cooling of Supernovae must not be unacceptably accelerated by KK graviton emissions; this turns out to be one of the most stringent constraints in the case that all extra dimensions have the same size (at least 3 extra dimensions are needed), but can be relaxed if the radii are allowed to be different;

- **cosmology** [16, 58], from the fact that relic KK gravitons must not be so numerous to over-close the universe and from the fact that KK gravitons can "come back" from the bulk and decay giving an unobserved distorsion of the photon spectrum; again these severe limits can be eased in models with enough extra dimensions or with a non degenerate structure of radii.

Moreover, one can investigate the modifications induced by KK gravitons in rare decays [16], ultra high energy cosmic ray physics [20], other astrophysical issues such as the additional heating of neutron stars [16], other cosmological points including Big Bang Nucleosynthesis [58] and so on.

In short, one can state that all phenomenological tests are passed, with the fundamental scale still fixed at $M_* \sim$ TeV (to solve the Hierarchy), at least paying the price of some uncomfortable flexibility in the constructions.

Probably the most important criticism to the Compact Extra Dimensions picture is related to the determination and stabilization of the compactification radii. In a sense, one introduces a new unmotivated hierarchy between the fundamental scale $M_* \sim$ TeV and the compactification scale of the extra dimensions ($\sim 10^{-3}$ eV when $R \sim 100\ \mu$m). Although the embedding in some string theory can support certain choices (see [17]) [5,6], the need for a more fundamental theory that can predict such structures is still alive.

2.1.2 Universal Extra Dimensions

Perhaps the most interesting realizations of theories with extra dimensions are the models in which also the fields of the Standard Model or MSSM propagate in the bulk.[7] Many possible variations on this theme have been implemented, particularly regarding the choice of the fields allowed in the bulk (all SM/MSSM fields, only gauge bosons with all or some matter fermions confined on a brane, only Higgs bosons...) but I argue that some general aspects can be outlined:

- the size of the extra dimensions have to be much smaller than the case where only gravity is higher dimensional, since of course ElectroWeak interactions are probed at much smaller distances; the

[5] The stabilization of the radii (seen as dynamical scalar fields) at large values requires very flat potentials, for which SuperSymmetry can help. One more time, SuperSymmetry (which fortunately is part of string theory) should better enter the game.

[6] Applying string theory to cosmology ("brane gas cosmology"), one can even aim to explain why 3+1 dimensions are allowed to expand while others remain compactified, and even also to set a non trivial morphology for the extra dimensions, see [21].

[7] For just some examples see [22, 23, 24, 25, 26].

typical compactification energy must indeed be larger than $\sim few{\cdot}100$ GeV $\div 1$ TeV, corresponding to radii smaller than $\sim 10^{-17}$ cm; [8]

- the focus here is not on a solution of the Hierarchy Problem but on possible beneficial effects with respect to other problems of the Standard Model or MSSM (flavour physics, ElectroWeak Symmetry Breaking, SuperSymmetry Breaking, neutrino masses, unification...), more in the spirit of the discussion developed in sections 1.1.3 and 1.1.4; gravitational interactions are not of interest here, as in usual ElectroWeak physics;

- the models usually need only one extra dimension, that is often compactified on $\mathbb{S}^1/\mathbb{Z}_2$; this structure is called an orbifold: a $\mathbb{Z}_2$ symmetry is introduced under which $y \to -y$ and all 5D fields are either even or odd;

- the chosen "reference model" (SM, 2HDSM, MSSM, NMSSM...) is usually reproduced by the zero modes of the KK fields.

I will concentrate on a specific realization [28] presented in chapter 4.

2.2 Warped Extra Dimensions

An alternative scenario [29, 30] that does not suffer of the residual hierarchy highlighted in section 2.1.1 can be built with a single extra dimension accessible to the graviton, provided that the metric of the space time distinguishes between the four traditional coordinates and the additional one. Indeed, the 4-dimensional metric is multiplied by a "warp" factor, a rapidly changing (exponential) function of the extra coordinate:

$$ds^2 = e^{-2k|y|}\eta_{\mu\nu}dx^\mu dx^\nu + dy^2 \tag{2.4}$$

where k is a free factor for the moment. The additional dimension is contained between two branes located at $y = 0$ and $y = \pi r_c$. This metric is a solution of Einstein equations provided that the tension on each brane is opposite in sign and equal to $24M_\star^3 k$ (where $M_\star$ is the only fundamental scale of the theory, which we assume to be of order of 10^{19} GeV) and the bulk is endowed with a negative cosmological constant, thus corresponding to a slice of Anti-de Sitter space. The value of the cosmological constant is fine tuned to the value $\lambda = -24M_\star^3 k^2$.

The Hierarchy Problem is solved thanks to the exponential factor in the metric. Indeed, any mass parameter (or energy scale) m_0 in the fundamental theory will generate a physical mass $m = e^{-\pi k r_c}\, m_0$ in the 4D theory; in particular, the 5-dimensional fundamental scale $M_\star$ produces the TeV scale of ElectroWeak interactions if only $kr_c \approx 50$. On the other hand, the old (4-dimensional) Planck mass is produced from $M_\star$ with only a slight dependance on the extra space: $M_{Pl} = (M_\star^3/k)(1 - e^{-2\pi k r_c})$.

[8] Of course hybrid models are possible, where some large extra dimensions are accessible to gravity and some smaller ones to the SM fields [27].

The message is that one can generate the Hierarchy and keep the extra space concealed at the same time, without introducing very large or very small numbers: it holds $M_\star \sim k \sim 50/r_c$. The picture is perfectly consistent with $r_c \to \infty$ [31], therefore opening the way to infinite, non-compact extra dimensions.[9]

This field is very active and developed several different directions, but my main focus from here on will be on the Compact Extra Dimensional scenario.

[9]Notice that in this case the focus is no more on the Hierarchy Problem.

Chapter 3

Limits on Extra Dimensions from Supernovae

In this chapter (based on ref. [42]) I focus on models with Gravitational Extra Dimensions, of which the general features have been described in section 2.1.1.

The firm points are the following:

- the fundamental scale M_* is set at ~ 1 TeV,
- I consider a single compact extra dimension (with flat metric),
- the Standard Model fields are confined on a brane while
- the graviton propagates in the bulk.

On top of this, the fundamental observation is that it is very natural to allow also the propagation of **fermionic fields in the extra dimension**. This can be supported in several ways, but the two most important points are the following:

1. ("bottom-up") once the existence of the Extra Dimension has been postulated, any field which is a singlet under the Standard Model gauge group (not only the graviton) has no reason to be confined on the brane; the most natural candidate is the right handed neutrino, a fermion;
2. ("top-down") if extra dimensions are inspired and implied by string/M theory, then several scalars are inevitably present in the bulk (e.g. the moduli that fix the internal radii); if scalars live in the bulk then also their fermionic superpartners do, since SuperSymmetry is also implied in string theory.

With an obvious extension of terminology, we will call these fermionic fields "bulk neutrinos" or "neutrinos from extra dimensions".

3.1 Overview

Sterile neutrinos from extra dimensions are not likely to play a primary role in atmospheric and solar neutrinos [43]. On the contrary, astrophysics, cosmology and rare decays still represent natural stages for their exotic performances. In this discussion, we focus on the implications of a possible mixing of the electron neutrino with a Kaluza-Klein tower of sterile neutrinos in supernova (SN) physics.

The potential relevance of bulk fermions for neutrino physics has first been pointed out and analyzed in [44, 45]. Fermions propagating in large extra dimensions appear as light, dense KK towers of sterile neutrinos in 4 dimensions, possibly mixing with the Standard Model ones.

The basic ideas about supernova explosion and cooling, nicely confirmed by the neutrino signal from SN 1987A [46], translate into significant constraints on the energy loss through invisible channels [47]. In fact, in order for the observed neutrino signal to be accounted for, the invisible energy loss should not cool the protoneutron star on a time scale shorter than about 10 seconds. The bulk of a large extra dimension provides at least two interesting examples of invisible channel: KK graviton emission [16, 48] and mixing of Standard Model and bulk neutrinos, the possibility we are interested in. With respect to the case of a single sterile neutrino [49], conversion into KK towers of sterile neutrinos is enhanced by the higher number of available states and especially by matter effects [50]. The constraints that follow on the parameter space of bulk neutrino models look at first sight quite severe [50]. However, those constraints are relaxed by an interesting feedback mechanism[1] that prevents unacceptable energy loss [52] and affects the protoneutron star deleptonization and cooling through a non trivial interplay with diffusion. By suppressing the neutrino MSW potential and then making it negative everywhere, the mechanism leads to a self-limiting of the potentially dangerous, MSW-enhanced, energy loss into the bulk and requires a revisitation of the bounds in the literature. The consequences for SN physics, in particular explosion, deleptonization, cooling and spectra, are not less interesting. From this point of view what we discuss here is an example of how the standard ideas about the protoneutron star evolution can be affected in presence of new physics in an unexpected and intriguing way.

This chapter is structured as follows. In Section 3.2 we shortly review the salient points about (electron) neutrino oscillations into bulk neutrinos. Section 3.3 is the central part of this chapter. Since a reliable study requires taking into account diffusion, we first set up in Section 3.3.1 a toy model of the protoneutron star core which, although minimal, contains all the neutrino transport physics relevant to our discussion. In Section 3.3.2 we incorporate in the model the effect of electron neutrino and antineutrino conversion into bulk neutrinos. The effect on the evolution of the protoneutron star core is described in Section 3.3.3. The consistency with SN 1987A is shown in Section 3.3.4, where the implications for the neutrino luminosity, the flux spectrum and the shock reheating are also discussed. Section 3.4 summarizes the constraints on subleading non self-limiting conversion probabilities, that provide one of the relevant bounds on our parameter space. We conclude in Section 3.5.

[1] A different type of feedback was considered in [51].

3.2 Framework

3.2.1 The supernova

Before embarking in the detailed analysis, let us shortly and qualitatively review the standard ideas about SN explosion and cooling [53, 54].

Type II Supernovae originate from evolved, massive stars whose iron core reaches the Chandrasekhar limit and collapses under gravitational pressure. During the collapse, neutrinos start to be produced by electron capture and get trapped when densities of order $10^{12}\,\mathrm{g\,cm^{-3}}$ are reached. The inner part of the iron core has an homologous collapse that stops when, after a fraction of a second, stiff nuclear densities of order $\rho_0 = 3 \cdot 10^{14}\,\mathrm{g\,cm^{-3}}$ are reached. The free falling outer material then builds up a shock that propagates outwards. It is believed that this "prompt" shock has not enough energy to give rise to a successful explosion and hence stalls after $\sim 0.1\,\mathrm{sec}$ at a radius of order 100 km. Below the shock, the protoneutron star has a high density inner part, the inner core, with a radius of 10–30 km and a bloated outer part, the mantle, that accretes mass falling through the shock. Let us leave for a moment the shock to its uncertain fate and follow the evolution of the protoneutron star below it. Most of the gravitational binding energy of the progenitor star, a few 10^{53} erg, is stored there. Only $\mathcal{O}(1\%)$ out of that will go into explosion kinetic energy or electromagnetic radiation. Most of it will be released through neutrino emission in a few tens of seconds.

The stiff inner core has a mass of order of the solar mass, $M_\odot \simeq 2 \cdot 10^{33}\,\mathrm{g}$, a density of order ρ_0, a temperature of 10–30 MeV and a lepton fraction per baryon $Y_L \sim 0.35$. Electrons and electron neutrinos are highly degenerate in such conditions, with Fermi momenta of order 300 and 200 MeV respectively. The mean free path of a 200 MeV neutrino is $\lambda \sim 10\,\mathrm{cm}$. This determines the time scale for neutrino diffusion and emission: $t_{\text{diff}} \sim 3R^2/\lambda \sim 10\,\mathrm{sec}$ for a neutrino at a depth $R = 10\,\mathrm{km}$ in the inner core. Analogously, the total neutrino flux and spectrum can be roughly estimated from the knowledge of the star structure and temperature where neutrinos experience their last energy exchange. The mantle looses most of its lepton number, accretes most of its mass, cools and contracts in only 0.5–1 sec. Then, as it cools, the whole protoneutron star slowly contracts to a radius of order 10 km. After a few tens of seconds, we are left with a proper neutron star.

Since supernovae do explode, we can be confident that the shock has in the meanwhile successfully expelled the outer matter. An important contribution to the revival of the stalled shock is given by the energy deposition of the neutrino flow. A $\mathcal{O}(1\%)$ fraction of the energy flowing might be enough to give rise to a sufficiently energetic explosion a second or so after collapse. Critical are of course the efficiency of the energy transfer mechanism and the intensity of the neutrino source.

Although this "delayed shock" mechanism is currently believed to play an important role, reproducing the explosion in computer simulations it is still non trivial at present [55]. This does not necessarily mean that something is missing in our general understanding. The problem is likely to originate from the complexity of the system to be modeled and the variety of the physics involved. It may just be necessary to turn to full 3D simulations able to account for non-spherically symmetric effects. Convection is likely to be important in this context, since it may boost the neutrino luminosity. Still, it is worth pointing out that the new physics and mechanism we discuss in this chapter might also play an important role by enhancing the neutrino luminosity. This will be discussed in Section 3.3.4.

The basic ideas about protoneutron star deleptonization and cooling have been nicely confirmed by the observation of a neutrino signal in the Superkamiokande and IMB detectors in coincidence with SN 1987A [46]. Despite the low statistics, there is definitely a significant agreement between the measured neutrino flux duration and intensity and the estimates above. This allows to set limits on drastic departures from the described picture, in particular on invisible energy loss channels that would waste the available energy on timescales shorter than 10 sec.

3.2.2 Bulk neutrinos and feedback

We consider a Kaluza-Klein (KK) tower of sterile neutrinos living in the bulk of a single, large, flat, gravitational extra dimension. Additional smaller dimensions will be in general present. What we consider is therefore an effective theory valid up to scales below the inverse scales of the smaller dimensions. The physics we are interested in involves bulk neutrinos with masses within $\sim 100\,\mathrm{keV}$. We therefore assume that the inverse scale of the additional smaller dimension is larger than $100\,\mathrm{keV}$ and neglect them in the following.

As for the size R of the extra dimension we consider, we only require it to be in the range

$$10^{-3}\,\mathrm{eV} \lesssim \frac{1}{R} \lesssim 1\,\mathrm{keV}\,. \tag{3.1}$$

The lower bound comes from tests of the Newton's law at small distances[2] and the origin of the upper bound, as well as the bounds below, will become clear by the end of the section.

Apart from R, which gives their density of states, all we need to know about bulk neutrinos is their mixing with the electron neutrino. We assume that the mixing θ_k of ν_e with the (almost) sterile k-th mass eigenstate N_k is inversely proportional to its mass M_k,

$$\theta_k \simeq \frac{m}{\sqrt{2}M_k}\,, \tag{3.2}$$

a generic feature of most models in the literature [44, 45, 50, 52, 56, 57]. Eq. (3.2) defines the mixing parameter m.[3]

We are interested in a range for m such that $mR \ll 1$, which ensures that all mixings θ_k are small, and

$$10^{-12}\,\mathrm{eV} \lesssim m^2R \lesssim 10^{-4}\,\mathrm{eV}\,. \tag{3.3}$$

[2] Depending on the specific model and on the scale of the mixing term m in eq. (3.2) below, it may be necessary to strengthen the lower bound to $1/R \gtrsim 10^{-1}\,\mathrm{eV}$ in order to avoid undesired effects in solar and atmospheric neutrino experiments. In fact, for $1/R \lesssim 10^{-1}\,\mathrm{eV}$, the first modes of the KK tower may participate to oscillations if their masses are given by n/R, $n = 0, 1, 2, \ldots$. This is not the case in presence of a Dirac or Majorana bulk mass μ, since in this case all bulk neutrinos are heavier than μ [56, 52]. Values of $1/R$ as low as $10^{-3}\,\mathrm{eV}$ would then be automatically compatible with not having effects in the observed oscillation signals. Provided that $\mu \ll \mathrm{keV}$, such a mass term would not affect SN physics.

[3] The exact dependence of M_k on $1/R$ may depend on the specific model. We only assume the density of states dk/dM to be R at scales around $10\,\mathrm{keV}$. The parameter m usually originates from Yukawa interactions involving the 5D neutrino, the lepton doublet and an Higgs field.

The parameter m^2R sets the scale of all the effects we discuss. The upper bound ensures the smallness of the transition probabilities over a mean free path and values of m^2R smaller than the lower bound give unobservable effects. The range in eq. (3.3) is further restricted by the expectation that subleading contributions to the oscillation probability give rise to the bound $mR \lesssim 10^{-5}$, as we will discuss in Section 3.4. Together with the upper bound on $1/R$, the latter gives $m^2R \lesssim 10^{-8}\,\mathrm{eV}$. We will therefore concentrate on the first four orders of magnitude of the range (3.3).

For appropriate sizes of the volume associated to the smaller dimensions, all values of $1/R$, m^2R in the ranges above are consistent with the relation $(M_{\mathrm{Pl}}/M_*)^2 = \prod_i 2\pi R_i M_*$ between the volume of the extra space with the 4D Planck mass, for appropriate sizes of the smaller dimensions. At the same time, those values are compatible with cosmological and astrophysical bounds from KK graviton production before Big-Bang nucleosyntesis [58] and in supernovae [16, 48].

Having described the neutrino parameter space, we now discuss neutrino oscillations in the inner core of the protoneutron star. Oscillations are dominated by matter effects. While bulk neutrinos are sterile and therefore unaffected by matter, the electron neutrinos acquire an effective squared mass $m^2_{\mathrm{eff}} = 2EV$, where

$$V = \sqrt{2} G_{\mathrm{F}} n_B \left(\frac{3}{2} Y_e + 2 Y_{\nu_e} - \frac{1}{2} \right) \tag{3.4}$$

is the MSW matter potential, n_B is the baryon number density and $Y_{e,\nu_e} = n_{e,\nu_e}/n_B$ is the number fraction of e, ν_e per baryon. More precisely, $n_{e,\nu_e} = N_{e^-,\nu_e} - N_{e^+,\bar{\nu}_e}$ denotes the difference of the particle and antiparticle number densities. Also, we denote by Y_L the total lepton fraction $Y_e + Y_{\nu_e}$.

The neutrino contribution to V is important in the inner core. Also important is the negative contribution from neutrons, that allows the potential to have both signs, as shown in Fig. 3.1. According to the sign of the potential, matter effects will enhance neutrino or antineutrino disappearance in the bulk.

The MSW potential ranges between $-10\,\mathrm{eV}$ and $5\,\mathrm{eV}$. Correspondingly, in the early stages of evolution, most electron neutrinos have an effective mass in the range

$$(10\,\mathrm{keV})^2 \frac{E}{100\,\mathrm{MeV}} \lesssim m^2_{\mathrm{eff}} \lesssim (50\,\mathrm{keV})^2 \frac{E}{100\,\mathrm{MeV}}\,,$$

where E is the neutrino energy, as shown in fig. 3.2. A resonance is met when the effective mass matches the mass of a state in the KK tower. The condition $mR \ll 1$ ensures that the width of the resonance is small compared to the distance between levels.

When an electron neutrino emerges from an interaction in the inner core, its mixing with the massive states in the KK tower depends on its effective mass m_{eff} and therefore on the values of n_B, Y_e, Y_{ν_e} where the interaction took place. If V is positive, ν_e is predominantly made of the mass eigenstate N_k such that $M_k < m_{\mathrm{eff}} < M_{k+1}$, with only a small component from the other eigenstates[4]. If $V < 0$, on the other hand, ν_e does not mix with the sterile states — the mixing takes place in the antineutrino sector in this case. After its interaction, the neutrino travels a distance of order of its mean free path, say

[4]This is always true except when m_{eff} coincides with some M_k within a resonance width. In such a case, ν_e will predominantly be made by a superposition of N_k and N_{k+1}. See [52] for a detailed discussion of mixing.

about 10 cm, before experiencing the next interaction. Let us determine the probability $P(\nu_e \to \text{bulk})$ that the electron neutrino has in the meanwhile oscillated into a bulk neutrino assuming that V is positive. If V is negative, the probability is negligible and what below applies to antineutrinos. Over 10 cm, the values of n_B, Y_e, Y_{ν_e} change only slightly, but the corresponding change in the effective mass may be sufficient for the neutrino to predominantly mix with a different mass eigenstate N_h. The dominant contribution to the disappearance probability $P(\nu_e \to \text{bulk})$ is then given by the probability that N_k has not turned into N_h. This level "non-crossing" probability can be computed by means of the Landau-Zener formula [45]

$$P(\nu_e \to \text{bulk}) \simeq 1 - e^{-\frac{\pi}{2}|\Delta n|\gamma} \simeq \frac{\pi}{2}|\Delta n|\gamma\,, \tag{3.5}$$

where Δn is the number of levels crossed, γ is the adiabaticity parameter and we assumed $P(\nu_e \to \text{bulk}) \ll 1$, as follows from $m^2R \ll 10^{-4}\,\text{eV}$ (for $P(\nu_e \to \text{bulk}) \sim 1$, the analysis is complicated by non linear effects and back conversion of bulk neutrinos into ν_e). The Landau-Zener formula can be extended to the case of multiple resonances because the latter are well separated.

The adiabaticity parameter is given by

$$\gamma = \frac{m^2V}{E(\partial V/\partial r)\cos\phi}\,, \tag{3.6}$$

where ϕ is the angle between the neutrino momentum and the radial direction. The number of levels crossed over a distance L is[5]

$$\Delta n = \frac{\partial V}{\partial r}\frac{RE}{m_{\text{eff}}}\,L\cos\phi\,. \tag{3.7}$$

We therefore conclude that

$$P(\nu_e \to \text{bulk}) \simeq \theta(V)L\,\frac{\pi}{2\sqrt{2}}m^2R\left(\frac{|V|}{E}\right)^{1/2} \tag{3.8a}$$

$$P(\bar\nu_e \to \text{bulk}) \simeq \theta(-V)L\,\frac{\pi}{2\sqrt{2}}m^2R\left(\frac{|V|}{E}\right)^{1/2}\,. \tag{3.8b}$$

The step function θ accounts for the fact that neutrinos (antineutrinos) do not cross any resonance if $V < 0$ ($V > 0$). Correspondingly, we have neutrino disappearance for $V > 0$ and antineutrino disappearance for $V < 0$. The probabilities depend on the neutrino parameters only through m^2R, to which they are proportional. The upper bound in eq. (3.3) ensures that $P(\nu_e \to \text{bulk}) \ll 1$.

In obtaining the previous equation, we have approximated the electron neutrino with the mass eigenstate of which it is predominantly made. Additional subleading contributions to $P(\nu_e \to \text{bulk})$ come from the small mixing with the neglected eigenstates, that amount to a fraction of order mR of the electron neutrino. Their effect will be discussed in Section 3.4.

Let us now discuss the motivation for restricting the range of $1/R$ to $1/R \lesssim$ keV. The number of resonances crossed in a mean free path can be estimated from eq. (3.7). Roughly speaking, for $1/R \lesssim$ eV

[5] For $1/R \gtrsim 1\,\text{eV}$, not all neutrinos cross a resonance and Δn should be considered as the average number of level crossed (see below).

most neutrinos are likely to cross at least a resonance in a mean free path — hundreds in the lower part of the allowed range. For $1/R \gtrsim$ eV, on the other hand, resonances are met only by neutrinos with energies within $\pm\delta E$ from a set of discrete values $E_k = M_k^2/(2V)$ in which $m_{\rm eff} = M_k$. The discrete values E_k are separated by $\Delta E_k = M_k/(RV)$. When $1/R \gtrsim$ eV, $\delta E = EL\cos\phi(\partial V/\partial r)/V$ is smaller than the separation ΔE_k and the resonances are not crossed for arbitrary values of the energy anymore. However, there will always be neutrinos crossing a resonance as long as some of the energies E_k fall in the neutrino spectrum. The condition $1/R \lesssim 1\,\text{keV}$ ensures that there are at least 20–50 points in the spectrum where neutrinos cross a resonance at the beginning of the evolution. It also ensures that there will be a few wells in the spectrum even when, at later stages, the product $V \cdot E$ will decrease by a factor 1000.

We now have all the ingredients to understand how ν_e conversion in the inner core tends to draw the MSW potential to zero everywhere through a feedback mechanism. Let us consider a region in the inner core where the MSW potential is positive. Eq. (3.8) shows that the neutrino conversion probability is proportional to $\sqrt{V}$. On the other hand, once a neutrino has been lost in the bulk, V decreases. This is because $V \propto 3Y_e/2 + 2Y_{\nu_e} - 1/2$. As a consequence of the loss, the electron and electron neutrino number densities will readjust to restore β equilibrium, but $3Y_e/2 + 2Y_{\nu_e}$ will certainly decrease. The more neutrinos are lost in the bulk the smaller V becomes. It may happen, and we will see that it does happen, that V approaches zero before all the lepton number and energy are lost. At this point the neutrino conversion through the MSW enhanced probability (3.8a) stops. In the region where the potential is negative, antineutrino escape would take place (at a much slower rate) drawing again the potential toward zero. As we will see, the possibility of reaching zero depends in this case on the local values of the thermodynamic variables.

The effect we are dealing with is potentially quite interesting. Besides limiting the energy loss, in fact, the condition $V = 0$ represents an important constraint on the relative abundances, with significant implications for the SN phenomenology. However, several issues have to be addressed. First of all, the $V = 0$ condition is spoiled by neutrino diffusion, which tends to lower V below zero. Antineutrino conversion into bulk neutrinos then tends to bring V back to zero at the expenses of an additional energy loss. The actual evolution will be determined by an interplay of diffusion and conversion. Moreover, it has to be proven that the mechanism is compatible with SN 1987A observation. Does the inner core loose all its lepton number and energy in the attempt of reaching the $V = 0$ condition? Or while neutrinos try to diffuse out? How quickly is the condition approached? Is the escape of the rare antineutrinos efficient enough? Qualitative arguments are not sufficient to reliably address the issues above, not to mention attacking the problem of implications for possible future SN observations. On the other hand, a full, detailed simulation of the protoneutron star evolution is clearly beyond the scope of this discussion. We therefore set up in the next section a toy model of inner core evolution which only incorporates the basic ingredients of neutrino diffusion but contains all the physics relevant to our study.

3.3 Inner core evolution

3.3.1 Standard evolution: equations and assumptions

We now discuss the equations we use to model the evolution of the inner core. We start from the case of no mixing with bulk neutrinos. We concentrate on the inner core because the bulk of energy and lepton number is stored there. Moreover, the loss rates and the effectiveness of the feedback on the MSW potential are highest in the core. That is because the neutrino densities are large and because the transition probability in eqs. (3.8) grows with the potential, which is proportional to the baryon density[6].

Focusing on the inner core has also practical advantages. Unlike the mantle, the core settles into local thermodynamic equilibrium very quickly after the collapse. The hydrodynamics is also much simpler, with the mass profile becoming essentially constant in a few hundreds milliseconds [54]. The mantle of the protoneutron, on the other hand, accretes matter for the first 0.5–1 sec and then slowly contracts.

Assuming thermodynamic equilibrium and neglecting general relativity effects, the basic equations of neutrino transport in absence of mixing are [59]

$$n_B \frac{\partial Y_L}{\partial t} = -\vec{\nabla} \cdot \vec{F}_L \tag{3.9a}$$

$$n_B T \frac{\partial s}{\partial t} = -\vec{\nabla} \cdot \vec{F}_\epsilon + \mu_\nu \vec{\nabla} \cdot \vec{F}_L \,, \tag{3.9b}$$

where s is the entropy per baryon and $\vec{F}_L = \vec{F}_\nu - \vec{F}_{\bar{\nu}}$, $\vec{F}_{\epsilon_L} = \vec{F}_{\epsilon_\nu} + \vec{F}_{\epsilon_{\bar{\nu}}}$ are the lepton number and lepton energy density currents respectively. The neutrino currents are

$$\vec{F}_\nu = -\frac{1}{3} \sum_{\nu=\nu_e,\nu_\mu,\nu_\tau} \int \frac{d\vec{p}}{(2\pi)^3} \lambda_\nu(E) \vec{\nabla} f_\nu(E) \tag{3.10a}$$

$$\vec{F}_{\epsilon_\nu} = -\frac{1}{3} \sum_{\nu=\nu_e,\nu_\mu,\nu_\tau} \int \frac{d\vec{p}}{(2\pi)^3} E\, \lambda_\nu(E) \vec{\nabla} f_\nu(E) \,, \tag{3.10b}$$

where $\vec{p}$ is the neutrino momentum, $E = p$ is the neutrino energy, λ_ν is the neutrino mean free path (mfp), which also depends on the local thermodynamic variables, and f_ν is the Fermi-Dirac distribution, $f_\nu(E) = (e^{(E-\mu_\nu)/T} + 1)^{-1}$, which depends on the temperature T and the neutrino chemical potential μ_ν. Analogous expressions hold for antineutrinos with $\mu_\nu \to -\mu_\nu$. We assume that muon and tau neutrinos have vanishing chemical potential[7]. As a consequence, they do not contribute to the lepton number current and only give a thermal contribution to the energy current. The neutrino chemical potential, as the electron, neutron and proton ones, μ_e, μ_n and μ_p, can be obtained in terms of the thermodynamic variables T, Y_L and ρ (ρ is the mass density), by solving the equilibrium equation

[6] The transition probability goes with $(V/E)^{1/2}$, where E also grows with the baryon density n_B. However, $V \propto n_B$, whereas $E \propto n_B^{1/3}$.

[7] Given the high energies involved, a non-vanishing number of muons could participate to the inner core life, giving a non-vanishing chemical potential.

$\mu_e - \mu_\nu = \mu_n - \mu_p$. Since we do not solve the whole protoneutron star evolution, we also have to specify boundary conditions for eqs. (3.9). We approximate them by imposing that the lepton number and energy fluxes at the border are proportional to the neutrino number and energy density. We assume spherical symmetry.

The transport equations (3.9) for Y_L and T incorporate all the physics we are interested in before inclusion of non-standard effects. Their solution however requires i) the knowledge of the mean free paths, ii) the knowledge of the equation of state, which enters the equilibrium condition and the entropy, and iii) the determination of the density $\rho(r,t)$. In order to prune our considerations from unnecessary complications and concentrate on the transport physics of eqs. (3.9), we address the three points above in the simplest possible way. First of all, we take advantage of the hydrodynamic stability of the inner core by using a constant (in time) density profile $\rho(r)$. As for the equation of state, we consider a core made only of n, p, $e^\pm$, $\nu_{e,\mu,\tau}$, $\bar{\nu}_{e,\mu,\tau}$, γ and we take into account the strong nuclear interactions through a modified dispersion relation for the nucleons. That is, the nucleons are approximated as a perfect Fermi gas, with an effective mass m_N^* carrying a dependence on the state variables. A detailed calculation of m_N^* has to rely on some effective theory of nucleon-nucleon interaction and, in general, will deviate substantially from the vacuum value $m_N = 939\,\mathrm{MeV}$. The result of such theories can be reproduced by a simple expression carrying only a dependence on the medium density [53]

$$m_N^* = \frac{m_N}{1 + \beta_0\ \rho/\rho_0} \tag{3.11}$$

where β_0 is chosen to be 0.5 and $\rho_0 = 3\ 10^{14}\ \mathrm{gr/cm^3}$ is the reference nuclear density.

Finally, we have to define a prescription for the mean free path of neutrinos of different flavors. For electron neutrinos the most important contributions to the opacity come from the absorption reaction $\nu_e + n \to e^- + p$ and from the scattering on neutrons. Scattering on protons and, to a smaller extent, on electrons, are also sizable. For ν_μ's and ν_τ's, only the scattering reactions are important. A detailed analysis of neutrino opacities should take into proper account the cross sections for these and several other subleading processes, as well as the status of the nuclear matter (degenerate or non-degenerate nucleons, consequent Fermi blocking effects), the nucleon-nucleon interactions, the multicomponent nature of dense matter (e.g. the presence of hyperons), etc. For a comprehensive discussion on this subject we refer the reader to [60] and references therein. For our purposes, it is sufficient to model the neutrino mean free path with a simple inverse quadratic dependence on the neutrino energy

$$\lambda_{\nu_e}(E) = \lambda^0_{\nu_e}\frac{E_0^2}{E^2}\,, \qquad \lambda_{\nu_\mu,\nu_\tau}(E) = \lambda^0_{\nu_\mu,\nu_\tau}\frac{E_0^2}{E^2}\,, \tag{3.12}$$

where we take $\lambda^0_{\nu_e} = 1.2$ cm and $\lambda^0_{\nu_\mu,\nu_\tau} = 4.8$ cm at the reference energy $E_0 = 260\,\mathrm{MeV}$. The values of $\lambda^0_{\nu_e}$ and $\lambda^0_{\nu_\mu,\nu_\tau}$ determine the diffusion time scale. When compared with the exact general expression of ref. [60] (taken at typical density, temperature and leptonic fraction), the above proves to be a good approximation for the upper portion of the range of neutrinos' energies of our interest while it turns out to be poorer in the lower part. Moreover, the above choices yield an evolution whose timescale agrees with the results of more sophisticated analysis [61].

With the choice above on the energy dependence of the mean free paths and setting $\lambda_{\bar\nu} = \lambda_\nu$ in the small antineutrino contribution, one finds the simple expressions

$$-\vec{F}_L = a_e \vec{\nabla}\mu_\nu \, , \qquad -\vec{F}_{\epsilon_L} = \frac{a_e}{2}\vec{\nabla}\mu_\nu^2 + (a_e + a_\mu + a_\tau)\frac{\pi^2}{6}\vec{\nabla}T^2 \, , \tag{3.13}$$

where $a_i = \lambda^0_{\nu_i} E_0^2/(6\pi^2)$, $i = e, \mu, \tau$.

3.3.2 Neutrino escape into the bulk

Eqs. (3.9,3.13), together with the equilibrium equations and the boundary conditions represent our simplified model of inner core deleptonization and cooling in absence of non standard dynamics. We now incorporate the effect of neutrino and antineutrino escape in the bulk.

Electron neutrinos with energy E contribute to the lepton number loss rate by $\langle P\rangle/\lambda$ each, where $P = P(\nu_e \to \text{bulk})$ and "$\langle\rangle$" indicates an average over the distance traveled L.[8] Since in our case the probability is linear in L, we simply have $\langle P\rangle/\lambda = P/L = \theta(V)\pi/(2\sqrt{2})m^2 R(|V|/E)^{1/2}$. The total neutrino number loss rate Γ_ν follows from integration over neutrino momenta and can be written by means of the Fermi integrals F_α as

$$\Gamma_\nu = \frac{\theta(V)}{4\sqrt{2}\pi} m^2 R\sqrt{|V|}T^{5/2}F_{3/2}\left(\frac{\mu_\nu}{T}\right) , \quad \Gamma_{\epsilon_\nu} = \frac{\theta(V)}{4\sqrt{2}\pi} m^2 R\sqrt{|V|}T^{7/2}F_{5/2}\left(\frac{\mu_\nu}{T}\right) ,$$
$$F_\alpha(y) = \int_0^\infty dx \frac{x^\alpha}{e^{x-y}+1} \, . \tag{3.14}$$

Analogously for antineutrinos. Putting all together, we find the following modified evolution equations for Y_L and T:

$$n_B \frac{\partial Y_L}{\partial t} = \vec{\nabla}\cdot(a_e\,\vec{\nabla}\mu_\nu) - \frac{\sigma}{4\sqrt{2}\pi} m^2 R\sqrt{|V|}\; T^{5/2}F_{3/2}\left(\sigma\frac{\mu_\nu}{T}\right) \tag{3.15a}$$

$$n_B T\frac{\partial s}{\partial t} = a_e\left(\vec{\nabla}\mu_\nu\right)^2 + \vec{\nabla}\cdot\left((a_e + a_\mu + a_\tau)\frac{\pi^2}{6}\vec{\nabla}T^2\right)$$
$$- \frac{1}{4\sqrt{2}\pi} m^2 R\sqrt{|V|}\; T^{7/2}\left(F_{5/2}\left(\sigma\frac{\mu_\nu}{T}\right) - \sigma\frac{\mu_\nu}{T}F_{3/2}\left(\sigma\frac{\mu_\nu}{T}\right)\right) , \tag{3.15b}$$

where $\sigma = \text{sign}(V)$. We recognize in eq. (3.15b) the heating term $a_e(\vec{\nabla}\mu_\nu)^2$ associated to the degradation of the degeneracy energy of the neutrinos reaching regions with lower chemical potential. This term partially originates from the chemical potential contribution to $T\,ds$. With the same origin, there is a heating term in the energy loss part proportional to $F_{3/2}$ that can overcome the cooling term proportional to $F_{5/2}$. In this case the temperature increases because of the degradation of the degeneracy energy of neutrinos at the Fermi surface that downscatter to replace neutrinos inside the Fermi sphere escaped in the bulk.

[8] Note the difference between $\langle P\rangle/\lambda$ and $\langle P/L\rangle$. While the latter expression looks at first sight more correct, it actually does not take into account, as the former does, the variation of the number densities in the time necessary to travel the distance L.

In eqs. (3.15) the potential V, as μ_ν and s, is a function of the thermodynamic variables ρ, T, Y_L. A simple approximation is useful to understand the dependence of V on those variables, in particular Y_L. By neglecting the $\mu_n - \mu_p$ term in the beta equilibrium equation $\mu_e - \mu_\nu = \mu_n - \mu_p$, one obtains $Y_e = 2/3\, Y_L$, $Y_\nu = 1/3\, Y_L$. Such a rough approximation turns out to be pretty good for V, where errors cancel to give, with an accuracy of 5% or less,

$$V \simeq \sqrt{2} G_{\mathrm{F}} n_B \left(\frac{5}{3} Y_L - \frac{1}{2} \right) , \tag{3.16}$$

which vanishes for $Y_L^0 \simeq 3/10$ independently of T, ρ. Eq. (3.16) illustrates what happens to the MSW potential when a neutrino or an antineutrino is lost in the unit volume. The lepton number lost or gained is redistributed by the beta equilibrium between neutrinos and electrons and the net effect is a variation of the potential by the amount $\mp(5/3)\sqrt{2} G_{\mathrm{F}}$. Moreover, through eq. (3.16) it is possible to explicitly see the effect of the feedback. Let us consider the limit in which the loss term dominates the evolution and diffusion is negligible. Then, when $Y_L > 3/10$, the RHS is negative and Y_L decreases. When $Y_L < 3/10$ the RHS is positive and Y_L increases. When $Y_L = 3/10$, the RHS vanishes and the lepton fraction is constant. In the approximation above, $3/10$ is the value of Y_L at which the non standard terms in eqs. (3.15) aim. We will see that for $m^2 R \gg 10^{-12}\,\mathrm{eV}$ this value is indeed reached and maintained for some time in some region of the inner core. In other regions, the value is not reached but its attraction on the lepton fraction affects the deleptonization. In our numerical implementation of eqs. (3.15), we do not make use of the approximation (3.16). The $V = 0$ condition then becomes a constraint on ρ, T, Y_L that translates into $Y_L = Y_L^0(\rho, T)$.

3.3.3 Phases of evolution

We start to follow the evolution of the inner core a few hundred milliseconds after collapse. We consider a core of $1.5\, M_\odot$ with a radius of 12.7 km and a typical density profile described by $\rho(r) = \rho_c/(1+(r/\bar{r})^3)$, with $\rho_c = 7.5\ 10^{14}$ gr/cm^3, $4/3\ \pi\ \bar{r}^3\ \rho_c = 1.1\, M_\odot$. The initial profiles for T and Y_L are shown in fig. 3.3 (the thick dashed lines). Their main features follow from models of core collapse [61]. The detailed structure of those profiles is not important for our purposes. Diffusion will in fact soon smooth them. Moreover, the mixing with bulk neutrinos, when important, also affects the early stages of SN evolution. This point will be discussed in more detail below.

Three processes contribute to the variation of the lepton fraction: diffusion, neutrino and antineutrino conversion into bulk neutrinos. Each of them has a characteristic time scale, t_{diff}, t_ν and $t_{\bar{\nu}}$ respectively, defined e.g. as the elapsed time per fraction of Y_L variation. While t_ν turns out to be finite and roughly the same in all the region where $V > 0$, $t_{\bar{\nu}}$ strongly depends on the position in the $V < 0$ region and may become infinite, as we will see. In any case, $t_\nu \ll t_{\bar{\nu}}$. In most of the inner core, in fact, the beta equilibrium forces μ_ν to be positive and the neutrinos to be degenerate, $\mu_\nu \gg T$. As a consequence, the antineutrino number is strongly suppressed and so is the lepton number variation due to antineutrino escape.

While the time scale for diffusion is typically $\sim 10\,\mathrm{sec}$, the escape time scale depends on $m^2 R$. Moreover, neglecting diffusion, the evolution due to the escape depends on $m^2 R$ only through an overall scale factor, $Y_L(r,t;k\,m^2R) = Y_L(r,k\,t;m^2R)$, $T(r,t;k\,m^2R) = T(r,k\,t;m^2R)$. The larger m^2R, the faster the variation of Y_L:[9]

$$t_\nu \sim 10\,\mathrm{sec}\,\frac{10^{-12}\,\mathrm{eV}}{m^2R}\left(\frac{\rho}{\rho_0}\right)^{1/2}\left(\frac{Y_L}{0.3}\right)^{1/3} . \tag{3.17}$$

We therefore distinguish two regimes:

- $m^2R \ll 10^{-12}\,\mathrm{eV}$, or $t_\nu \gg t_{\mathrm{diff}}$. Neutrino and antineutrino escape are too slow to affect significantly the evolution of the protoneutron star. Consistency with the observed neutrino signal from SN 1987A is ensured.

- $m^2R \gg 10^{-12}\,\mathrm{eV}$, or $t_\nu \ll t_{\mathrm{diff}}$. Neutrino escape changes Y_L faster than diffusion. The consistency with the SN 1987A signal would be in question if the feedback were not taken into account. Deleptonization and cooling are affected.

In the remaining of this subsection, we will concentrate on the case of fast escape, say $m^2R \gtrsim 10^{-11}\,\mathrm{eV}$.

We can distinguish two phases in the evolution. In the first one neutrino escape dominates and diffusion can be neglected. The second is a mixed phase where antineutrino escape dominates in some region and for some time and is comparable to diffusion elsewhere.

The first phase takes place in the $V > 0$ region, corresponding to $Y_L > Y_L^0$, on the left of the vertical lines in fig. 3.3. The change of Y_L and T due to antineutrino conversion (where $V < 0$) and diffusion is negligible, since the time scales are slower. Due to neutrino disappearance, both Y_L and the energy density start decreasing. The essential point is whether the value of Y_L that stops the MSW conversion is reached before all the energy has been lost. This turns out to be the case in all the region where $V > 0$. In fact, by neglecting the diffusion terms in eqs. (3.15) we find the following relation between lepton fraction and the entropy variation:

$$\frac{\partial s}{\partial Y_L} = \left(\frac{F_{5/2}(\mu_\nu/T)}{F_{3/2}(\mu_\nu/T)} - \frac{\mu_\nu}{T}\right) \sim -\frac{2}{7}\frac{\mu_\nu}{T} , \tag{3.18}$$

where the partial derivative is taken at a fixed position and the approximation $\partial s/\partial Y_L \sim -2/7\,\mu_\nu/T$ holds for degenerate neutrinos. Since such an approximation does hold for $Y_L \gtrsim 0.3$ and $T \gtrsim 30\,\mathrm{MeV}$, eq. (3.18) shows that the temperature in the $V > 0$ region actually grows while it deleptonizes. In turn, that means that the $V = 0$ condition is comfortably attained spending only a fraction of the available energy. Within a time $t = 0.5$–$1\,\mathrm{sec}(10^{-11}\,\mathrm{eV}/m^2R)$, Y_L has reached Y_L^0 in all the $V > 0$ region and the fastest phase of evolution has ended. The profiles are now shown as solid thick lines in fig. 3.3. The temperature has increased as a consequence of the conversion of degeneracy energy into thermal energy. As mentioned in Section 3.3.2, such a conversion takes place when states deep inside the neutrino Fermi sphere are emptied by neutrinos escaping in the bulk. In summary, after the initially dramatic energy leak into the bulk, most of the energy in the $V > 0$ region gets locked as Y_L reaches Y_L^0, which happens

[9] For $m^2R \gtrsim 10^{-7}$ the thermal processes would not be fast enough to maintain equilibrium. The time scale above would be affected, but the results below would not.

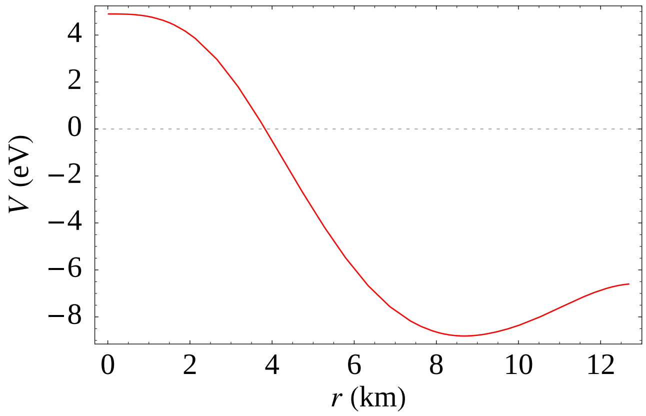

Figure 3.1: *Profile of the MSW potential of electron neutrinos corresponding to the initial profiles in fig. 3.3.*

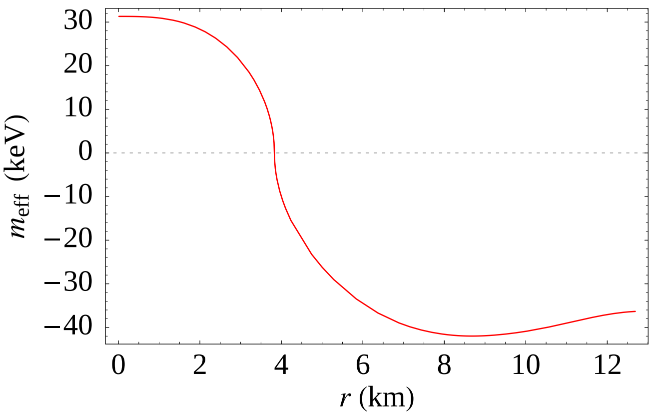

Figure 3.2: *Effective mass of a* 100 MeV *neutrino (where* $V > 0$*) or antineutrino (where* $V < 0$*) induced by the potential in fig. 3.1.*

on the t_ν time scale. The thick lines in fig. 3.3 can therefore be considered as the initial condition for the subsequent evolution.

Before discussing the next phase, a comment on the initial condition we used is in order. As mentioned at the beginning of the subsection, for $m^2R \gg 10^{-12}$ eV the initial profiles are likely to be affected by the neutrino escape. For $m^2R = 10^{-8}$ eV, for example, moving from the initial to the $Y_L = Y_L^0$ profile only takes about a millisecond. Therefore, the initial profiles in fig. 3.3, following from analysis that do not take into account the new effect, cannot be trusted hundreds milliseconds after core bounce. On the other hand, given the fixed point character of the evolution in the fast phase, we can be confident that the thick solid profile is indeed reached as soon as the core settles. We are therefore entitled to use that profile in the subsequent evolution. Why not to use it in the first place and ignore the fast phase of evolution, then? Because the simulation based on eq. (3.18), although it does not take into account the conditions met in the early stages of the SN, still gives a conservative estimate of the temperature variation and of the amount of the energy loss, a key piece of information for what follows. In summary, the thick profiles in fig. 3.3 can be considered realistic initial profiles for the next phase within the approximations and uncertainties associated to our approach and to core collapse models. Needless to say, the original initial profiles are suitable as initial conditions for the standard diffusive regime ($m^2R \lesssim 10^{-12}$ case) within the same uncertainties.

After neutrinos in what was initially the $V > 0$ region have been locked, antineutrinos loss begins to be significant in the $V < 0$ region. This happens on the slower time scale $t_{\bar\nu}$, which depends on the position in the core. Since antineutrinos are lost, the lepton fraction Y_L, initially smaller than Y_L^0, grows and V becomes less and less negative. Again, the essential point is whether the $V = 0$ condition,

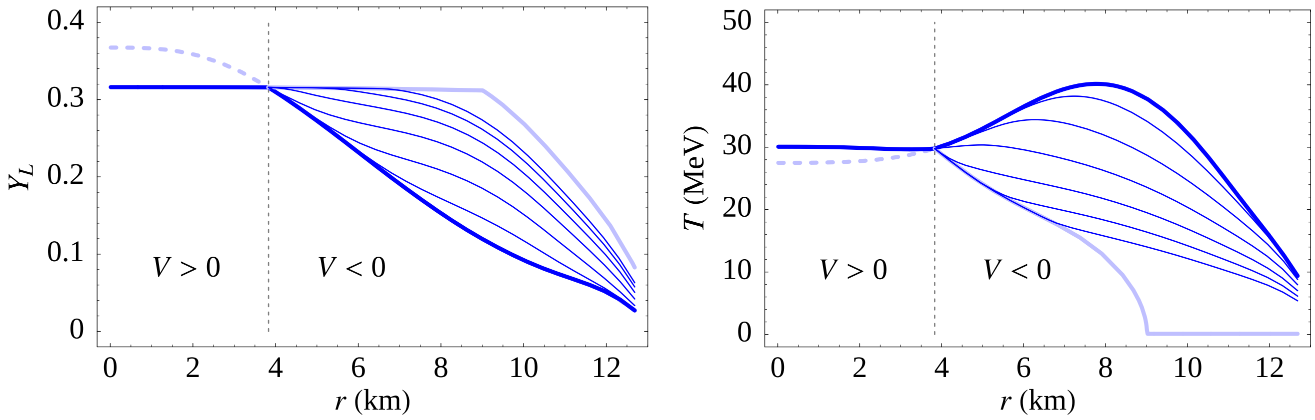

Figure 3.3: *Lepton fraction and temperature profiles in the initial phase of the evolution. The thick dashed lines (dark solid in the $V < 0$ region) represent the initial profiles. The dark thick lines show the profiles at the end of the neutrino escape phase. The thin lines show the effect of antineutrino escape 1 second later for $m^2R = 10^{-(10,9,8,7,6,5)}\,\mathrm{eV}$. They can also be considered as the profiles at times $t = 10^{-(5,4,3,2,1,0)}\,\mathrm{sec}\,(m^2R/(10^{-5}\,\mathrm{eV}))$ provided that $t \lesssim 1\,\mathrm{sec}$. Finally, the light thick lines show the values that would be asymptotically approached if diffusion could be indefinitely neglected.*

or $Y_L = Y_L^0$, is reached before all the available energy is lost. The relevant equation is in this case

$$\frac{\partial s}{\partial Y_L} = -\left(\frac{F_{5/2}(-\mu_\nu/T)}{F_{3/2}(-\mu_\nu/T)} + \frac{\mu_\nu}{T}\right) \sim -\left(\frac{\mu_\nu}{T} + \frac{5}{2}\right) . \tag{3.19}$$

The loss turns out to be more pronounced than in the previous phase. Actually, the energy loss per unit of lepton number change is smaller, since the average antineutrino energy is $5/2\,T$ whereas the average neutrino energy was $5/7\mu_\nu$. However, the entropy variation is larger since the increase of Y_L leads to an increase of the energy stored in the degenerate neutrino or electron sea at the expenses of the temperature and entropy. That is why the RHS in eq. (3.19) is larger than in eq. (3.18). Furthermore, the change in Y_L needed to reach Y_L^0 is larger in the external part of the inner core, where Y_L is lower. In order to clarify the situation, we need to numerically solve eq. (3.19). The result is that $V = 0$ is reached before all the local energy is gone only in the inner part of the $V < 0$ region. The outer part cools completely while Y_L is still lower than Y_L^0, as it is apparent from Figs. 3.3. There, the light thick lines represent the asymptotic lepton fraction and temperature profiles that would be reached if the antineutrino escape phase continued indefinitely without diffusion. In the $r \gtrsim 9\,\mathrm{km}$ region, the asymptotic temperature profile reaches zero. Correspondingly, the maximum value of Y_L attainable before complete cooling is not Y_L^0 anymore. In practice, complete cooling does not occur. The profiles reached after one second, before diffusion becomes essential, are shown by the thin lines in the $V < 0$ regions of figs. 3.3. The lines correspond to $m^2R = 10^{-(10,9,8,7,6,5)}\,\mathrm{eV}$. The three largest values, that are not in the parameter space we are interested in, illustrate the asymptotic behavior of the profiles. Alternatively, they can be considered as the profiles at times $t = 10^{-(5,4,3,2,1,0)}\,\mathrm{sec}\,(m^2R/(10^{-5}\,\mathrm{eV}))$ for a given value of m^2R — as long as $t \lesssim 1\,\mathrm{sec}$, of course. The $V = 0$ condition is reached and antineutrinos are locked in a portion of the initially $V < 0$ region which is larger the larger is m^2R. In a sufficiently large but finite time that would happen in all the region where the asymptotic Y_L profile is constant and the T one is non vanishing. In the outer part of the inner core, on the other hand, neither Y_L^0 nor the asymptotic profile will ever be reached. However, the attraction of the fixed point on Y_L has the effect of raising the Y_L profile, with interesting implications that will be discussed in section 3.3.4. The total energy loss in this phase is again a small fraction of the total available energy.

After the first, fast phase of neutrino escape and the second slower phase of antineutrino escape, diffusion begins to play a significant role. This happens on the slowest time scale t_{diff}. Diffusion "unlocks" the energy stored in the $V = 0$ region. Some of it gets lost in the bulk, the rest diffuses out in the outer part and eventually is emitted mainly as active neutrinos. The diffusion regime however is different from the standard one that takes place in absence of transitions into the bulk. We have in this case a mixed regime in which the evolution is determined by an interplay of diffusion and escape. Let us consider first the inner part of the core, where $V = 0$. Due to diffusion, the densities change, thus spoiling the $V = 0$ condition. The lepton fraction decreases and V becomes slightly negative. As V becomes negative, though, antineutrinos start to escape in the bulk thus giving a positive contribution to V. At some point, the positive contribution to V from conversion into bulk neutrinos will balance the negative contribution from diffusion. In this regime, some of the energy is lost in the bulk and some is diffused out. The amount of energy lost in the invisible channel turns out to be independent of m^2R as long as the conversion of antineutrinos (slower than the neutrino conversion) is efficient enough to keep $|V|$ small. The evolution in such a regime is well described by a single equation for the temperature. In fact, denoting $Y_L = Y_L^0 + \delta Y_L$, we have

$$V = V(\rho, T) \simeq \frac{\partial V}{\partial Y_L}\delta Y_L \,. \tag{3.20}$$

When inserted in eqs. (3.15), the previous expression allows to recover $\delta Y_L(\rho, T)$ from eq. (3.15a). Eq. (3.15b) then becomes

$$\begin{aligned} n_B T\frac{\partial s}{\partial t} = a_e\left(\vec{\nabla}\mu_\nu\right)^2 + \vec{\nabla}\cdot\left((a_e + a_\mu + a_\tau)\frac{\pi^2}{6}\vec{\nabla}T^2\right) \\ + \left(\mu_\nu - \sigma T\frac{F_{5/2}(\sigma\mu_\nu/T)}{F_{3/2}(\sigma\mu_\nu/T)}\right)\left(\vec{\nabla}\cdot\left(a_e\,\vec{\nabla}\mu_\nu\right) - n_B\frac{\partial Y_L}{\partial t}\right)\,. \end{aligned} \tag{3.21}$$

Eq. (3.21) always holds. In the small $|V|$ limit, one can approximate $Y_L \simeq Y_L^0$ everywhere, in which case the equation becomes selfconsistent and the evolution becomes independent of m^2R. This of course will not hold forever since the efficiency of antineutrino conversion decreases as the star cools. Moreover, it certainly does not hold in the outer region where V is well below zero in the first place.

In fig. 3.4 we show the evolution of the Y_L and T profiles that follows from eqs. (3.15) for three values of m^2R: $10^{-10}\,\mathrm{eV}$, $10^{-9}\,\mathrm{eV}$ and $10^{-8}\,\mathrm{eV}$. The case of no new physics is also showed in each plot for comparison (dashed lines). We do not aim at reproducing the results of the most sophisticated analysis in the literature for the latter case. However, a comparison between the solid and dashed lines in figure well illustrates the effect of new physics on the evolution. Due to neutrino conversion, Y_L quickly drops to Y_L^0 in the inner part of the core. Then, on a longer time scale, diffusion further lowers Y_L, thus starting antineutrino conversion. For large values of m^2R, the latter is efficient enough to keep Y_L close to Y_L^0 for a few seconds, until the region becomes too cool to sustain the necessary conversion. After the initial dramatic fall, the lepton fraction is higher than in the case of pure diffusion. The same happens in the outer part of the core, where the effect is more pronounced because neutrino loss never took place and $|V|$ is larger during antineutrino conversion. The lepton fraction even grows in the first second and then decreases slower than in the case of pure diffusion, at the expenses of a quicker cooling. The consequences of this effect will be discussed in the next subsection. For $m^2R = 10^{-8}\,\text{eV}$, the temperature in the inner core essentially never increases.

3.3.4 Implications for supernova physics

Fig. 3.4 shows that deleptonization and cooling do take place on the same time scale as in absence of new physics despite the time scale of neutrino disappearance can be orders of magnitude faster than the diffusion one. What cannot be inferred from fig. 3.4 is the size of the portion of the available lepton number and energy that disappears in the bulk. Is something left to give rise to the SN 1987A neutrino signal and to revive the shock in the delayed explosion scenario? This issue is addressed in fig. 3.5, where the energy and lepton number lost by the inner core in the first 10 seconds are plotted against m^2R and split in the component that goes into the observable neutrino flux and the component that is irremediably lost in the bulk. The latter grows with m^2R but is never larger than 25% of the total. The total energy loss also grows with m^2R. This is just a consequence of the faster evolution of the temperature profile due to the additional loss (see fig. 3.4). The net effect of the growth of both the total and the invisible energy loss is that the energy emitted in the visible channel in the first 10 seconds (as well as in the following 10 seconds) remains within 10% of the $m^2R = 0$ value.

The lepton number lost in the bulk in the first 10 seconds is negative, a consequence of the dominance of the antineutrino escape phase. The reluctance of the lepton fraction to get away from the $V = 0$ value shows in fig. 3.5 in the reduction of the total lepton number loss with m^2R. It is also apparent how the large negative loss in the invisible channel translates into an enhancement up to a factor four of the emitted lepton number. Fig. 3.6 shows that the enhancement takes place on the time scale of the initial antineutrino loss rate and is therefore effective already in the first second.

The enhancement of the emitted lepton number has interesting consequences on the SN phenomenology. In order to discuss them, we first comment on the temperature of the neutrinosphere and the spectrum of the neutrino flux. A quantitative analysis of this and the following issues would require solving the evolution of the mantle, which is beyond the scope of this discussion. We will therefore confine ourselves to some qualitative considerations. The disappearance probability is negligible at the density and temperature T_ν of the neutrinosphere, thus the latter can hardly be affected. Moreover, T_ν might even increase due to compressional heating until the mantle settles. The faster inner core cooling will therefore affect T_ν only later on. Finally, as the temperature of the neutrinosphere decreases, the neutrino mean free path grows and the neutrinosphere moves in the hotter interior, partially compen-

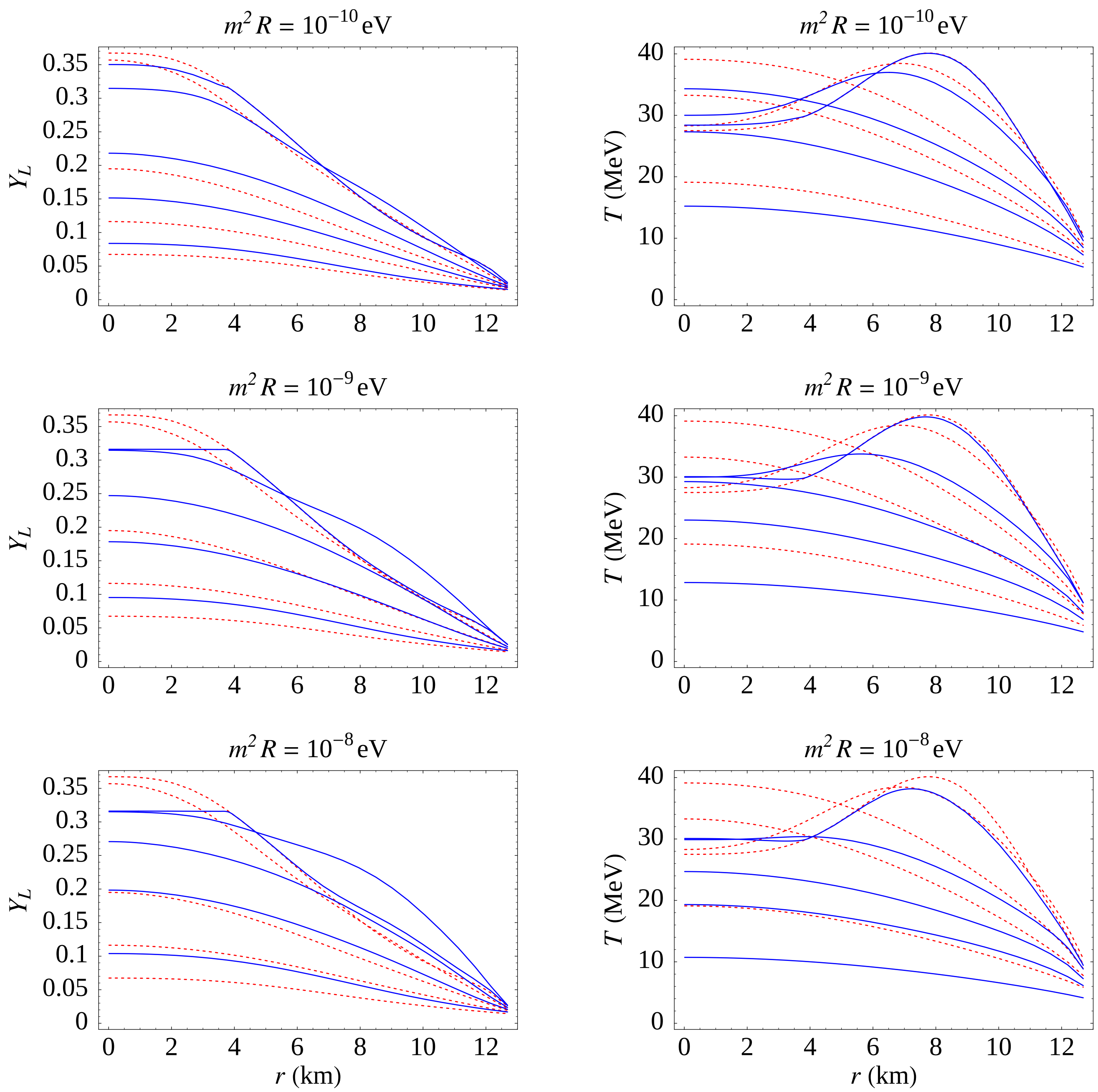

Figure 3.4: *Lepton fraction and temperature profiles at* $t = (0.01,\ 1,\ 10,\ 20,\ 40)$ sec *for different values of* m^2R *(solid lines). The profiles for* $m^2R = 0$ *are also shown for comparison (dashed lines).*

sating the temperature change. We do not expect the spectrum of the neutrino flux to be significantly affected either.

The composition of the neutrino flux depends in first approximation on T_ν and on the energy radiated

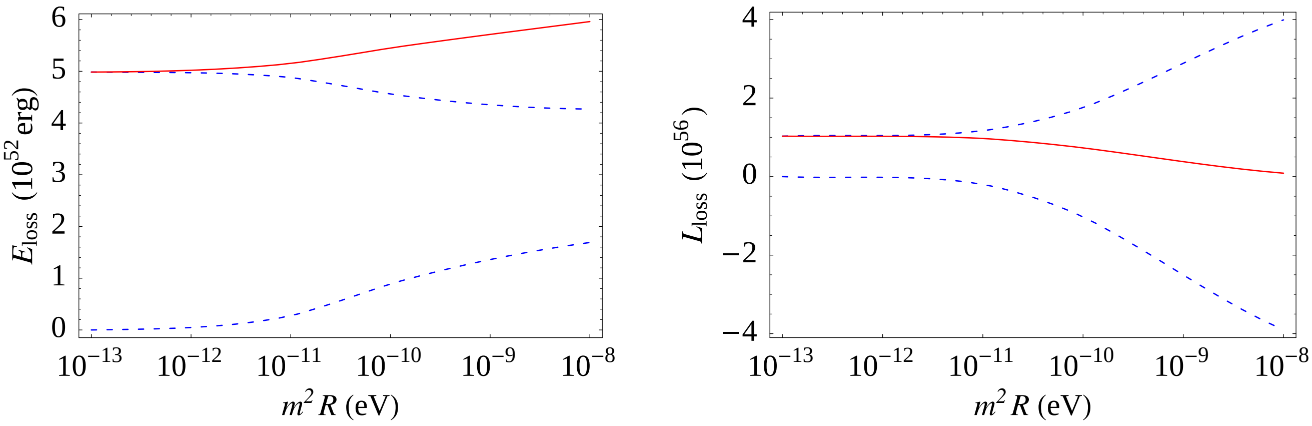

Figure 3.5: *Energy and lepton number loss in the first 10 seconds. The total loss (solid lines) is shown together with its visible (upper dashed lines) and invisible (lower dashed lines) components as a function of* m^2R*.*

per unit of lepton number. Neglecting the difference among the neutrino spectra [62], the number of neutrinos emitted per unit of lepton number is $N \sim kE/(LT_\nu)$, where E is the energy radiated with the lepton number L and k characterizes the shape of the energy spectrum at the neutrinosphere. In absence of new physics one has $N \sim 10$. Since the total electron lepton number of those neutrinos must be 1, there is a slight prevalence of electron neutrinos over the other species. Consider now our situation in the extreme limit $m^2R = 10^{-8}\,$eV. The lepton number emitted in say the first second is 4–5 times larger than in the standard case, while the energy emitted is about the same. Each electron neutrino emitted will be therefore accompanied in average by only a couple of neutrinos of other species. Such a peculiar neutrino flux composition could be observed in the existing neutrino detectors when the signal of a SN explosion in our galaxy will reach us.

The prevalence of electron neutrinos in the neutrino flux for large m^2R has two further consequences. First, it reduces the electron antineutrino component, which is constrained by the SN 1987A signal. Moreover, the electron neutrinos are much more effective than muon or tau neutrinos in depositing energy in the matter outside the neutrinosphere. As a consequence, a larger ν_e component might help a stalling shock in ejecting the SN envelope. In fact, the heating rate of matter irradiated by a hotter ν_e flux is proportional to T_ν^2, which we expect not to be significantly affected by a large m^2R, and to the ν_e luminosity. As the left panel of fig. 3.5 shows, the total luminosity in all neutrino species (integrated over 10 seconds, but the same holds for the luminosity itself) is not significantly affected. Therefore, an increase of the ν_e component has the effect of increasing the ν_e luminosity and, in turn, the heating rate. The enhancement can be significant and is only limited by the reduction of the $\bar{\nu}_e$ flux one is willing to accept.

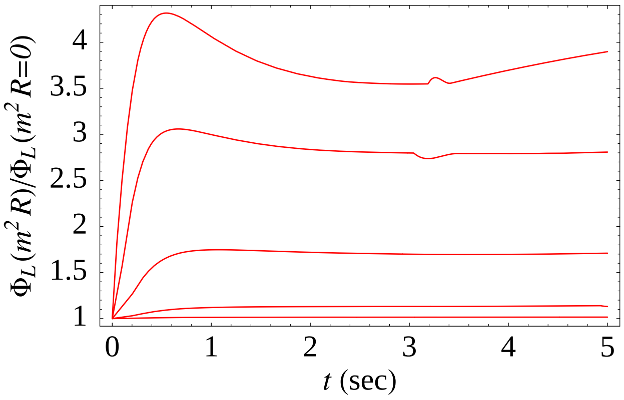

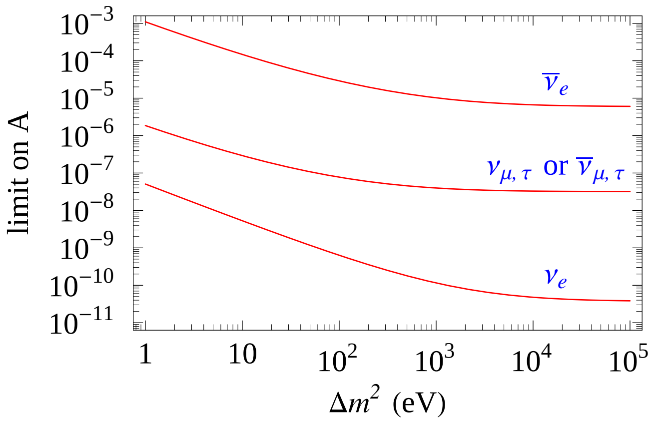

Figure 3.6: *Enhancement of the lepton number flux over the* $m^2R = 0$ *case. The five lines correspond to* $m^2R = 10^{-(12,11,10,9,8)}\,\mathrm{eV}$. *The enhancement grows with* m^2R.

Figure 3.7: *Limits on the amplitude of* ν_e, $\bar{\nu}_e$ *and* $\nu_{\mu,\tau}$ *or* $\bar{\nu}_{\mu,\tau}$ *oscillations into an invisible channel as functions of the squared mass difference* Δm^2.

3.4 "Conventional" invisible channels

Before concluding, we discuss the limits on conventional (non self-limiting) invisible cooling channels. This simple application of the formalism set up in the previous section is relevant to our discussion because it provides the condition under which subleading contribution to the disappearance probability are under control.

Let $P_\nu(L,E)$ be the probability that a neutrino of type $\nu = \nu_e, \nu_\mu, \nu_\tau, \bar{\nu}_e, \bar{\nu}_\mu, \bar{\nu}_\tau$ with energy E disappears in an invisible channel while traveling a distance L and let us assume that there is no reappearance[10]. In order to obtain a limit on P_ν, we compare the consequent lepton number loss rate with the diffusion one. The simplest case is that of a power-law disappearance probability $P_\nu(L,E) = P_0(L/L_0)^\alpha(E/E_0)^\beta$. For example, the mixing with a tower of KK states gives rise to a contribution to the escape probability which is essentially constant in the relevant range for L, E: $P_{\nu_e,\bar{\nu}_e} \sim (mR)^2$.

The neutrino number density loss rate is

$$\Gamma_\nu = \int \frac{d\vec{p}}{(2\pi)^3} \frac{\langle P\rangle_E}{\lambda_\nu(E)} f_\nu(E)\,, \tag{3.22}$$

where $\langle P\rangle = \int_0^\infty dx P(x\lambda_\nu(E), E)e^{-x}$ is the average over the distance traveled of the disappearance probability. In the case of a power law probability and within the approximations discussed in Section 3.3.1, one has

$$\Gamma_\nu = \frac{\Gamma(\alpha+1)}{12\pi^4 a_\nu} T^5 F_{4+\beta-2\alpha}\left(\frac{\mu_\nu}{T}\right)\,, \tag{3.23}$$

where $a_\nu = \lambda_\nu E^2/(6\pi^2)$. By definition of t_{diff}, the diffusion rate is $\Gamma_{\mathrm{diff}} = n_B \partial Y_L/\partial t = n_B Y_L/t_{\mathrm{diff}}$. The

[10] In the case of oscillations, reappearance can be neglected when $P \ll 1$. The case of large mixing is not covered here.

limit on the probability following from $\Gamma_\nu < \Gamma_{\rm diff}$ reflects the abundance of the neutrino type considered,

$$P_\nu(\lambda(\mu_\nu),\mu_\nu) < 2\cdot 10^{-11} a_{\alpha\beta} \left(\frac{200\,\mathrm{MeV}}{\mu_\nu}\right)^5 \frac{\rho}{\rho_0}\frac{Y_L}{0.3}\frac{10\,\mathrm{sec}}{t_{\rm diff}} \qquad \text{for } \nu=\nu_e \tag{3.24a}$$

$$P_\nu(\lambda(T),T) < 1.5\cdot 10^{-8} b_{\alpha\beta} \left(\frac{30\,\mathrm{MeV}}{T}\right)^5 \frac{\rho}{\rho_0}\frac{Y_L}{0.3}\frac{10\,\mathrm{sec}}{t_{\rm diff}} \qquad \text{for } \nu=\nu_{\mu,\tau} \text{ or } \bar\nu_{\mu,\tau} \tag{3.24b}$$

$$P_\nu(\lambda(T),T) < 3\cdot 10^{-6} b_{\alpha\beta}\, e^{(\mu_\nu/T-20/3)} \left(\frac{30\,\mathrm{MeV}}{T}\right)^5 \frac{\rho}{\rho_0}\frac{Y_L}{0.3}\frac{10\,\mathrm{sec}}{t_{\rm diff}} \qquad \text{for } \nu=\bar\nu_e\,, \tag{3.24c}$$

where $a_{\alpha\beta} = (5+\beta-2\alpha)/(5\Gamma(\alpha+1))$, $b_{\alpha\beta} = 24/(\Gamma(5+\beta-2\alpha)\Gamma(\alpha+1))$ are numerical coefficients normalized to $a_{00}=b_{00}=1$. In particular, in the case of a constant electron neutrino disappearance probability $P_{\nu_e}=(mR)^2$ we get the limit $mR \lesssim 0.5\cdot 10^{-5}(200\,\mathrm{MeV}/\mu_\nu)^{5/2}(10\,\mathrm{sec}/t_{\rm diff})$ that we used to determine the conservative upper bound $m^2R \lesssim 10^{-8}\,\mathrm{eV}$.

For completeness, we also give the limit on the amplitude of a simple oscillation probability $P_\nu(L,E) = A\sin^2(\Delta m^2 L/(4E))$ into an invisible channel. The limit on A as a function of Δm^2 for the case of ν_e, $\bar\nu_e$ and $\nu_{\mu,\tau}$ or $\bar\nu_{\mu,\tau}$ oscillations is plotted in Fig. 3.7 for $\rho=\rho_0$, $Y=0.3$, $t_{\rm diff}=10\,\mathrm{sec}$, $\mu_\nu = 200\,\mathrm{MeV}$ and $T=30\,\mathrm{MeV}$.

3.5 Summary

The supernova plays an important role in the phenomenology of a possible mixing between SM neutrinos and fermions propagating in the bulk of large extra dimensions. We studied both the constraints on such a mixing following from the necessity of avoiding unacceptable energy loss and the implications for supernova physics. We considered the simple case of mixing between the electron neutrino and a single KK tower of 5D bulk neutrinos. The parameter space where interesting effects arise is quite broad, with the size of the extra dimension in the range $10^{-2}\,\mathrm{eV} \lesssim 1/R \lesssim 1\,\mathrm{keV}$ and the mixing mass parameter m such that $10^{-12}\,\mathrm{eV} \lesssim m^2R \lesssim 10^{-8}\,\mathrm{eV}$ and $mR \lesssim 10^{-5}$. The interplay of neutrino diffusion and conversion into bulk neutrinos has an important role in the phenomenology we study and requires taking into account the relevant aspects of neutrino transport, which we did in the context of a simplified model of the protoneutron star core.

Due to the large number of available states and especially to matter effects, the rate at which neutrino disappearance in the bulk cools the protoneutron star is initially dangerously high. If taken at face value, such a rate would set quite a stringent bound on m^2R, $m^2R \lesssim 10^{-12}\,\mathrm{eV}$ in the case of neutrino conversion. However, the disappearance rate quickly reduces itself to acceptable values. This happens for different reasons. In the region where the MSW potential V is positive, neutrinos escape in the bulk and the lepton fraction quickly drops to the value $Y_L^0 \simeq 0.3$ at which $V=0$, thus stopping the potentially most dangerous MSW enhanced conversion before a significant amount of energy is lost. Then, on a much slower time scale, neutrino diffusion spoils the $V=0$ condition and unlocks the energy frozen in what was initially the $V>0$ region. The potential becomes slightly negative and antineutrinos start escaping in the bulk to restore the $V=0$ condition. This feedback keeps Y_L close to Y_L^0 until the temperature becomes too low to sustain the necessary antineutrino escape rate. In the region where the potential was initially negative, neutrino conversion never takes place. The initial loss rate is smaller because of the much lower antineutrino density. Still, it would be too high for large values of m^2R. However, in the inner part of the $V < 0$ region the antineutrino loss stops itself by drawing V up to zero before all the local energy is lost, analogously to the $V > 0$ case. In the outer part of the $V < 0$ region, there is not enough energy to reach $V = 0$. However, the conversion again controls itself. This happens this time because the energy loss, proportional to $T^{7/2}$, becomes less and less effective as the region cools.

The described mechanism allows to gain four orders of magnitude in the allowed range for m^2R ($10^{-12}\,\mathrm{eV} \to 10^{-8}\,\mathrm{eV}$). In the subsequent four orders of magnitudes, the MSW enhanced conversion would still be under control but what were previously neglected as subleading contributions to the oscillation probability become too large. Such contributions, as well as the limits on other "conventional" invisible cooling channels, were discussed in Section 3.4. In the gained portion of the parameter space, the implications for supernova physics are particularly interesting. Although compatible with the SN 1987A signal, the evolution of the protoneutron star is significantly affected, especially for large values of m^2R. Deleptonization and cooling take place on the same time scale as in absence of new physics. However, the reluctance of the lepton fraction to get away from $Y_L^0 \sim 0.3$ slows the deleptonization, while the energy loss accelerates the cooling. Up to a fourth of the energy lost by the protoneutron star goes to the bulk but the total luminosity in all neutrino species turns out to be approximately the same as in the standard case, at least in the first 20 seconds. Antineutrinos escape in the bulk in the effort of keeping Y_L close to Y_L^0, which boosts the lepton number radiated from the neutrinosphere. A quantitative study of the consequences of such an enhancement would require solving the evolution of the mantle. However, we expect it to result in an enhancement of the ν_e component of the neutrino flux and therefore of the ν_e luminosity, an effect observable in the existing neutrino detectors. Since we expect the temperature of the neutrinosphere not to be significantly affected, the energy deposition in a possibly stalling shock would also be enhanced at the expenses of a smaller $\bar{\nu}_e$ luminosity.

The exotic phenomenology discussed in this chater represents an example of how the standard ideas about protoneutron star evolution could be affected in an unexpected way by the presence of new physics.

Chapter 4

A Constrained Standard Model with one Extra Dimension

In this chapter I move to a different realization of the idea of Extra Dimensions. Namely, I move to the framework of Universal Extra Dimensions, which I briefly introduced in section 2.1.2. I focus on the model proposed by Barbieri, Hall and Nomura in [28].

4.1 The model

The model in [28] is a 5D theory with $\mathcal{N} = 1$ SuperSymmetry, compactified on $\mathbb{S}^1/\mathbb{Z}_2 \times \mathbb{Z}'_2$ (see figure 4.1), and the gauge group is the Standard Model one: $SU(3) \times SU(2) \times U(1)$. The fields content is given by the embedding of the usual SM fields in the extra dimension: for every gauge boson A^μ there is a 5D vector supermultiplet $(A^M, \lambda, \lambda', \sigma)$; for every matter field Q, U, D, L, E and for the single Higgs H there are 5D matter supermultiplets $(\psi, \varphi, \varphi^c, \psi^c)$.

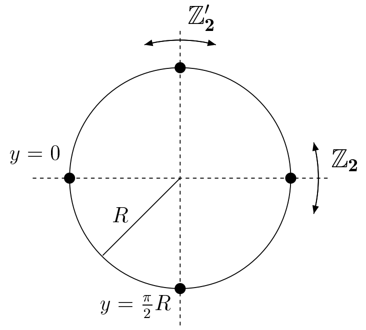

Figure 4.1: The double orbifold. The $\mathbb{Z}_2$ symmetry can be seen as a reflection with respect to the horizontal axis ($y \to -y$); the $\mathbb{Z}'_2$ with respect to the vertical axis ($y' \to -y'$, $y' = y - \pi R/2$).

From a 4D point of view, a matter hypermultiplet splits into a pair of chiral supermultiplets with conjugate quantum numbers (property that I indicate with a ^{c}), while a vector hypermultiplet splits into a vector and a chiral supermultiplet. Under the double orbifolding, global supersymmetry is completely broken *à la* Scherk-Schwarz, leaving the SM fields as the only zero modes. Anyhow, restricted local supersymmetric transformations still hold. The most general Lagrangian, according to this set of symmetries (gauge group, orbifold parities and local supersymmetry), is:

$$\mathcal{L}(x,y) = \mathcal{L}_5 + \delta(y)\, \mathcal{L}_4 + \delta(y - \pi R/2)\, \mathcal{L}_4' \tag{4.1}$$

where $\mathcal{L}_5$ is $\mathcal{N} = 1$ supersymmetric in 5D whereas $\mathcal{L}_4$ and $\mathcal{L}_4'$ are 4D lagrangians invariant under different $\mathcal{N} = 1$ supersymmetries valid on the fixed points of the two parities.

In particular the 4D pieces include the Yukawa couplings

$$\begin{aligned} & \frac{1}{2}\left(\delta(y) + \delta(y - \pi R)\right) \int d^2\theta \left(\lambda_U Q U H\right) \\ + \; & \frac{1}{2}\left(\delta(y - \frac{\pi}{2}R) + \delta(y + \frac{\pi}{2}R)\right) \int d^2\theta' \left(\lambda_D Q' D' H^{c\prime} + \lambda_E L' E' H^{c\prime}\right) + \text{h.c.} \end{aligned} \tag{4.2}$$

Under the two parities all the fields have definite transformation properties, given in Table 4.1 and in figure 4.2, together with the corresponding eigenfunctions and the spectrum of every tower of Kaluza-Klein states.

A_μ, ψ_M, ϕ_H	$(+,+)$	$\cos \frac{2n}{R} y$	$\frac{2n}{R}$, $n = 0, 1, 2, 3...$
λ, ϕ_M, ψ_H	$(+,-)$	$\cos \frac{2n-1}{R} y$	$\frac{2n-1}{R}$, $n = 1, 2, 3...$
ψ_Σ, $\phi_M^{c\dagger}$, $\psi_H^{c\dagger}$	$(-,+)$	$\sin \frac{2n-1}{R} y$	$\frac{2n-1}{R}$, $n = 1, 2, 3...$
ϕ_Σ, $\psi_M^{c\dagger}$, $\phi_H^{c\dagger}$	$(-,-)$	$\sin \frac{2n}{R} y$	$\frac{2n}{R}$, $n = 1, 2, 3...$

Table 4.1: Gauge, Matter and Higgs fields content of the theory with their orbifolding properties

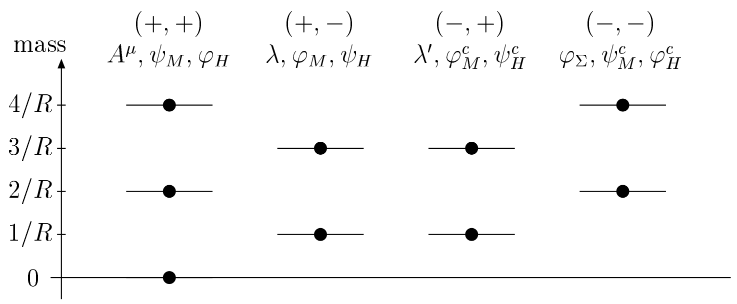

Figure 4.2: The tree-level spectrum of the theory (before EWSB).

The tree-level Higgs potential in the low energy effective theory is constrained to have the form

$$V_{H,tree} = \frac{g^2 + g'^2}{8} |\phi_H|^4, \tag{4.3}$$

where g and g' are the standard model $SU(2)$ and $U(1)$ gauge couplings.

No free parameter is present in $V_{H,tree}$, unlike in the Standard Model, and ElectroWeak Symmetry is unbroken. The next step is of course to compute the radiative corrections. The one loop contribution from the top loop to the Higgs mass reads

$$\begin{aligned} \delta m_H^2 &= -\frac{3\,\widehat{y}_t^2}{16\,R^2} \int_0^\infty \mathrm{d}x\, x^3 \left[\coth^2\left(\frac{\pi x}{2}\right) - \tanh^2\left(\frac{\pi x}{2}\right)\right] \\ &= -\frac{63\,\zeta(3)}{8\,\pi^4} \frac{\widehat{y}_t^2}{R^2} \end{aligned} \tag{4.4}$$

where $\zeta(3) = 1.20$ and $\widehat{y}_t = \lambda_t/(2\pi R)^{3/2}$ is the top Yukawa coupling in 4D. The contribution is negative thus ElectroWeak Symmetry is (radiatively) broken. This formula should be compared to the corresponding results in the Standard Model (eq. 1.1) and in "traditional" SuperSymmetry (eq. 1.2): notice that this is finite, no sort of residual divergence is present, and that the top/stop mass has been replaced by $1/R$, a feature that could be expected since it corrisponds to the shift of the squark tower masses. Above all, the only parameter showing in the formula is R so that the Fermi constant can be used to determine it via the minimization of the potential and a mass for the physical Higgs boson can be predicted. In the context of [28] one obtains

$$m_H = 127 \pm 8 \text{ GeV}, \tag{4.5}$$

$$1/R = 370 \pm 70 \text{ GeV}. \tag{4.6}$$

Some **modifications** [32, 33, 34, 35, 36, 37, 38] have occourred since the first proposal of the model. Without entering in the details, the main consequence on the theory is the appearance of 5D mass terms for every hypermultiplet, allowed by all the residual symmetries:

$$\begin{aligned} \mathcal{L}_m &= -\left(\psi m(y) \psi^c + \text{h.c.}\right) - M^2 \left(|\varphi|^2 + |\varphi^c|^2\right) \\ &\quad -2M \left(\delta(y) + \delta(y - \pi R/2)\right) \left(|\varphi|^2 - |\varphi^c|^2\right) \end{aligned} \tag{4.7}$$

where $m(y)$ has to be a jumping function on the circle

$$m(y) = M\ \eta(y)\,, \quad \eta(y) = \begin{cases} +1, & y \in (0, \pi R/2) \cup (\pi R, 3\pi R/2) \\ -1, & y \in (\pi R/2, \pi R) \cup (3\pi R/2, 2\pi R) \end{cases} \tag{4.8}$$

The values of the various M are new free parameters in the theory; moreover, they also receive a piece that is proportional to the contribution of a Fayet-Iliopoulos term (multiplied by the hypercharge of the hypermultiplet). This carries a quadratic dependance on the cut-off. The phenomenology of the theory ($1/R, m_H$...) can be re-examined in presence of these terms and turns out, in a certain sense, to be even more appealing [37, 38].

However, it is not inconceivable to put all the masses to zero from the beginning: indeed (i) if the values M are vanishing at tree level for some underlying reason, then the non–renormalisation theorems guarantee to keep them negligibly small; (ii) one can design a suitable extension of the theory (e.g. including two Higgs doublets – of which however only one takes a vev – and some relations among the bulk masses) where the Fayet-Iliopoulos induced term is consistently fixed to zero [36, 38].

From now on, I will always work in the case of all $M = 0$, or, which is the same, in the framework of the original theory described above.

4.2 Virtues of the model

I ended section 1.1.3 and 1.1.4 above with a sense of dissatisfaction coming from the open problems of (Little) Hierarchy and ElectroWeak Symmetry Breaking.

In the spirit of that discussion, let us see how the theory that I described in this chapter can give some comfort. A list of its achievements can be outlined as follows:

- **EW Symmetry Breaking**: The theory do provide a physical description of EWSB and an origin of the lightness of the Higgs boson. In particular, the radiative correction to the Higgs mass due to the top loop is finite, not even logarithmically divergent as in traditional SuperSymmetry. Nevertheless, this finiteness can be traced back to the residual local supersymmetry.

- **Raising of the mass of new particles**: The superpartner spectrum begins at $\sim 1/R \sim 370$ GeV. The perplexing low scale of new particles highlighted in section 1.1.3 is moved at least a factor 2 away.

- **Frugality of new parameters**: The only new parameter in the theory is the radius R (barring the hypermultiplet masses, see above). This replaces the two parameters μ^2 and λ in the scalar potential of the Standard Model in the implementation of EWSB. No new parameters are introduced to realize the SuperSymmetry breaking (compare with the 105 additional parameters of the MSSM): unlike the usual approach of adding soft supersymmetry breaking terms adjusted by hand, the SM spectrum is supersymmetrized in 5D and then the boundary conditions do the job by themselves.

- **Predictiveness and Calculability**: As is obvious for a Yang-Mills theory in 5 dimensions, the model is non-renormalizable and possesses an energy cut-off ($\sim 5/R \sim 2$ TeV). It must then be thought as an effective theory valid up to that scale [1]. However, working at energies much lower

[1] The cut-off is not too low with respect to the characteristic scale of the theory set by $1/R$, compare with the case of chiral lagrangians where a similar factor $4 \div 5$ splits the pion mass and the characteristic scale f_π.

than the cut-off, the effects of unknown UV physics are under control and in this sense the theory is *predictive*.

Moreover, in this model several quantites are provided with calculability, thanks to the residual local supersymmetry. Indeed, it ensure that them can be computed in terms of other parameters of the theory and are not spoilt by tree level contributions. In this sense the theory is *calculable*.

4.3 Calculations

The most important quantity predicted by this theory is, of course, the Higgs mass.

The zoology of the spectrum after ElectroWeak Symmetry Breaking and the collider phenomenology are developed in ref. [28, 39].

Precision loop observables are also interesting as sensitive probes of new physics: the branching ratio of $B \to X_s \gamma$ has been computed in [40], while in chapter 5 we compute the muon anomalous magnetic moment a_μ.

An interesting feature emerges from the computation of the Higgs boson production rate via gluon fusion, performed in chapter 6.

Chapter 5

Muon g-2 in a model with one extra dimension

In this chapter, based on ref. [63, 64], I discuss the computation of the muon anomalous magnetic moment a_μ in the framework of the theory presented in chapter 4.

5.1 The muon anomalous magnetic moment

The measurement of a_μ is one of the most stringent tests for "new physics" scenarios, thanks to its current impressive precision. Moreover, the recent results of E821 experiment at BNL [65] have highlighted a discrepancy with the present Standard Model prediction and have therefore made even more interesting the comparison with reliable predictions made by new models. In particular, attempts have been made in order to study the effect of extra space dimensions [66].

Let us briefly review the present status of the SM prediction [67]. The QED contribution has been computed up to order α^5 and it gives the core of the experimental value: $a_\mu^{QED} = (11\ 658\ 470.0 \pm 0.3) \cdot 10^{-10}$. The purely weak terms are also known with a small uncertainty, up to two loops: $a_\mu^{weak} = (15.1 \pm 0.4) \cdot 10^{-10}$. On the contrary, hadronic loop corrections provide relevant contributions but also carry the greatest theoretical uncertainty [68]. In fact, since it is quite hard to deal with low energy QCD, experimental inputs are also needed. Light-by-light scattering yields $a_\mu^{lbl} = -(8.6 \pm 3.2) \cdot 10^{-10}$ and hadronic vacuum polarization $a_\mu^{hvp} = (684.9 \pm 6.4) \cdot 10^{-10}$. Summing up all these contributions and uncertainties, the SM prediction is:

$$a_\mu^{SM} = (11\ 659\ 162.0 \pm 7.5) \cdot 10^{-10}$$

On the other hand, the present world average for the experimental value (including BNL results) is [67]:

$$a_\mu^{exp} = (11\ 659\ 202.3 \pm 15.1) \cdot 10^{-10}$$

This leads to a discrepancy a bit larger than 2σ:

$$a_\mu^{exp} - a_\mu^{SM} = (40.3 \pm 16.9) \cdot 10^{-10} \tag{5.1}$$

Actually, this result is not well established. On the theoretical side, recent results [69] [70] claim that the light-by-light contribution has opposite sign, thus reducing the discrepancy to about 1σ. At the same time, the error on the experimental value should be improved by further results at BNL.

In this chapter we compute the corrections Δa_μ to the anomalous magnetic moment due to the new fields in the theory, up to order $(M_W R)^2$ where R is the compactification radius of the 5^{th} dimension.

5.2 Necessary ingredients from the theory

The terms in the 5D action, that are relevant for the following calculation, are:

$$\begin{aligned} S \; = \int d^5x \; & \Big\{ -\frac{1}{4}\mathbf{Tr}F_{MN}F^{MN} - \mathbf{Tr}\left[i\lambda\sigma^\rho\mathcal{D}_\rho\overline{\lambda} - i\lambda'\sigma^\rho\mathcal{D}_\rho\overline{\lambda}' \right] + i\psi_X\sigma^\rho\mathcal{D}_\rho\overline{\psi}_X + i\psi_X^c\sigma^\rho\mathcal{D}_\rho\overline{\psi}_X^c + \\ & +(\mathcal{D}_M\phi_X)^\dagger(\mathcal{D}^M\phi_X) + (\mathcal{D}_M\phi_X^c)^\dagger(\mathcal{D}^M\phi_X^c) + \sqrt{2}g_{(5)}\left[\phi_X^\dagger\lambda\psi_X - \psi_X^c\lambda\phi_X^{c\dagger} + h.c. \right] + \\ & +\sqrt{2}g_{(5)}\left[\psi_X^c\lambda'\phi_X + \phi_X^c\lambda'\psi_X + \psi_X^c\Sigma\psi_X + h.c. \right] + \\ & +\delta(y - \frac{\pi}{2}R)\lambda_\mu\left[\psi_L\psi_E\phi_{H^0}^\dagger + \psi_L\psi_{H^0}^c\phi_E^{c\dagger} + \psi_E\psi_{H^0}^c\phi_L^{c\dagger} + \right. \\ & \left. -(\psi_\nu\psi_E\phi_{H^+}^\dagger + \psi_\nu\psi_{H^+}^c\phi_E^{c\dagger} + \psi_E\psi_{H^+}^c\phi_\nu^{c\dagger}) \right] \Big\} \end{aligned} \tag{5.2}$$

where the fermionic fields are Weyl spinors, the gauge fields W_M, λ, λ' and σ contains the group generators, e.g. $\lambda \equiv \lambda^a T^a$ (the generators being normalized according to $\mathbf{Tr}(T^aT^b) = \delta^{ab}$) and the index X can run over E, L, H. The gauge coupling g is intended to be the $U_Y(1)$ coupling g' or the $SU_L(2)$ coupling g according to the gauge fields involved.

From now on, for the four gauge hypermultiplets we use the notation:

$$\begin{aligned} QED \quad & \left(A_\rho, \tilde{\gamma}, \tilde{\gamma}_c, \Sigma_\gamma\right) \\ Z's \quad & \left(Z_\rho, \tilde{z}, \tilde{z}_c, \Sigma_z\right) \\ W's \quad & \left(W_\rho^\pm, \tilde{w}^\pm, \tilde{w}_c^\pm, \Sigma_w^\pm\right) \end{aligned}$$

(we remind that, also in this case, the subscribed c only means that the second spinors have conjugate quantum numbers).

5.2.1 Mass Eigenstates

The brane interactions introduce mass mixing among the states of muon and smuon KK towers: since it will be useful for our calculation to work with the mass eigenstates, we proceed to determine eigenvalues and eigenvectors from the very beginning (see e.g. the discussion in [40]). For the fermions, the mass eigenvalues turn out to be:

$$m_0 = m \equiv \frac{\epsilon}{R}, \qquad m_n^{\pm} = m \pm \frac{2n}{R} \qquad (n = 1, 2, ...)$$

corresponding to mass eigenvectors whose Weyl spinor components we denote by (μ_0, μ_0^c) and $(\mu_n^{\pm}, \mu_n^{c\pm})$. Thus m is the mass of the ordinary muon. For the scalars:

$$\tilde{m}_n^{\pm} = \frac{(2n-1)}{R} \pm m \qquad (n = 1, 2, ...)$$

corresponding to eigenvectors $\Phi_n^{\pm}$ and $\Phi_n^{c\pm}$.

The interaction eigenstates[1] are expressed in terms of the mass eigenstates (at order ϵ) by

$$\psi_{L,0} = \mu_0 + \epsilon \sum_n \frac{1}{2n} (\mu_n^+ - \mu_n^-) \tag{5.3}$$

$$\psi_{L,l} = \frac{1}{\sqrt{2}} \left\{ \left(1 + \frac{\epsilon}{2(2n)}\right) \mu_l^+ + \left(1 - \frac{\epsilon}{2(2n)}\right) \mu_l^- + \epsilon \sum_n \kappa_{nl} (\mu_n^+ - \mu_n^-) \right\} \tag{5.4}$$

$$\psi_{E,l}^c = \frac{1}{\sqrt{2}} \left\{ \left(1 - \frac{\epsilon}{2(2n)}\right) \mu_l^+ - \left(1 + \frac{\epsilon}{2(2n)}\right) \mu_l^- - \epsilon \sum_n \kappa_{ln} (\mu_n^+ + \mu_n^-) \right\} - \frac{\sqrt{2}}{2l} \epsilon\, \mu_0 \tag{5.5}$$

$$\phi_{L,l} = \frac{1}{\sqrt{2}} \left\{ \left(1 + \frac{\epsilon}{2(2n-1)}\right) \Phi_l^+ + \left(1 - \frac{\epsilon}{2(2n-1)}\right) \Phi_l^- + \epsilon \sum_n J_{ln} (\Phi_n^+ - \Phi_n^-) \right\} \tag{5.6}$$

$$\phi_{E,l}^c = \frac{1}{\sqrt{2}} \left\{ -\left(1 - \frac{\epsilon}{2(2n-1)}\right) \Phi_l^+ + \left(1 + \frac{\epsilon}{2(2n-1)}\right) \Phi_l^- + \epsilon \sum_n J_{nl} (\Phi_n^+ + \Phi_n^-) \right\} \tag{5.7}$$

with $\kappa_{ln} = \frac{2(2l)}{(2l)^2 - (2n)^2}$ and $J_{ln} = \frac{2(2l-1)}{(2l-1)^2 - (2n-1)^2}$, and zero for $n = l$. Expressions which are identical to (5.3), (5.4), (5.5) hold for $(\psi_{E,0},\ \psi_{E,n},\ \psi_{L,n}^c)$ if $(\mu_0,\ \mu_n^{\pm})$ are replaced by $(\mu_0^c,\ \mu_n^{c\pm})$; for $(\phi_L^c,\ \phi_E)$ it is sufficient to replace $\Phi_n^{\pm}$ with $\Phi_n^{c\pm}$ in equations (5.6), (5.7).

5.2.2 Couplings to the mass eigenstates

Starting from eq. (5.2), one has to integrate out the 5^{th} dimension y and rewrite the interaction vertices in terms of the mass eigenstates (5.3)-(5.7). Taking into account momentum conservation along the 5^{th} direction, p_5, the bulk interactions give rise to several trilinear vertices. The muon masses and Higgs vertices, on the other hand, being located on the brane, violate p_5-conservation and are proportional to ϵ. As we are interested in $\mathcal{O}(R^2)$ contributions, only graphs where the internal lines carry the same index n, in terms of the mass eigenstates, have to be taken into account. This simplifies the calculation of the relevant vertices. As an explicit example, the interaction terms between KK photons and the various components in the muon towers, in the mass eigenstate basis, are:

[1]Note that in this chapter the brane lagrangians $\mathcal{L}_4$ and $\mathcal{L}'_4$ are reversed respect to ref. [28]. For more details, see appendix A in chapter 6.

$$\begin{aligned}
e\overline{\psi}_{L,0}\overline{\sigma}_\rho\psi_{L,n}A_n^\rho &= e\overline{\mu}_0\overline{\sigma}_\rho\frac{1}{\sqrt{2}}\left\{\left(1-\frac{\epsilon}{2(2n)}\right)\mu_n^+ + \left(1+\frac{\epsilon}{2(2n)}\right)\mu_n^-\right\}A_n^\rho \\
\frac{e}{\sqrt{2}}\overline{\psi}^c_{E,2n}\overline{\sigma}_\rho\psi^c_{E,n}A_n^\rho &= -e\frac{\epsilon}{2(2n)}\overline{\mu}_0\overline{\sigma}_\rho\frac{1}{\sqrt{2}}\{\mu_n^+ - \mu_n^-\}A_n^\rho
\end{aligned}$$

In this particular case, summing up the two contributions, the couplings of order ϵ vanish, so that the net result is:

$$e\overline{\mu}_0\overline{\sigma}_\rho\frac{1}{\sqrt{2}}\left(\mu_n^+ + \mu_n^-\right)A_n^\rho \tag{5.8}$$

This allows to recognize $e/\sqrt{2}$ as the correct coupling with a KK photon.

On the other hand, the interactions of the zero mode gauge bosons are still diagonal in n and have a universal coupling, e.g. $e = e_{(5)}/\sqrt{2\pi R}$ for the photon. Note that this relation holds for all gauge couplings, so in the following $g = g_{(5)}/\sqrt{2\pi R}$ is the 4D gauge coupling, while $s = \sin\theta_W$ and $c = \cos\theta_W$ are functions of the usual SM Weinberg angle.

5.3 Calculation of a_μ

The effective Lagrangian term which fixes the notation for the anomalous magnetic moment $a_\mu = (g_\mu - 2)/2$ is:

$$\mathcal{L} = \frac{ie}{2m}\,a_\mu\left(\overline{\mu}\sigma_{\rho\sigma}F^{\rho\sigma}\mu\right) \tag{5.9}$$

In the Feynman–'t Hooft gauge ($\xi = 1$, see below), one can identify the five general types of diagrams in fig. 5.1, each giving a contribution Δa_μ whose explicit expressions are listed in app. A.

As in the following we will distinguish between diagrams with chirality flip on the external or internal fermionic line, in eq. (5.50)-(5.53) it is easy to trace back the external cross contribution and the internal cross one (the latter proportional to m_f/m). On the other hand, in graph V the chirality flip is provided by the only scalar interaction with the fermion.

5.3.1 QED

In this section we consider all the diagrams involving QED hypermultiplet fields. The one loop Standard Model contribution [71] simply comes from graph IV with a massless photon in the loop, with $g_+ = g_- = e$:

$$a_\mu^\gamma = \frac{\alpha}{2\pi} \tag{5.10}$$

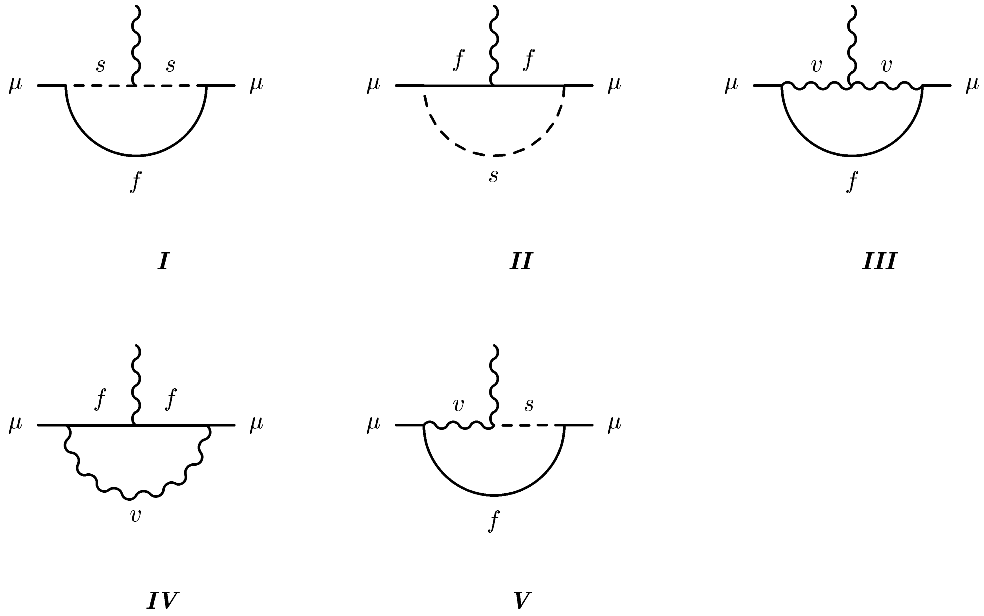

Figure 5.1: General patterns of graphs contributing to the $(g-2)$.

KK vectors

The interaction lagrangian for KK photons has been displayed in (5.8) and the graphs are of type IV. As a general rule, dealing with the diagrams involving KK fields, it is useful to separate the external and internal cross contributions. This is motivated by the fact that in the latter case it is necessary to use couplings and loop masses at order ϵ while in the former $\mathcal{O}(1)$ is enough. The following sketched diagrams are drawn in terms of Weyl fermions and the emitted zero-mode photon is implicitly attached to any internal charged line. The states in the loop are KK modes of the field indicated, always carrying the same index n for the reasons explained above. The resulting Δa_μ, for a given internal KK state, are:

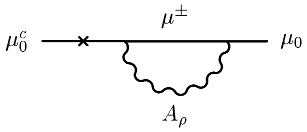

$$\Rightarrow \quad \frac{e^2}{16\pi^2}\frac{\epsilon^2}{(2n)^2}\int dx\,\left[4x(1-x)^2-8x(1-x)\right] \tag{5.11}$$

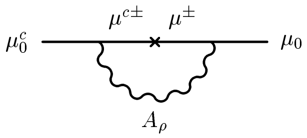

$$\Rightarrow \quad \frac{e^2}{16\pi^2}\frac{\epsilon^2}{(2n)^2}\int dx\,\left[8x(1-x)-16x(1-x)^2\right] \tag{5.12}$$

and the trivial integration over the Feynman parameter x is left explicit in order to discuss supersymmetric cancellations (see below).

Scalars

The gauge scalar field A_5 mixes mode by mode with the massive vector A_ρ. Including also the mass term for the gauge scalar σ_γ, the mass lagrangian, for each mode n, is:

$$\mathcal{L}_{mass} = -\partial_\rho A^\rho \left(\frac{2n}{R} A_5\right) - \frac{1}{2}\left(\frac{2n}{R}\right)^2 \sigma_\gamma^2 - \frac{1}{2\xi}\left(\partial_\rho A^\rho - \xi \frac{2n}{R} A_5\right)^2 \tag{5.13}$$

where the R_ξ gauge fixing term is there to cancel the mixing terms. It is convenient to work in the $\xi = 1$ gauge: we obtain a photon propagator with no longitudinal modes and two scalars σ_γ and A_5 (with equal mass) that can be combined in the complex scalar Σ_γ. The interaction terms are then:

$$\sqrt{2} e \left(\psi_E^c \Sigma_\gamma \psi_E + \psi_L^c \Sigma_\gamma \psi_L + h.c.\right) \tag{5.14}$$

so that at the relevant order in ϵ, only an external cross graph is possible. Equivalently, in terms of the real scalar fields it happens that the internal cross diagram with an A_5 field is cancelled out by the same diagram with a σ_γ. The external cross diagram is of type *II* so that the resulting Δa_μ is

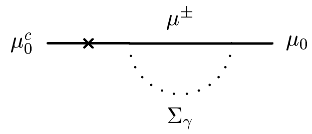

$$\Rightarrow \frac{e^2}{16\pi^2} \frac{\epsilon^2}{(2n)^2} \int dx \left[4x(1-x)^2\right] \tag{5.15}$$

Fermions

The gauge fermions $\tilde{\gamma}$ and $\tilde{\gamma}_c$ are mixed by the kinetic term along the 5^{th} direction. They are involved in the following interaction terms

$$\begin{aligned} &-\sqrt{2} e \mu_0 \tilde{\gamma}_n \frac{1}{\sqrt{2}} \left\{ \left(\Phi_n^{\dagger -} - \Phi_n^{\dagger +}\right) + \frac{\epsilon}{2n-1}\left(\Phi_n^{\dagger -} + \Phi_n^{\dagger +}\right) \right\} \\ &+\sqrt{2} e \mu_0^c \tilde{\gamma}_{c,n} \frac{1}{\sqrt{2}} \left\{ \left(\Phi_n^{+} + \Phi_n^{-}\right) + \frac{\epsilon}{2n-1}\left(\Phi_n^{+} - \Phi_n^{-}\right) \right\} \end{aligned} \tag{5.16}$$

and in similar expressions (replacing Φ with Φ^c) for the interactions of μ_0^c with $\tilde{\gamma}_n$ and μ_0 with $\tilde{\gamma}_{c,n}$. From graph *II*, one gets

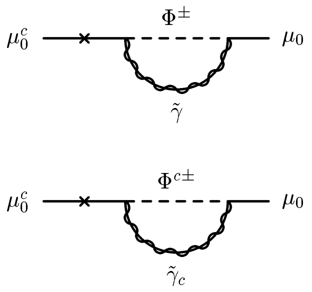

$$\Rightarrow -\frac{e^2}{16\pi^2}\frac{\epsilon^2}{(2n-1)^2}\int dx\ \left[4x(1-x)^2\right]\times 2 \tag{5.17}$$

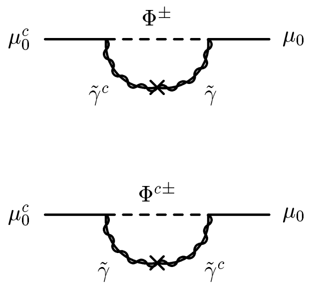

$$\Rightarrow \frac{e^2}{16\pi^2}\frac{\epsilon^2}{(2n-1)^2}\int dx\ \left[8x(1-x)^2\right]\times 2 \tag{5.18}$$

Total QED contribution

First of all, in order to test the computation, we consider the supersymmetric limit in which both fermions and bosons have the same parities and therefore the same bulk mass. In this case, we find that the total contributions of the KK modes vanishes, as expected. Of course, the appearance of zero modes for the matter and gauge partners also cancels the SM result.

Then, we collect all the QED contributions and we obtain:

$$\Delta a_\mu^{QED} = \frac{e^2}{16\pi^2}(mR)^2\frac{\pi^2}{18} \tag{5.19}$$

5.3.2 Neutral Weak sector

In this section we consider all the diagrams involving Z hypermultiplet fields and neutral Higgs. We define

$$\begin{aligned} g_L &= \frac{1}{c}\left(-\frac{1}{2}+s^2\right)\ g \\ g_R &= -\frac{s^2}{c}\ g \end{aligned}$$

The one loop SM result [72] comes from graph IV with a zero mode Z boson and couplings $g_- = g_L$, $g_+ = -g_R$:

$$a_\mu^Z = \frac{g^2}{48\pi^2}\frac{m^2}{M_Z^2}\frac{4s^4 - 2s^2 - 1}{c^2} \tag{5.20}$$

The discussion for the KK modes mimics the QED case, thus in the following we only point out the differences.

KK vectors

The interaction lagrangian consists in

$$\overline{\mu}_0\overline{\sigma}_\rho\frac{1}{\sqrt{2}}\{j_L^+\mu_n^+ + j_L^-\mu_n^-\}Z_n^\rho + \overline{\mu}_0^c\overline{\sigma}_\rho\frac{1}{\sqrt{2}}\{j_R^+\mu_n^{c+} + j_R^-\mu_n^{c-}\}Z_n^\rho + h.c. \tag{5.21}$$

where:

$$\begin{aligned} j_L^+ &= g_L + \frac{\epsilon}{2(2n)}\left(g_L + g_R\right) \qquad & j_R^+ &= -g_R - \frac{\epsilon}{2(2n)}\left(g_R + g_L\right) \\ j_L^- &= g_L - \frac{\epsilon}{2(2n)}\left(g_L + g_R\right) \qquad & j_R^- &= -g_R + \frac{\epsilon}{2(2n)}\left(g_R + g_L\right) \end{aligned} \tag{5.22}$$

The two Δa_μ then amount to

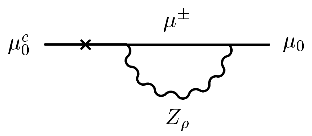

$$\Rightarrow \frac{1}{16\pi^2}\frac{\epsilon^2}{(2n)^2}\int dx(g_L^2 + g_R^2)\left[2x(1-x)^2 - 4x(1-x)\right] \tag{5.23}$$

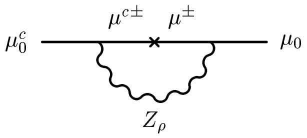

$$\Rightarrow -\frac{1}{16\pi^2}\frac{\epsilon^2}{(2n)^2}\int dx\left[\left(g_Lg_R + \frac{1}{2}(g_L+g_R)^2\right)8x(1-x) - g_Lg_R16x(1-x)^2\right] \tag{5.24}$$

Scalars

With respect to the QED case (5.13), the lagrangian for scalar fields is a bit more complicated, involving also mixing terms with φ_{H^0}, the imaginary part of ϕ_{H^0}. With the gauge fixing piece already included, the lagrangian for each mode n is:

$$\mathcal{L}_{mass} = -\partial_\rho Z^\rho\left(\frac{2n}{R}Z_5 - M_Z\varphi_{H^0}\right) - \frac{1}{2}\left[\frac{2n}{R}\varphi_{H^0} - M_ZZ_5\right]^2 - \frac{1}{4}M_Z^2\varphi_{H^0}^2 - \frac{1}{2}\left(\frac{2n}{R}\right)^2\sigma_Z^2 - \frac{1}{2\xi}\left[\partial_\rho Z^\rho - \xi\left(\frac{2n}{R}Z_5 - M_Z\varphi_{H^0}\right)\right]^2 \tag{5.25}$$

Vector-scalar mixings are again cancelled and, for $\xi = 1$, there are no off-diagonal terms $\varphi_{H^0} Z_5$, so the three real scalars σ_Z, Z_5, φ_{H^0} are the mass eigenstates. The first two combine in the complex field Σ_Z in terms of which, at the relevant order in ϵ, only the external cross graph is possible:

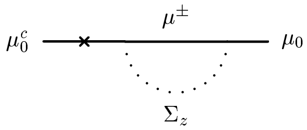

$$\Rightarrow \frac{1}{16\pi^2} \frac{\epsilon^2}{(2n)^2} \int dx (g_L^2 + g_R^2)\, 2x(1-x)^2 \tag{5.26}$$

Fermions

The mixing matrix for the four neutralinos $\tilde{z}$, $\tilde{z}_c$, ψ_{H^0}, $\psi^c_{H^0}$, for each mode n, is:

$$\mathcal{L}_{mass} = (\psi_{H^0}, \tilde{z}) \begin{pmatrix} \frac{2n-1}{R} & M_Z \\ -M_Z & \frac{2n-1}{R} \end{pmatrix} \begin{pmatrix} \psi^c_{H^0} \\ \tilde{z}_c \end{pmatrix} \tag{5.27}$$

They are involved in the following interaction terms:

$$\begin{aligned} &\sqrt{2}\mu_0 \tilde{z}_n \frac{1}{\sqrt{2}} \left\{ g_L(\Phi_n^{\dagger -} - \Phi_n^{\dagger +}) + (g_L - g_R) \frac{\epsilon}{2(2n-1)} (\Phi_n^{\dagger -} + \Phi_n^{\dagger +}) \right\} + \\ &+ \sqrt{2}\mu_0^c \tilde{z}_n \frac{1}{\sqrt{2}} \left\{ g_L \leftrightarrow g_R \quad \text{and} \quad \Phi \leftrightarrow \Phi^c \right\} + \\ &+ \sqrt{2}\mu_0^c \tilde{z}_n^c \frac{1}{\sqrt{2}} \left\{ g_R(\Phi_n^- + \Phi_n^+) - (g_R - g_L) \frac{\epsilon}{2(2n-1)} (\Phi_n^- - \Phi_n^+) \right\} + \\ &+ \sqrt{2}\mu_0 \tilde{z}_n^c \frac{1}{\sqrt{2}} \left\{ g_L \leftrightarrow g_R \quad \text{and} \quad \Phi \leftrightarrow \Phi^c \right\} + \\ &+ 2\frac{\epsilon}{v} \left\{ \mu_0 \frac{1}{\sqrt{2}} (\Phi_n^- + \Phi_n^+) + \mu_0^c \frac{1}{\sqrt{2}} (\Phi_n^{c-} + \Phi_n^{c+}) \right\} \psi^c_{H,n} \end{aligned} \tag{5.28}$$

The external cross graphs are readily computed:

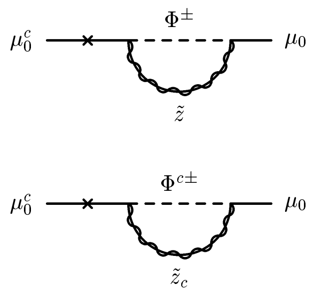

$$\Rightarrow -\frac{1}{16\pi^2} \frac{\epsilon^2}{(2n-1)^2} \int dx (g_L^2 + g_R^2)\, 2x(1-x)^2 \times 2 \tag{5.29}$$

and it is possible to write three internal cross diagrams, using also the off-diagonal propagator in eq. (5.27):

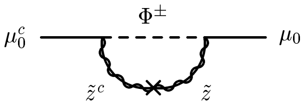

$$\Rightarrow -\frac{1}{16\pi^2}\frac{\epsilon^2}{(2n-1)^2}\int dx\,\left[(g_L^2-g_R^2)2x(1-x)+g_Lg_R8x(1-x)^2\right] \quad (5.30)$$

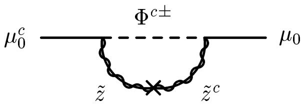

$$\Rightarrow -\frac{1}{16\pi^2}\frac{\epsilon^2}{(2n-1)^2}\int dx\,\left[(g_R^2-g_L^2)2x(1-x)+g_Lg_R8x(1-x)^2\right] \quad (5.31)$$

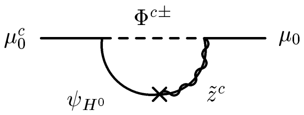

$$\Rightarrow -\frac{1}{16\pi^2}\frac{\epsilon^2}{(2n-1)^2}\int dx\frac{g}{c}(g_L+g_R)\,4x(1-x) \quad (5.32)$$

Total neutral weak contribution

Again, as in case of QED, one can check that in the supersymmetric limit, discussed above, the contribution of the KK modes vanishes. Moreover, in the limit $g_L = -g_R = e$, the QED results are recovered.

Then, we sum up all the results of the neutral weak sector and obtain:

$$\Delta a_\mu^Z = \frac{g^2}{16\pi^2}(mR)^2\frac{1}{c^2}\left(\frac{1}{4}-\frac{s^2}{3}+\frac{2s^4}{3}\right)\frac{\pi^2}{12} \quad (5.33)$$

5.3.3 Charged Weak sector

In this section we consider all the diagrams involving $W^{\pm}$ hypermultiplets fields and charged Higgs. The SM result [73] comes from graph *III*, where the loop contains a zero mode W boson and a neutrino and $g_+ = g/\sqrt{2}$, $g_- = 0$:

$$a_\mu^W = \frac{5g^2}{96\pi^2}\frac{m^2}{M_W^2} \quad (5.34)$$

KK vectors

The interaction terms involving the KK vectors are quite simple

$$\frac{g}{\sqrt{2}}W_n^\rho\,\mu_0\sigma_\rho\overline{\psi}_{\nu,n} - \frac{g}{2\sqrt{2}}\frac{\epsilon}{2n}W_n^\rho\,\mu_0^c\sigma_\rho\overline{\psi}_{\nu,n} \quad (5.35)$$

and the external and internal cross diagrams are readily computed using graph *III*:

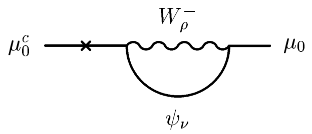

$$\Rightarrow\ -\frac{g^2}{16\pi^2}\frac{\epsilon^2}{(2n)^2}\int dx\ (1-x)^2(x-3/2) \tag{5.36}$$

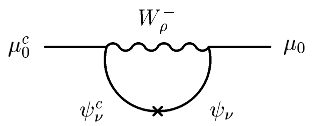

$$\Rightarrow\ \frac{g^2}{16\pi^2}\frac{\epsilon^2}{(2n)^2}\int dx\ \frac{3}{2}(1-x)^2 \tag{5.37}$$

There also are diagrams of type V. The only nonvanishing one has a Higgs scalar, since the contributions of W_5 and σ_W cancel out:

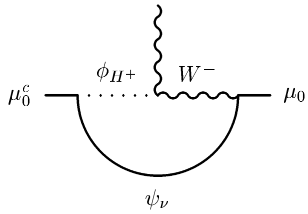

$$\Rightarrow\ \frac{g^2}{16\pi^2}\frac{\epsilon^2}{(2n)^2}\int dx\ (1-x)^2 \tag{5.38}$$

Scalars

The gauge fixing procedure works as in the Z's case: the interaction lagrangian terms only allow for an external cross contribution:

$$g\big(\psi_\nu^c\Sigma^+\psi_L+\psi_L^c\Sigma^-\psi_\nu+h.c.\big)$$

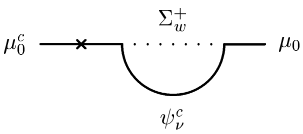

$$\Rightarrow -\frac{g^2}{16\pi^2}\frac{\epsilon^2}{(2n)^2}\int dx\ x(1-x)^2 \tag{5.39}$$

Fermions

The charginos $\tilde{w}^-$, $\tilde{w}_c^-$, ψ_{H^+}, $\psi_{H^+}^c$ mix for each n according to:

$$\mathcal{L}_{mass}=\big(\psi_{H^+},\tilde{w}_c^-\big)\begin{pmatrix}\frac{2n-1}{R} & \sqrt{2}M_W\\ -\sqrt{2}M_W & \frac{2n-1}{R}\end{pmatrix}\begin{pmatrix}\psi_{H^+}^c\\ \tilde{w}^-\end{pmatrix}-\frac{2n-1}{R}\tilde{w}_c^+\tilde{w}^+ \tag{5.40}$$

They enter the following interaction terms

$$
\begin{aligned}
& g\phi^{\dagger}_{\nu,n}\tilde{w}^{+}_{n}\mu_0 - g\frac{\epsilon}{2(2n-1)}\phi^{c\dagger}_{\nu,n}\tilde{w}^{-}_{n}\mu^{c}_{0} + \\
& g\phi^{c}_{\nu,n}\tilde{w}^{-}_{c,n}\mu_0 + g\frac{\epsilon}{2(2n-1)}\phi_{\nu,n}\tilde{w}^{+}_{c,n}\mu^{c}_{0} \\
& -\frac{2m}{v}\mu^{c}_{0}\psi^{c}_{H^+,n}\phi^{c\dagger}_{\nu,n}
\end{aligned} \tag{5.41}
$$

The external cross diagrams are of the usual form

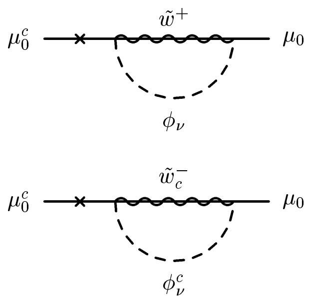

$$
\Rightarrow \frac{g^2}{16\pi^2}\frac{\epsilon^2}{(2n-1)^2}\int dx\; x(1-x)^2 \times 2 \tag{5.42}
$$

and there are three internal cross diagrams with propagators $(\tilde{w}^+)^\dagger$— $\tilde{w}^+_c$, $(\tilde{w}^-_c)^\dagger$— $\tilde{w}^-$ and $(\tilde{w}^-_c)^\dagger$— $\phi^c_{H^+}$:

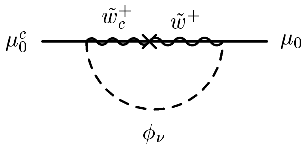

$$
\Rightarrow \frac{g^2}{16\pi^2}\frac{\epsilon^2}{(2n-1)^2}\int dx\; (1-x)^2 \tag{5.43}
$$

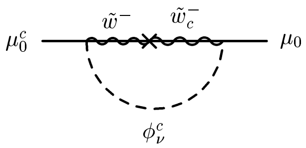

$$
\Rightarrow -\frac{g^2}{16\pi^2}\frac{\epsilon^2}{(2n-1)^2}\int dx\; (1-x)^2 \tag{5.44}
$$

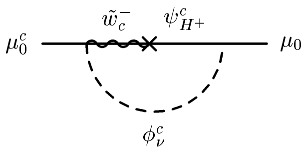

$$
\Rightarrow -\frac{g^2}{16\pi^2}\frac{\epsilon^2}{(2n-1)^2}\int dx\; 4(1-x)^2 \tag{5.45}
$$

Total charged weak contribution

Again in this case, we correctly find that in the supersymmetric limit the sum of the KK states contributions vanishes.

We then gather all the contributions of the charged weak sector into the result:

$$\Delta a_\mu^W = -\frac{g^2}{16\pi^2}(mR)^2\frac{7}{6}\frac{\pi^2}{12} \tag{5.46}$$

5.3.4 Result to leading order in $(M_W R)^2$

Collecting all partial results (5.19), (5.33) and (5.46) we have:

$$\Delta a_\mu^{KK} = -\frac{g^2}{192}\frac{m^2}{M_W^2}\frac{11-18s^2}{12c^2}(M_W R)^2 \tag{5.47}$$

Numerically, for $1/R = 370 \pm 70\,GeV$, it is

$$\Delta a_\mu^{KK} = 0.07\,{}^{+0.06}_{-0.02} \cdot a_\mu^{weak} = -(1.1\,{}^{+0.6}_{-0.3}) \cdot 10^{-10},$$

which means that, for any sensible value of R (see [33]), Δa_μ^{KK} is well inside the uncertainties that affect the SM prediction.

5.4 $M_W R$ corrections

In the previous section, we have neglected the ElectroWeak Symmetry Breaking in the masses of the KK modes for the gauge fields, since this was enough to get eq. (5.47). However, in this way we are neglecting contributions that in principle can be quite relevant, since the dimensionless expansion parameters $M_W R$ or $M_Z R$ can be as large as 1/3. In this chapter we estimate these contributions. They are recovered if the full gauge fields masses are kept in the denominators of eq. (5.50)–(5.54), so the corrections to our previous results can be expressed in a simple way. Of course, these corrections only apply to the pure weak sector.

To begin with, let us focus on the neutral weak sector. First of all, what we have to do is to study the exact spectrum: defining the dimensionless parameter $\zeta = M_Z R$, for every n there is a vector boson Z_μ whose full mass squared is $(2n)^2 + \zeta^2$, in unit of $1/R^2$. The scalars fields masses are determined from eq. (5.25): the n^{th} KK mode of Σ_z has mass squared $(2n)^2 + \zeta^2$, while, for the real field φ_{H^0}, it has mass squared $(2n)^2 + \frac{3}{2}\zeta^2$. For the neutralinos, diagonalization of eq. (5.27) shows that there are two degenerate states with mass squared $(2n-1)^2 + \zeta^2$. The rest of the computation proceeds as in the previous section. To get the modified results, it is sufficient to substitute the sum $\sum \frac{1}{(2n)^2}$ in eqs. (5.23), (5.24), (5.26), (5.29)–(5.32) with:

$$\sum \frac{1}{N^2+\zeta^2} \quad \text{or} \quad \sum \frac{N^2}{(N^2+\zeta^2)^2}$$

where $N = 2n$ for bosons and $N = 2n-1$ for fermions. The first is the one to be used in all external cross diagrams, while for internal cross ones the formulae are a bit more involved. To be specific, in the case of the vectors, eq. (5.24) becomes:

$$
-\frac{1}{16\pi^2}\epsilon^2 \int dx \left[\left(g_L g_R + \frac{1}{2}(g_L + g_R)^2 \right) 8x(1-x)\frac{1}{(2n)^2+\zeta^2} - g_L g_R\, 16x(1-x)^2 \frac{(2n)^2}{((2n)^2+\zeta^2)^2} \right] \quad (5.48)
$$

With a bit of algebra, all contributions can be recast in a common form and the net result is:

$$
\Delta a_\mu^Z = \frac{1}{16\pi^2}\frac{m^2}{M_W^2}(M_W R)^2 \left\{ (g_L^2 + g_R^2)\, f_1(\zeta) + g_L g_R\, f_2(\zeta) \right\} \quad (5.49)
$$

where the functions f_1 and f_2 are defined in app. B. This replaces eq. (5.33), with all corrections to any order in $(M_W R)^2$ included. Numerically, for $1/R = 370 \pm 70\, GeV$, the result is only about 3% smaller than eq. (5.33). In the case of the charged weak sector, the calculation is very similar, so we expect the correction to be not so far from a few percent.

5.5 Conclusions

In this chapter we have performed the calculation at one loop of the corrections to muon anomalous magnetic moment coming from the presence of one extra dimension in the model in ref. [28], to first order in $(mR)^2$ and in $(M_W R)^2$. We have also shown that the complete calculation in $(M_W R)^2$ yields small deviations, so to our purposes the simple analytic form given in eq. (5.47) is a good approximation. The corrections are relatively small, for any sensible value of R, at the 10% level of the pure weak contribution in the SM, and well inside the uncertainties of the hadronic contribution.

Appendix A

In this appendix we list the contributions to a_μ from the five graphs[2] in figure 5.1:

$$\Delta a_\mu^I = \frac{Q_s}{16\pi^2} m^2 \int_0^1 dx \left[\frac{h_+^2 + h_-^2}{2} 2x(1-x)^2 + \frac{m_f}{m} h_+ h_- 2x(1-x) \right] \frac{1}{x m_f^2 + (1-x) m_s^2 - x(1-x) m^2} \tag{5.50}$$

$$\Delta a_\mu^{II} = -\frac{Q_f}{16\pi^2} m^2 \int_0^1 dx \left[\frac{h_+^2 + h_-^2}{2} 2x(1-x)^2 + \frac{m_f}{m} h_+ h_- 2(1-x)^2 \right] \frac{1}{x m_s^2 + (1-x) m_f^2 - x(1-x) m^2} \tag{5.51}$$

$$\Delta a_\mu^{III} = \frac{Q_v}{16\pi^2} m^2 \int_0^1 dx \left[\frac{g_+^2 + g_-^2}{2} 2(1-x)^2(2x-3) + g_+ g_- \frac{m_f}{m} 6(1-x)^2 \right] \frac{1}{x m_f^2 + (1-x) m_v^2 - x(1-x) m^2} \tag{5.52}$$

$$\Delta a_\mu^{IV} = -\frac{Q_f}{16\pi^2} m^2 \int_0^1 dx \left[\frac{g_+^2 + g_-^2}{2} \left(4x(1-x)^2 - 8x(1-x)\right) + \frac{m_f}{m} g_+ g_- 8x(1-x) \right] \frac{1}{x m_v^2 + (1-x) m_f^2 - x(1-x) m^2} \tag{5.53}$$

$$\Delta a_\mu^V = \frac{Q_v}{16\pi^2} m\tau \int_0^1 dx (g_+ h_+ + g_- h_-)(1-x)^2 \frac{1}{x m_f^2 + (1-x) m_v^2 - x(1-x) m^2} \tag{5.54}$$

where $Q_{s,f,v}$ are the electric charges of the particles emitting the zero-mode photon and $m_{s,f,v}$ are the masses in the loop. Note that in eq. (5.54) we assume $m_s = m_v$. The couplings are defined by:

$$\begin{gathered} v_\rho \overline{f} \gamma^\rho \left[g_+ \mathcal{P}^+ + g_- \mathcal{P}^- \right] \mu \\ s \overline{f} \left[h_+ \mathcal{P}^+ + h_- \mathcal{P}^- \right] \mu \\ e\tau s^+ W_\rho^- A^\rho \\ e \left[g^{\nu\rho}(k - p_+)^\sigma + g^{\rho\sigma}(p_+ - p_-)^\nu + g^{\sigma\nu}(p_- - k)^\rho \right] W_\rho^+ W_\sigma^- A_\nu \end{gathered}$$

where $P^\pm$ are projectors on the two Weyl components of the Dirac fields.

[2]Similar results can also be found in refs. [74].

Appendix B

In this appendix we list the functions to be inserted in eq. (5.49):

$$
\begin{aligned}
f_1 &= \frac{1}{\zeta^8}\int_0^\zeta dy\; 2(\zeta^4-y^4)\left(\pi y^2 \tanh\left(\frac{\pi}{2}y\right)-\pi y^2 \coth\left(\frac{\pi}{2}y\right)+2y\right)= \\
&= \frac{4}{3\zeta^2}+\frac{1}{3\pi^6\zeta^8}\Big[48\pi^5\zeta^5\left(\mathrm{Li}_2\left(-e^{-\pi\zeta}\right)-\mathrm{Li}_2\left(e^{-\pi\zeta}\right)\right)+336\pi^4\zeta^4\left(\mathrm{Li}_3\left(-e^{-\pi\zeta}\right)-\mathrm{Li}_3\left(e^{-\pi\zeta}\right)\right) \\
&+1440\pi^3\zeta^3\left(\mathrm{Li}_4\left(-e^{-\pi\zeta}\right)-\mathrm{Li}_4\left(e^{-\pi\zeta}\right)\right)+4320\pi^2\zeta^2\left(\mathrm{Li}_5\left(-e^{-\pi\zeta}\right)-\mathrm{Li}_5\left(e^{-\pi\zeta}\right)\right)+ \\
&+8640\pi\zeta\left(\mathrm{Li}_6\left(-e^{-\pi\zeta}\right)-\mathrm{Li}_6\left(e^{-\pi\zeta}\right)\right)+8640\left(\mathrm{Li}_7\left(-e^{-\pi\zeta}\right)-\mathrm{Li}_7\left(e^{-\pi\zeta}\right)\right)+ \\
&-42\pi^4\zeta^4\,\zeta(3)+17145\,\zeta(7)\Big]
\end{aligned}
$$

$$
\begin{aligned}
f_2 &= \frac{1}{\zeta^8}\int_0^\zeta dy\; 8(y^2-\zeta^2)(3y^2-2\zeta^2)\left(\pi y^2 \tanh\left(\frac{\pi}{2}y\right)-\pi y^2 \coth\left(\frac{\pi}{2}y\right)+2y\right)= \\
&= \frac{4}{\zeta^2}-\frac{4}{\pi^6\zeta^8}\Big[8\pi^5\zeta^5\left(\mathrm{Li}_2\left(-e^{-\pi\zeta}\right)-\mathrm{Li}_2\left(e^{-\pi\zeta}\right)\right)+136\pi^4\zeta^4\left(\mathrm{Li}_3\left(-e^{-\pi\zeta}\right)-\mathrm{Li}_3\left(e^{-\pi\zeta}\right)\right)+ \\
&+960\pi^3\zeta^3\left(\mathrm{Li}_4\left(-e^{-\pi\zeta}\right)-\mathrm{Li}_4\left(e^{-\pi\zeta}\right)\right)+3840\pi^2\zeta^2\left(\mathrm{Li}_5\left(-e^{-\pi\zeta}\right)-\mathrm{Li}_5\left(e^{-\pi\zeta}\right)\right)+ \\
&+8640\pi\zeta\left(\mathrm{Li}_6\left(-e^{-\pi\zeta}\right)-\mathrm{Li}_6\left(e^{-\pi\zeta}\right)\right)+8640\left(\mathrm{Li}_7\left(-e^{-\pi\zeta}\right)-\mathrm{Li}_7\left(e^{-\pi\zeta}\right)\right)+ \\
&+28\pi^4\zeta^4\,\zeta(3)-930\pi^2\zeta^2\,\zeta(5)+17145\,\zeta(7)\Big]
\end{aligned}
$$

where $\zeta(n)$ is the Riemann zeta function, not to be confused here with our variable $\zeta = M_Z R$. In the integrals, the hyperbolic tangent is produced by the sum over the fermionic KK states, while the cotangent and the "$2y$" pieces by the bosonic states.

Chapter 6

Gluon fusion into Higgs in a model with one extra dimension

In this chapter, based on ref. [75], I deal with the computation of the Higgs decay width into two gluons in the framework of the theory presented in chapter 4.

The main interest about this process is that it can be related to the cross section for Higgs production [76] through gluon fusion. At a large hadron collider (LHC), this is expected to be the most important channel for light SM Higgs [77].

Motivated by the modifications mentioned in chapter 4, I will consider here a limited band of variability for the Higgs mass and the compactification radius: m_H lies in the range $120 \div 160$ GeV, while $1/R$, which is correlated to the Higgs mass, can increase up to about a TeV [33, 37]. Recall that the center values in the unmodified theory are $m_H = 127 \pm 8$ GeV and $1/R = 370 \pm 70$ GeV.

Moreover, we will focus only on zero mode gluon fusion since we expect the parton distribution of KK gluons in the proton to be negligibly small.

6.1 Necessary ingredients from the theory

The relevant lagrangian for our calculation comes from the quark Yukawa interactions, located on the branes. We remind that the vertices of gluon emission are the same for all the KK states, with 4-dimensional coupling $g_s = g_s^{(5)}/\sqrt{2\pi R}$. In terms of mass eigenstates, for every flavour q the Lagrangian is:

$$\mathcal{L}_{int} = -\sum_{n=1}^{\infty} \Big\{ \big(\tilde{m}_n^{\pm}(\phi_H)\big)^2 \big(\Phi_n^{\dagger\pm}\Phi_n^{\pm} + \Phi_n^{c\dagger\pm}\Phi_n^{c\pm}\big) + \big(m_n^{\pm}(\phi_H)\,\psi_n^{c\pm}\psi_n^{\pm} + h.c.\big) \Big\} - \big(m_0(\phi_H)\,\psi_0^c\psi_0 + h.c.\big) \quad (6.1)$$

where m_0, $m_n^{\pm}$ and $\tilde{m}_n^{\pm}$ are the field dependent masses for quark and squark towers. They have the same form for every flavor q, even if the mass matrices arising from Yukawa couplings, y_q, located on different branes are not the same (see Appendix):

$$\begin{cases} \tilde{m}_n^{\pm} &= \frac{2n-1}{R} \pm m_q(\phi_H) \\ m_n^{\pm} &= m_q(\phi_H) \pm \frac{2n}{R} \\ m_0 &= m_q(\phi_H) = \frac{2}{\pi R}\arctan\left(\frac{\pi}{2} y_q R \phi_H\right) \end{cases} \tag{6.2}$$

Substituting for the complex field $\phi_H = v + H/\sqrt{2}$, this provides us with the full expression of the couplings of the Higgs field H to the mass eigenstates. Taking the linear terms in H and keeping all orders in $m_q R = \epsilon_q$, we find:

$$\mathcal{L}_{int} = -\lambda_q\, \psi_0 \psi_0^c H - \lambda_q \sum_{n=1}^{\infty} \psi_n^{\pm} \psi_n^{\pm c} H + h.c. - \lambda_q \sum_{n=1}^{\infty} (\pm) 2 \tilde{m}_n^{\pm}(v) \left(\Phi_n^{\pm\dagger} \Phi_n^{\pm} + \Phi_n^{c\pm\dagger} \Phi_n^{c\pm}\right) H \tag{6.3}$$

where

$$\lambda_q = \frac{1}{\sqrt{2}} y_q \frac{1}{1+\tan^2(\frac{\pi}{2}\epsilon_q)} = \sqrt{\frac{G_F}{\sqrt{2}}}\, \frac{2\sqrt{2}}{\pi R} \frac{\tan(\frac{\pi}{2}\epsilon_q)}{1+\tan^2(\frac{\pi}{2}\epsilon_q)} \tag{6.4}$$

Note that the Yukawa coupling is related to the Fermi constant $\frac{G_F}{\sqrt{2}} = \frac{1}{4v^2}$ in a non trivial way, due to the mixing with the massive KK states. The standard expression, $\lambda_q = \sqrt{\frac{G_F}{\sqrt{2}}} \sqrt{2} m_q$, is recovered for $R \to 0$.

6.2 The calculation

The graphs that contribute at one loop are shown in figure 6.1. For a color triplet scalar ϕ and a color triplet fermion Ψ with mass m_s and m_f respectively, coupled to the Higgs field via $\mathcal{L} = \lambda_f \overline{\Psi} \Psi H + \lambda_s \phi^\dagger \phi H$, the amplitude can be written as:

$$\mathcal{A}^{ab} = -\frac{\alpha_s}{4\pi} \frac{\delta^{ab}}{2} \left[(p_1 \cdot \varepsilon_2)(p_2 \cdot \varepsilon_1) - (p_1 \cdot p_2)(\varepsilon_1 \cdot \varepsilon_2)\right] \mathcal{F} \tag{6.5}$$

where ε_i and p_i are the gluon polarizations and momenta, and

$$\begin{aligned} \mathcal{F}_{ferm} &= -8 \lambda_f m_f \int_0^1 dx \int_0^{1-x} dy\, \frac{1-4xy}{m_f^2 - p^2 xy} \\ \mathcal{F}_{scal} &= -2\lambda_s \int_0^1 dx \int_0^{1-x} dy\, \frac{4xy}{m_s^2 - p^2 xy}. \end{aligned} \tag{6.6}$$

Let us first review the Standard Model result [80]. In the present context it comes from the zero mode fermionic graph for $\lambda_f = y_q$, and it amounts to:

$$\mathcal{F}_{SM} = \frac{8}{3} \frac{1}{v} \sum_q A_{SM}(\xi_q) \tag{6.7}$$

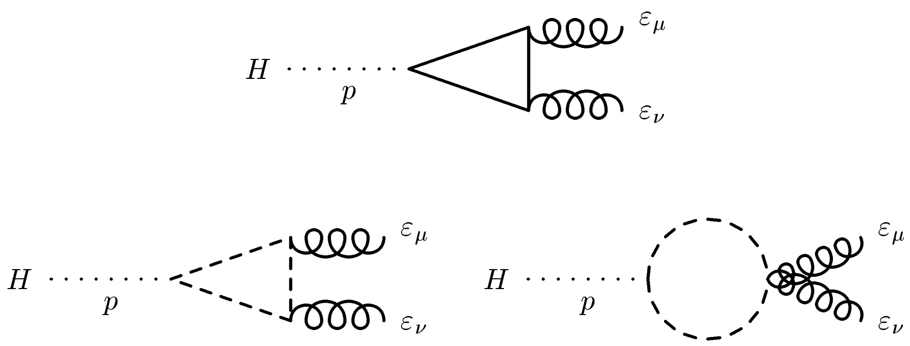

Figure 6.1: Feynman diagrams contributing at 1-loop to $H \to gg$. Dashed lines stand for scalars, full lines for fermions.

where $\xi_q = \dfrac{p^2}{m_q^2} = \dfrac{m_H^2}{m_q^2}$,

$$A_{SM}(\xi) = \frac{3}{\xi^2}\left\{2\xi + \left(\xi - 4\right) g(\xi)\right\}$$

and the function g is

$$g(\xi) = \begin{cases} 2\arcsin^2\left(\frac{\sqrt{\xi}}{2}\right) & \xi \leq 4 \\ -\frac{1}{2}\left[\log\left(\frac{1+\sqrt{1-4\xi^{-1}}}{1-\sqrt{1-4\xi^{-1}}}\right) - i\pi\right]^2 & \xi > 4 \end{cases}$$

The decay width is related to the amplitude, after summing over polarizations and color indices of the final state gluons. In the SM it is:

$$\Gamma_{SM}(H \to gg) = \frac{G_F}{\sqrt{2}}\frac{\alpha_s^2 m_H^3}{36\pi^2}\left|\sum_q A_{SM}(\xi_q)\right|^2 = \Gamma_0 \left|\sum_q A_{SM}(\xi_q)\right|^2 \tag{6.8}$$

The main contribution comes from top loops, while the other quarks contribute to a few percent. The dependence on the Higgs mass, apart from the m_H^3 factor in Γ_0, is encoded in ξ, in such a way that the functions A_{SM} run from ≈ 0.9, for $m_H = 120\, GeV$, up to ≈ 1 for $m_H = 160\, GeV$.

Let us now move to our model. The couplings are given in eq. (6.4), and we consider contributions from top and stop KK towers. Defining $\epsilon = m_t R$ and $\xi = \dfrac{m_H^2}{m_t^2}$, the result can be written as:

$$\mathcal{F}_f = 8\lambda_t R \int dxdy\, (1 - 4xy)\left\{\frac{1}{\epsilon}\frac{1}{1-\xi xy} + f(x,y,\xi,\epsilon)\right\} \tag{6.9}$$

$$\mathcal{F}_s = 4\lambda_t R \int dxdy\, 4xy\; s(x,y,\xi,\epsilon) \times 2 \tag{6.10}$$

where the factor two in $\mathcal{F}_s$ takes in account the two KK towers of scalar partners and the functions f and s contain the contributions of the KK modes:

$$\begin{cases} f &= \sum_{n=1}^{\infty} \left(\frac{\epsilon + 2n}{(2n+\epsilon)^2 - \xi\epsilon^2 xy} + \frac{\epsilon - 2n}{(2n-\epsilon)^2 - \xi\epsilon^2 xy} \right) \\ s &= \sum_{n=1}^{\infty} \left(\frac{\epsilon + 2n - 1}{(2n-1+\epsilon)^2 - \xi\epsilon^2 xy} + \frac{\epsilon - 2n + 1}{(2n-1-\epsilon)^2 - \xi\epsilon^2 xy} \right) \end{cases} \tag{6.11}$$

Let us remind that the Higgs mass depends on R, so that in our model the two parameters ϵ and ξ are related to each other.

6.2.1 $\xi \to 0$ limit

To compute the KK state contribution exactly is not a trivial task. As a first step we note that the sums in f and s simplify in the limit $\xi \to 0$. In this case we are neglecting contributions of relative order $\mathcal{O}(m_H R)^2$. These contributions may be important expecially for large R, where $m_H \approx 120\, GeV$ and then $m_H R \gtrsim 0.4$. However, we use this limit just to have a reliable estimate for small radius ($1/R \approx 1\, TeV$), where $m_H \approx 160\, GeV$ and then $m_H R \approx 0.15$, and to have an analytic control on the calculation.

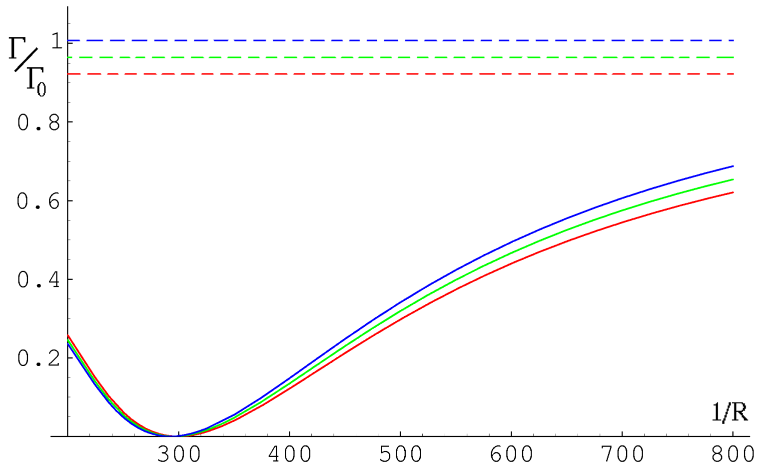

Figure 6.2: Plot of Γ/Γ_0 as a function of $1/R$, for fixed values of $m_H = 120$ (red), 140 (green) and 160 GeV (blue); the upper three lines are the corresponding SM results.

In this case, the result is:

$$\Gamma(H \to gg) = \Gamma_0 \left| \frac{2}{\pi\epsilon} \frac{\tan\left(\frac{\pi}{2}\epsilon\right)}{1 + \tan^2\left(\frac{\pi}{2}\epsilon\right)} \left[A_t - 1 + \frac{1}{2}\pi\epsilon\cot\left(\frac{\pi}{2}\epsilon\right) - \frac{1}{4}\pi\epsilon\tan\left(\frac{\pi}{2}\epsilon\right) \right] + A_b \right|^2 \tag{6.12}$$

where $A_{t,b} = A_{SM}(\xi_{t,b})$.

As we can see from figure 6.2, the dependence on the Higgs mass in eq. (6.12) is smooth in the range $120 \div 160\, GeV$ and then the correlation between m_H and R can be consistently neglected. The decay width is significantly different from the SM one and, in particular, it vanishes for $1/R \approx 300\, GeV$ (that corresponds to $m_H \approx 120\, GeV$ [33, 37]). This means that the contributions of the top and stop KK modes cancel the SM result. It is relevant that this happens for every value of A_b.[1]

Also notice that for the unphysical value $1/R = m_t$ the decay width diverges. This is a remnant of the approximation we are working in, as corrections $\mathcal{O}(m_H R)^2$ are relevant in this region.

6.2.2 Full calculation

In the previous paragraph, the dependence on m_H has been kept only in the SM result. This is, as we saw, an approximation less appropriate for small values of $1/R$. In order to evaluate how the result fully depends on m_H, one could keep the ξ dependence in eq. (6.11) and then expand in the parameter ϵ. But, two issues arise. The first one is that if we expand eq. (6.12), the series is oscillatory, and stabilizes only at very high order in ϵ. The second point is that for small $1/R$ the parameter ϵ is too large and the expansion is not meaningfull.

What one can rather do is to perform the sums in f and s and then evaluate numerically the residual integrals on Feynman parameters x and y. The functions f and s can be simplified to:

$$\begin{aligned}
f &= -2\epsilon \sum_{n=1}^{\infty} \frac{1}{(2n+\epsilon\sqrt{\xi xy})^2-\epsilon^2} &= \frac{1}{2}\left[\psi\left(\frac{2+\epsilon\left(\sqrt{\xi xy}-1\right)}{2}\right)-\psi\left(\frac{2+\epsilon\left(\sqrt{\xi xy}+1\right)}{2}\right)\right] \\
s &= -2\epsilon \sum_{n=1}^{\infty} \frac{1}{(2n-1+\epsilon\sqrt{\xi xy})^2-\epsilon^2} &= \frac{1}{2}\left[\psi\left(\frac{1+\epsilon\left(\sqrt{\xi xy}-1\right)}{2}\right)-\psi\left(\frac{1+\epsilon\left(\sqrt{\xi xy}+1\right)}{2}\right)\right]
\end{aligned} \tag{6.13}$$

where $\psi(z) = \Gamma'(z)/\Gamma(z)$ is the polygamma function of order zero. Now, the net result is:

$$\Gamma = \Gamma_0 \left| \frac{2}{\pi\epsilon} \frac{\tan\left(\frac{\pi}{2}\epsilon\right)}{1+\tan^2\left(\frac{\pi}{2}\epsilon\right)} \Big[A_t + 3\epsilon\, \Xi(\xi,\epsilon)\Big] + A_b \right|^2 \tag{6.14}$$

where

$$\Xi = \int_0^1 dx \int_0^{1-x} dy\, \big[(1-4xy)f + 4xys\big].$$

Eq. (6.14) contains the exact dependence on the related parameters ϵ and ξ. In order to estimate how the approximation in the previous paragraph works, we fix $m_H = 127\, GeV$ and in fig. 6.3 we plot the result as a function of R compared to eq. (6.12) in the same limit. The two curves differ only slightly in the region $1/R > 300\, GeV$. Moreover, for small values of $1/R$ the apparent divergence of eq. (6.12) is not present any more.

In figure 6.3, we can also read the value of the decay width for $1/R = 370 \pm 70\, GeV$. To do this, we first have to take into account the effect of the brane z factors discussed in [28], that are the main

[1]We have checked that working out a formula similar to eq. (6.12) including also bottom KK towers, there is no significant change since the parameter ϵ_b is quite small.

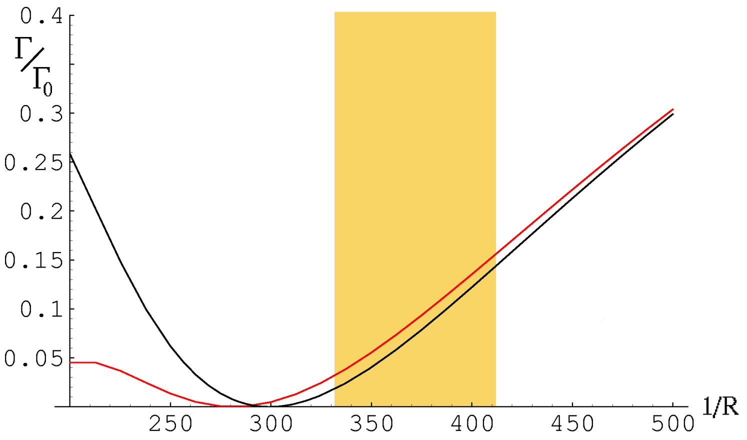

Figure 6.3: Plot of Γ/Γ_0 as a function of $1/R$ for $m_H = 127\, GeV$ (red curve). The black one is eq. (6.12), i.e. the $\xi \to 0$ limit.

source of the error on $1/R$. Eqs. (6.12) and (6.14) are actually functions of $\tilde{R} = R/(1-\overline{z})$ instead of R, since the dependence on the radius only comes from the top and stop mass eigenvalues. It is $\tilde{R}$ which is determined by the minimization of the Higgs potential, so that its uncertainty does not come from the z factors but from other sources. It is therefore estimated to be smaller, at 10% level [33]. Thus, it follows that the decay width, in the case of the center value for $1/R$, is at 5% $\div$ 15% level of the SM one and is only affected at quadratic order in z.

6.3 Conclusions

In this chapter we have calculated the full one loop amplitude for the decay width of the Higgs boson into two gluons for any value of the compactification radius. We find a result significantly suppressed with respect to the SM value. This is due to a partial cancellation between the SM and the top and stop KK tower contributions. In particular, this cancellation is complete and the cross section goes to zero for a value of $1/R \approx 300\, GeV$.

For the center value of the compactification radius of $1/R \sim 370 \pm 70 GeV$, the one loop cross section is reduced below the 15% level of the SM prediction. Notice, however, that the two loop amplitude, of order α_s^2, is expected to be relevant, since in the SM [81] it is as large as 40% of the 1-loop one.

Appendix: Mass matrices

In ref. [40], the diagonalization of the mass matrices arising from Yukawa couplings located on the brane $y = 0$ is presented. Dealing with couplings located on the brane $y = \frac{\pi}{2}R$, some subtleties appear. First of all, the matrices are, for scalars and fermions:

$$\Phi^\dagger \mathcal{M}^2 \Phi = \left(\phi^{c\dagger}_{U,l}, \phi^\dagger_{T,l}\right) \begin{pmatrix} \tilde{M}^2 + 4m^2\eta E & -2mE \cdot \tilde{M} \\ -2m\tilde{M} \cdot E & \tilde{M}^2 \end{pmatrix} \begin{pmatrix} \phi^c_{U,k} \\ \phi_{T,k} \end{pmatrix} \tag{6.15}$$

$$\overline{\Psi} \mathcal{M} \Psi^c = \left(\psi_{T,0}, \psi_{T,l}, \psi^c_{U,l}\right) \begin{pmatrix} m & \sqrt{2}m\mathcal{J}^T & 0 \\ \sqrt{2}m\mathcal{J} & 2m\mathcal{J}\mathcal{J}^T & M \\ 0 & M & 0 \end{pmatrix} \begin{pmatrix} \psi_{U,0} \\ \psi_{U,k} \\ \psi^c_{T,k} \end{pmatrix} \tag{6.16}$$

where $\eta = \sum_k 1$, $M_{lk} = \frac{2l}{R}\delta_{lk}$, $\tilde{M}_{lk} = \frac{2l-1}{R}\delta_{lk}$, $\mathcal{J}_k = (-1)^k$, $E_{lk} = (-1)^{l+k}$ and $m = y_q v$. The difference with ref. [40] is the presence of some -1 signs that come from the values of the wave functions of the fields, whose dependence on y in given by their parity. But, carefully performing the calculation, it is clear that the eigenvalues coincide with those produced by the matrices on the brane $y = 0$, eq. (6.2). Note also that in this case ϕ^c is the field in the $\mathcal{N} = 1$ supermultiplet of ψ. The effect of these signs is physically relevant only when the two branes interfere. This happens when the observable receives contributions from both the branes (see for example [40]).

The calculation of these matrices deserves another comment. In fact, if we write the bulk lagrangian as in [82] and add the two brane interactions as in [28], it is not trivial how to get rid of the auxiliary fields F and F^c. For F it is straightforward since both the bulk and the $y = 0$ brane lagrangians are written in terms of the same multiplets, while for F^c we refer the reader to [83]. The result is that the term $\delta(y - \pi R/2)\partial_5\phi \frac{d}{d\phi^c} W'$, where W' is the superpotential localized on the $y = \pi R/2$ brane, has a minus sign with respect to the analogous term generated by F.

Chapter 7

Conclusions

In this thesis I briefly sketched the generic empasse that currently seems to tie particle phenomenology (chapter 1) and then I described a proposed way–out to some of those problems: the existence of Extra space Dimensions (chapter 2).
I then discussed some specific realization of the general idea.

In particular (chapter 3), in the framework of Gravitational Extra Dimensions, I dealt with the phenomenology of neutrino mixing with bulk fermions in the context of supernova physics, a sort of *bridge* linking physics beyond the Standard Model and astrophysics. On the first bank I showed that SN physics sets a much larger limit on the parameters of Extra Dimensions then previously thought. On the other bank I argued that beneficial effects for the comprehension of SN evolution can come also from the existence of Extra Dimensions.

Then (chapter 4), in the framework of Universal Extra Dimensions, I described the theory proposed by Barbieri, Hall and Nomura and then presented some examples of computations in this context.

First (chapter 5), I presented the computation of the muon anomalous magnetic moment, a sensitive test for new physics scenario thanks to its impressive precision. The deviations from the SM value are found small and well inside its errors; in this sense the model under consideration is a viable extension of the SM. Moreover, the predictive capability of the model has been shown for this quantity: the computation is reliable, i.e. insensitive to the cutoff and stable under higher order effects.

Then (chapter 6), I presented the full one loop amplitude for the decay width of the Higgs boson into two gluons, that is in turn relevant for its production rate via gluon fusion at hadron colliders. I showed that the result is significantly suppressed with respect to the SM value, a fact that is important for the possible discovery of the Higgs boson predicted by the model.

Needless to say, the discussed topics cover only a small part of the large amount of work that has been done and is to be done yet on the subject of Extra Dimensions, not to speak of the possible surprises coming from this very active field.
No one knows about the future (except for [41]) but certainly Extra Dimensions are a nice possible springboard for a jump across the present energy frontier.

Bibliography

Bibliography for introductory chapters 1, 2, 4, 7

[1] J. L. Rosner, "Resource letter: The standard model and beyond," arXiv:hep-ph/0206176;

S. Willenbrock, "The standard model and the top quark," arXiv:hep-ph/0211067, Chapter 1 only;

J. R. Ellis, "Beyond the standard model for hillwalkers," arXiv:hep-ph/9812235;

Z. Kunszt, "Bread and butter standard model", arXiv:hep-ph/0004103;

C. Quigg, "The state of the standard model", arXiv:hep-ph/0001145;

J. Womersley, "Physics beyond the standard model," J. Phys. G **26** (2000) 505 [arXiv:hep-ex/0001039].

[2] The Lep ElectroWeak Working Group, results presented at 2002 summer conferences, http://www.cern.ch/LEPEWWG/

[3] G. Altarelli, R. Barbieri and F. Caravaglios, "Electroweak precision tests: A concise review," Int. J. Mod. Phys. A **13** (1998) 1031 [arXiv:hep-ph/9712368].

[4] H. E. Montgomery, "XXXVIIieme Rencontres de Moriond: Electroweak 2002 conference summary," arXiv:hep-ex/0207002.

P. Langacker, "Recent developments in precision electroweak physics," arXiv:hep-ph/0211065.

[5] Y. Fukuda *et al.* [Super-Kamiokande Collaboration], "Evidence for oscillation of atmospheric neutrinos," Phys. Rev. Lett. **81** (1998) 1562 [arXiv:hep-ex/9807003].

[6] One can also see the very accessible and nice reviews (and references therein):

N. Schmitz, "The discovery of neutrino masses," arXiv:hep-ex/0211041.

H. Pas, "Neutrino masses and particle physics beyond the standard model," Annalen Phys. **11** (2002) 551 [arXiv:hep-ph/0209018].

[7] F. Wilczek, "Beyond the standard model: This time for real," Nucl. Phys. Proc. Suppl. **77** (1999) 511 [arXiv:hep-ph/9809509].

[8] T. Hambye and K. Riesselmann, "Matching conditions and Higgs mass upper bounds revisited," Phys. Rev. D **55** (1997) 7255 [arXiv:hep-ph/9610272], and references inside.

See also the Lep Higgs Working Group, http://lephiggs.web.cern.ch/LEPHIGGS/www/Welcome.html.

[9] R. Barbieri and A. Strumia, "The 'LEP paradox'," arXiv:hep-ph/0007265.

[10] M. Schmaltz, "Physics beyond the standard model (Theory): Introducing the little Higgs," arXiv:hep-ph/0210415.

[11] See the Lep SuSy Working Group, http://www.cern.ch/lepsusy/.

[12] V. A. Rubakov, "Large and infinite extra dimensions: An introduction," Phys. Usp. **44** (2001) 871 [Usp. Fiz. Nauk **171** (2001) 913] [arXiv:hep-ph/0104152].

M. Besancon, "Experimental introduction to extra dimensions," arXiv:hep-ph/0106165.

A. Perez-Lorenzana, "Theories in more than four dimensions," AIP Conf. Proc. **562** (2001) 53 [arXiv:hep-ph/0008333].

R. Tabbash, "Physics of extra dimensions: Higher-dimensional virtual environments," arXiv:hep-ph/0111334.

[13] K. R. Dienes, "Beautified with goodly shape: Rethinking the properties of large extra dimensions," arXiv:hep-ph/0211211.

[14] N. Arkani-Hamed, S. Dimopoulos and G. R. Dvali, "The hierarchy problem and new dimensions at a millimeter," Phys. Lett. B **429** (1998) 263 [arXiv:hep-ph/9803315].

See also:

I. Antoniadis, "A Possible New Dimension At A Few Tev," Phys. Lett. B **246** (1990) 377;

J. D. Lykken, "Weak Scale Superstrings," Phys. Rev. D **54** (1996) 3693 [arXiv:hep-th/9603133];

[15] J. C. Long, H. W. Chan, A. B. Churnside, E. A. Gulbis, M. C. Varney and J. C. Price, "New experimental limits on macroscopic forces below 100-microns," arXiv:hep-ph/0210004.

[16] N. Arkani-Hamed, S. Dimopoulos and G. R. Dvali, "Phenomenology, astrophysics and cosmology of theories with sub-millimeter dimensions and TeV scale quantum gravity," Phys. Rev. D **59** (1999) 086004 [arXiv:hep-ph/9807344].

[17] I. Antoniadis, N. Arkani-Hamed, S. Dimopoulos and G. R. Dvali, "New dimensions at a millimeter to a Fermi and superstrings at a TeV," Phys. Lett. B **436** (1998) 257 [arXiv:hep-ph/9804398].

[18] G. F. Giudice, R. Rattazzi and J. D. Wells, "Quantum gravity and extra dimensions at high-energy colliders," Nucl. Phys. B **544** (1999) 3 [arXiv:hep-ph/9811291].

See also:

G. F. Giudice, R. Rattazzi and J. D. Wells, "Graviscalars from higher-dimensional metrics and curvature-Higgs mixing," Nucl. Phys. B **595** (2001) 250 [arXiv:hep-ph/0002178].

[19] G. F. Giudice, R. Rattazzi and J. D. Wells, "Transplanckian collisions at the LHC and beyond," Nucl. Phys. B **630** (2002) 293 [arXiv:hep-ph/0112161].

[20] L. Anchordoqui, T. Paul, S. Reucroft and J. Swain, "Ultrahigh energy cosmic rays: The state of the art before the Auger observatory," arXiv:hep-ph/0206072, sections VII and IX

R. Emparan, M. Masip and R. Rattazzi, "Cosmic rays as probes of large extra dimensions and TeV gravity," Phys. Rev. D **65** (2002) 064023 [arXiv:hep-ph/0109287].

[21] R. Brandenberger, invited seminar at Scuola Normale Superiore, Pisa, Italy, 14 February 2002; based on

S. Alexander, R. H. Brandenberger and D. Easson, "Brane gases in the early universe," Phys. Rev. D **62** (2000) 103509 [arXiv:hep-th/0005212].

[22] A. Pomarol and M. Quiros, "The standard model from extra dimensions," Phys. Lett. B **438** (1998) 255 [arXiv:hep-ph/9806263].

A. Delgado, A. Pomarol and M. Quiros, "Supersymmetry and electroweak breaking from extra dimensions at the TeV-scale," Phys. Rev. D **60** (1999) 095008 [arXiv:hep-ph/9812489].

A. Delgado, A. Pomarol and M. Quiros, "Electroweak and flavor physics in extensions of the standard model with large extra dimensions," JHEP **0001** (2000) 030 [arXiv:hep-ph/9911252].

[23] T. Appelquist, H. C. Cheng and B. A. Dobrescu, "Bounds on universal extra dimensions," Phys. Rev. D **64** (2001) 035002 [arXiv:hep-ph/0012100].

[24] Y. Kawamura, "Triplet-doublet splitting, proton stability and extra dimension," Prog. Theor. Phys. **105** (2001) 999 [arXiv:hep-ph/0012125].

[25] G. Altarelli and F. Feruglio, "SU(5) grand unification in extra dimensions and proton decay," Phys. Lett. B **511** (2001) 257 [arXiv:hep-ph/0102301].

[26] Lectures at Corfu Summer Institute, September 2001; based on

A. Muck, A. Pilaftsis and R. Ruckl, "An introduction to 5-dimensional extensions of the standard model," arXiv:hep-ph/0209371.

[27] J. Lykken and S. Nandi, "Asymmetrical large extra dimensions," Phys. Lett. B **485** (2000) 224 [arXiv:hep-ph/9908505].

[28] R. Barbieri, L. J. Hall and Y. Nomura, "A constrained standard model from a compact extra dimension," Phys. Rev. D **63** (2001) 105007 [arXiv:hep-ph/0011311].

[29] L. Randall and R. Sundrum, "A large mass hierarchy from a small extra dimension," Phys. Rev. Lett. **83** (1999) 3370 [arXiv:hep-ph/9905221].

[30] W. D. Goldberger and M. B. Wise, "Modulus stabilization with bulk fields," Phys. Rev. Lett. **83** (1999) 4922 [arXiv:hep-ph/9907447].

[31] L. Randall and R. Sundrum, "An alternative to compactification," Phys. Rev. Lett. **83** (1999) 4690 [arXiv:hep-th/9906064].

[32] D. M. Ghilencea, S. Groot Nibbelink and H. P. Nilles, "Gauge corrections and FI-term in 5D KK theories," Nucl. Phys. B **619** (2001) 385 [arXiv:hep-th/0108184].

[33] R. Barbieri, L. J. Hall and Y. Nomura, "A constrained standard model: Effects of Fayet-Iliopoulos terms," arXiv:hep-ph/0110102.

[34] C. A. Scrucca, M. Serone, L. Silvestrini and F. Zwirner, "Anomalies in orbifold field theories," Phys. Lett. B **525** (2002) 169 [arXiv:hep-th/0110073].

[35] L. Pilo and A. Riotto, "On anomalies in orbifold theories," Phys. Lett. B **546** (2002) 135 [arXiv:hep-th/0202144].

[36] R. Barbieri, R. Contino, P. Creminelli, R. Rattazzi and C. A. Scrucca, "Anomalies, Fayet-Iliopoulos terms and the consistency of orbifold field theories," Phys. Rev. D **66** (2002) 024025 [arXiv:hep-th/0203039].

[37] R. Barbieri, G. Marandella and M. Papucci, "Breaking the electroweak symmetry and supersymmetry by a compact extra dimension," Phys. Rev. D **66** (2002) 095003 [arXiv:hep-ph/0205280].

[38] R. Barbieri, L. J. Hall, G. Marandella, Y. Nomura, T. Okui, S. J. Oliver and M. Papucci, "Radiative electroweak symmetry breaking from a quasi-localized top quark," arXiv:hep-ph/0208153.

[39] M. Chertok, G. D. Kribs, Y. Nomura, W. Orejudos, B. Schumm and S. Su, "Phenomenology of a constrained standard model from an extra dimension," in *Proc. of the APS/DPF/DPB Summer Study on the Future of Particle Physics (Snowmass 2001)* ed. N. Graf, arXiv:hep-ph/0112001.

[40] R. Barbieri, G. Cacciapaglia and A. Romito, "b $\rightarrow$ s gamma in a calculable model of electroweak symmetry breaking," Nucl. Phys. B **627** (2002) 95 [arXiv:hep-ph/0107148].

[41] J. R. Ellis, "Looking back at the first decade of 21st century high-energy physics," arXiv:hep-ph/0208109.

Bibliography for chapter 3 "Limits on Extra Dimensions from Supernovae"

[42] G. Cacciapaglia, M. Cirelli, Y. Lin and A. Romanino, "Bulk neutrinos and core collapse supernovae," arXiv:hep-ph/0209063.

[43] Q. R. Ahmad *et al.* [SNO Collaboration], "Measurement of the charged current interactions produced by B-8 solar neutrinos at the Sudbury Neutrino Observatory," Phys. Rev. Lett. **87** (2001) 071301 [arXiv:nucl-ex/0106015];

Q. R. Ahmad *et al.* [SNO Collaboration], "Direct evidence for neutrino flavor transformation from neutral-current interactions in the Sudbury Neutrino Observatory," Phys. Rev. Lett. **89** (2002) 011301 [arXiv:nucl-ex/0204008];

Q. R. Ahmad *et al.* [SNO Collaboration], "Measurement of day and night neutrino energy spectra at SNO and constraints on neutrino mixing parameters," Phys. Rev. Lett. **89** (2002) 011302 [arXiv:nucl-ex/0204009].

[44] K. R. Dienes, E. Dudas and T. Gherghetta, "Light neutrinos without heavy mass scales: A higher-dimensional seesaw mechanism," Nucl. Phys. B **557** (1999) 25 [arXiv:hep-ph/9811428];

N. Arkani-Hamed, S. Dimopoulos, G. R. Dvali and J. March-Russell, "Neutrino masses from large extra dimensions," Phys. Rev. D **65** (2002) 024032 [arXiv:hep-ph/9811448].

[45] G. R. Dvali and A. Y. Smirnov, "Probing large extra dimensions with neutrinos," Nucl. Phys. B **563** (1999) 63 [arXiv:hep-ph/9904211].

[46] K. Hirata *et al.* [KAMIOKANDE-II Collaboration], "Observation Of A Neutrino Burst From The Supernova Sn1987a," Phys. Rev. Lett. **58** (1987) 1490;

R. M. Bionta *et al.*, "Observation Of A Neutrino Burst In Coincidence With Supernova Sn1987a In The Large Magellanic Cloud," Phys. Rev. Lett. **58** (1987) 1494.

[47] G. G. Raffelt, "Particle physics from stars," Ann. Rev. Nucl. Part. Sci. **49** (1999) 163 [arXiv:hep-ph/9903472].

[48] T. Han, J. D. Lykken and R. J. Zhang, "On Kaluza-Klein states from large extra dimensions," Phys. Rev. D **59** (1999) 105006 [arXiv:hep-ph/9811350];

S. Cullen and M. Perelstein, "SN1987A constraints on large compact dimensions," Phys. Rev. Lett. **83** (1999) 268 [arXiv:hep-ph/9903422];

C. Hanhart, D. R. Phillips, S. Reddy and M. J. Savage, "Extra dimensions, SN1987a, and nucleon nucleon scattering data," Nucl. Phys. B **595** (2001) 335 [arXiv:nucl-th/0007016];

C. Hanhart, J. A. Pons, D. R. Phillips and S. Reddy, "The likelihood of GODs' existence: Improving the SN 1987a constraint on the size of large compact dimensions," Phys. Lett. B **509** (2001) 1 [arXiv:astro-ph/0102063].

[49] A. D. Dolgov, S. H. Hansen, G. Raffelt and D. V. Semikoz, “Cosmological and astrophysical bounds on a heavy sterile neutrino and the KARMEN anomaly,” Nucl. Phys. B **580** (2000) 331 [arXiv:hep-ph/0002223].

[50] R. Barbieri, P. Creminelli and A. Strumia, “Neutrino oscillations from large extra dimensions,” Nucl. Phys. B **585** (2000) 28 [arXiv:hep-ph/0002199].

[51] H. Nunokawa, J. T. Peltoniemi, A. Rossi and J. W. Valle, “Supernova bounds on resonant active-sterile neutrino conversions,” Phys. Rev. D **56** (1997) 1704 [arXiv:hep-ph/9702372].

[52] A. Lukas, P. Ramond, A. Romanino and G. G. Ross, “Neutrino masses and mixing in brane-world theories,” JHEP **0104** (2001) 010 [arXiv:hep-ph/0011295].

[53] For general reviews and extensive references, see H. A. Bethe, “Supernova Mechanisms,” Rev. Mod. Phys. **62** (1990) 801;

G. G. Raffelt, “ Stars and as laboratories for fundamental physics: The astrophysics of neutrinos, axions, and other weakly interacting particles,” Chicago Univ.Press, Chicago, 1996.

[54] J. M. Lattimer, “The Nuclear Equation of State and Supernovae,” in “Nuclear Equation of State”, ed. A. Ansari and L. Satpathy (World Scientific, Singapore), pp. 83-208 (1996);

M. Prakash, J. M. Lattimer, J. A. Pons, A. W. Steiner and S. Reddy, “Evolution of a Neutron Star From its Birth to Old Age,” Lect. Notes Phys. **578** (2001) 364 [arXiv:astro-ph/0012136];

H. T. Janka, K. Kifonidis and M. Rampp, “Supernova explosions and neutron star formation,” Lect. Notes Phys. **578** (2001) 333 [arXiv:astro-ph/0103015].

[55] M. Rampp and H. T. Janka, “Spherically symmetric simulation with Boltzmann neutrino transport of core collapse and post-bounce evolution of a 15 solar mass star,” Astrophys. J. **539** (2000) L33 [arXiv:astro-ph/0005438];

A. Mezzacappa, M. Liebendorfer, O. E. Messer, W. R. Hix, F. K. Thielemann and S. W. Bruenn, “The Simulation of a Spherically Symmetric Supernova of a 13 Solar Mass Star with Boltzmann Neutrino Transport, and Its Implications for the Supernova Mechanism,” Phys. Rev. Lett. **86** (2001) 1935 [arXiv:astro-ph/0005366];

M. Liebendorfer, A. Mezzacappa, F. K. Thielemann, O. E. Messer, W. R. Hix and S. W. Bruenn, “Probing the gravitational well: No supernova explosion in spherical symmetry with general relativistic Boltzmann neutrino transport,” Phys. Rev. D **63** (2001) 103004 [arXiv:astro-ph/0006418].

[56] A. Lukas, P. Ramond, A. Romanino and G. G. Ross, Phys. Lett. B **495** (2000) 136 [arXiv:hep-ph/0008049].

[57] A. E. Faraggi and M. Pospelov, “Phenomenological issues in TeV scale gravity with light neutrino masses,” Phys. Lett. B **458** (1999) 237 [arXiv:hep-ph/9901299];

R. N. Mohapatra, S. Nandi and A. Perez-Lorenzana, "Neutrino masses and oscillations in models with large extra dimensions," Phys. Lett. B **466** (1999) 115 [arXiv:hep-ph/9907520];

A. Ioannisian and A. Pilaftsis, "Cumulative non-decoupling effects of Kaluza-Klein neutrinos in electroweak processes," Phys. Rev. D **62** (2000) 066001 [arXiv:hep-ph/9907522];

A. Lukas and A. Romanino, "A brane-world explanation of the KARMEN anomaly," arXiv:hep-ph/0004130;

K. R. Dienes and I. Sarcevic, "Neutrino flavor oscillations without flavor mixing angles," Phys. Lett. B **500** (2001) 133 [arXiv:hep-ph/0008144];

A. Lukas, P. Ramond, A. Romanino and G. G. Ross, "Brane-Bulk Neutrino Oscillations," Int. J. Mod. Phys. A **16S1C** (2001) 934;

D. O. Caldwell, R. N. Mohapatra and S. J. Yellin, "Large extra dimensions, sterile neutrinos and solar neutrino data," Phys. Rev. Lett. **87** (2001) 041601 [arXiv:hep-ph/0010353];

A. S. Dighe and A. S. Joshipura, "Neutrino anomalies and large extra dimensions," Phys. Rev. D **64** (2001) 073012 [arXiv:hep-ph/0105288];

A. De Gouvea, G. F. Giudice, A. Strumia and K. Tobe, "Phenomenological implications of neutrinos in extra dimensions," Nucl. Phys. B **623** (2002) 395 [arXiv:hep-ph/0107156];

H. Davoudiasl, P. Langacker and M. Perelstein, "Constraints on large extra dimensions from neutrino oscillation experiments," Phys. Rev. D **65** (2002) 105015 [arXiv:hep-ph/0201128].

[58] L. J. Hall and D. R. Smith, "Cosmological constraints on theories with large extra dimensions," Phys. Rev. D **60** (1999) 085008 [arXiv:hep-ph/9904267];

S. Hannestad, "Strong constraint on large extra dimensions from cosmology," Phys. Rev. D **64** (2001) 023515 [arXiv:hep-ph/0102290].

[59] A. Burrows, T. J. Mazurek, J. M. Lattimer, "The deleptonization and heating of proton-neutron stars," Astrophys. J. **251** (1981) 325;

A. Burrows and J. M. Lattimer, "The Birth Of Neutron Stars," Astrophys. J. **307** (1986) 178.

[60] S. Reddy, M. Prakash and J. M. Lattimer, "Neutrino interactions in hot and dense matter," Phys. Rev. D **58** (1998) 013009 [arXiv:astro-ph/9710115].

[61] W. Keil and H. T. Janka, "Hadronic Phase Transitions At Supranuclear Densities And The Delayed Collapse Of Newly Formed Neutron Stars," Astron. Astrophys. **296** (1995) 145;

K. Sumiyoshi, H. Suzuki and H. Toki, "Influence of the symmetry energy on the birth of neutron stars and supernova neutrinos," Astron. Astrophys. **303** (1995) 475 [arXiv:astro-ph/9506024];

J. A. Pons, S. Reddy, M. Prakash, J. M. Lattimer and J. A. Miralles, "Evolution of protoneutron stars," Astrophys. J. **513** (1999) 780 [arXiv:astro-ph/9807040].

[62] For a recent discussion of spectra formation, see e.g. M. T. Keil *et al.*, "Monte Carlo Study of Supernova Neutrino Spectra Formation," [arXiv:astro-ph/0208035].

Bibliography for chapter 5 "Muon g-2 in a model with one extra dimension"

[63] G. Cacciapaglia, M. Cirelli and G. Cristadoro, "Muon anomalous magnetic moment in a calculable model with one extra dimension," Nucl. Phys. B **634** (2002) 230 [arXiv:hep-ph/0111288].

[64] M. Cirelli, "Muon g-2 in a model with one extra dimension," arXiv:hep-ph/0205140, Talk given at 37th Rencontres de Moriond on Electroweak Interactions and Unified Theories, Les Arcs, France, 9-16 Mar 2002.

[65] H.N.Brown et al. (Muon g-2 Collaboration), *Phys.Rev.Lett.* **86**:2227-2231,2001, arXiv:hep-ex/0102017;

A.Czarnecki, W.J.Marciano, *Phys.Rev.* **D64**:013014,2001, arXiv:hep-ph/0102122;

[66] P.Nath, M.Yamaguchi, *Phys.Rev.* **D60**:116006,1999, arXiv:hep-ph/9903298;

R.Casadio, A.Gruppuso, G.Venturi, *Phys. Lett.* **B495**:378, 200, arXiv:hep-th/0010065;

Seong Chan Park, H.S.Song, *Phys. Lett.* **B506**:99,2001, arXiv:hep-ph/0103072;

K.Agashe, N.G.Deshpande, G.-H.Wu, *Phys.Lett.* **B511**:85,2001, arXiv:hep-ph/0103235;

T.Appelquist, B.A.Dobrescu, *Phys.Lett* **B516**:85,2001, arXiv:hep-ph/0106140;

[67] J.Prades, invited talk at "Kaon 2001", 6-13 June 2001, Pisa, Italy, arXiv:hep-ph/0108192;

[68] for a recent review: W.J.Marciano, B.L.Roberts, arXiv:hep-ph/0105056;

[69] M.Knecht, A.Nyffeler, arXiv:hep-ph/0111058;

M.Knecht, A.Nyffeler, M.Perrottet, E.de Rafael, arXiv:hep-ph/0111059;

[70] I.Blokland, A.Czarnecki and K.Melnikov, arXiv:hep-ph/0112117;

[71] J.Schwinger, *Phys.Rev.* **73**:416-417,1948;

Phys.Rev. **76**:790-817:1949;

[72] G.Altarelli, N.Cabibbo, L.Maiani, *Phys.Lett.* **B40**:415,1972;

[73] S.J.Brodsky, J.D.Sullivan, *Phys.Rev.* **156**:1644,1967;

[74] I.Vendramin, *Nuovo Cim.* **A101**:731,1989;

K.R.Lynch, arXiv:hep-ph/0108080 and arXiv:hep-ph/0108081 .

Bibliography for chapter 6 “Gluon fusion into Higgs in a model with one extra dimension”

[75] G. Cacciapaglia, M. Cirelli and G. Cristadoro, “Gluon fusion production of the Higgs boson in a calculable model with one extra dimension,” Phys. Lett. B **531** (2002) 105 [arXiv:hep-ph/0111287].

[76] H.M.Georgi, S.L.Glashow, M.E.Machacek and D.V.Nanopoulos, *Phys.Rev.Lett.* **40** (1978) 692;

[77] M.Spira, contribution to the *Proceedings of the International Europhysics Conference on High-Energy Physics*, 19-26 Aug. 1997, Jerusalem, Israel, arXiv:hep-ph/9711394;

[78] D.M.Ghilencea, S.Groot Nibbelink and Hans Peter Nilles, *Nucl.Phys.* **B619** (2001) 385, arXiv:hep-th/0108184;

[79] R.Barbieri, L.J.Hall and Y.Nomura, *Nucl.Phys.* **B624** (2002) 63, arXiv:hep-th/0107004;

[80] J.R.Ellis, M.K.Gaillard and D.V.Nanopoulos, *Nucl.Phys.* **B106** (1976) 292;

A.I.Vainstein, M.B.Voloshin, V.I.Zakharov and M.A.Shifman, *Sov.J.Nucl.Phys.* **30** (1979) 711;

[81] M.Spira, A.Djouadi and P.M.Zerwas, *Phys.Lett.* **B264** (1991) 440;

for recent reviews see: M.Spira, A.Djouadi, D.Gaudenz and P.M.Zerwas, *Nucl.Phys.* **B453** (1995) 17, arXiv:hep-ph/9504378; M.Spira, *Fortsch.Phys.* **46** (1998) 203, arXiv:hep-ph/9705337;

[82] N.Arkani-Hamed, T.Gregoire and J.Wacker, arXiv:hep-th/0101233;

[83] E.A.Mirabelli and M.E.Peskin, *Phys.Rev.* **D58** (1998) 065002, arXiv:hep-th/9712214.